



**UNIVERSITY OF
BIRMINGHAM**



John Innes Centre

**BIOFORTIFICATION OF WHEAT USING DIFFERENT MOLECULAR BREEDING
TECHNIQUES**

By

MUHAMMAD WAQAS ALI

A thesis submitted to the University of Birmingham for the degree of

DOCTOR OF PHILOSOPHY

School of Biosciences

College of Life and Environmental Sciences

University of Birmingham

August 2023

UNIVERSITY OF
BIRMINGHAM

University of Birmingham Research Archive

e-theses repository

This unpublished thesis/dissertation is copyright of the author and/or third parties. The intellectual property rights of the author or third parties in respect of this work are as defined by The Copyright Designs and Patents Act 1988 or as modified by any successor legislation.

Any use made of information contained in this thesis/dissertation must be in accordance with that legislation and must be properly acknowledged. Further distribution or reproduction in any format is prohibited without the permission of the copyright holder.

Abstract

Wheat grains are a poor source of iron and zinc, and identifying genetic ways to improve these through breeding could improve human health. In this thesis, we aimed to characterise the *ZIP* (zinc-regulated, iron-regulated transporter-like protein) family in wheat and identify novel variation for Fe content using an EMS population.

In our first project, we identified and functionally characterised the *ZIP* genes in wheat, identifying 15 *TaZIP* genes in total. Using publicly available RNA-seq data, we found that in both wheat and rice, *TaZIP11*, *TaZIP13*, and *TaZIP14* showed the highest expression in most tissues. We functionally characterised these three ZIPs. We found that *TaZIP11* could transport Fe and Zn in a yeast complementation assay but did not observe consistent effects on micronutrients in any wheat mutant lines. Although *TaZIP13* did not transport Fe and Zn in yeast complementation assay, our TILLING mutants showed altered Fe contents, while these were inconsistent between different crosses. *TaZIP14* showed no effect in yeast or in *planta*.

Secondly, we screened a hundred EMS lines cv. Cadenza using Perls staining and selected three high Fe lines to develop the mapping populations. For Fe phenotyping in mapping population, we developed a computational method to quantify the Fe levels. Additionally, this method also localized the Fe contents in grain tissues. Bulk segregant analysis of F₂ lines identified significant QTL for Fe content in one population, including a highly significant QTL on Chromosome 3B.

In summary, we identified and characterised three *ZIP* genes in wheat, found that EMS mutagenesis can increase grain iron content and found a novel QTL for Fe content.

Dedication

I would like to dedicate my PhD thesis to my loving parents, Muhammad Ramzan and Riaz Bibi, my sisters and my younger brother Muhammad Rizwan Ali. Their steady support, encouragement, and belief in my capabilities have been the foundation of my academic achievements. Your sacrifices, understanding, and endless encouragement have allowed me to pursue my dreams with confidence. Your presence in my life has provided me with the strength to overcome challenges and the belief that anything is possible.

Acknowledgements

I would like to express my heartfelt gratitude to my supervisor, Dr Philippa Borrill from John Innes Centre. Throughout my PhD, her tremendous help, direction, motivation, and support with kindness, tenderness, and patience were extremely helpful to me. Without her encouragement and motivation, I would not have been able to complete this thesis. She assisted me with my scientific writing and mentored me throughout my research. You are my ideal supervisor and mentor.

As a member of my supervisory committee, Dr Marco Catoni from University of Birmingham provided me with excellent advice during my PhD, to whom I am grateful. I would like to thank to our lab for being so supportive. I would love to mention Catherine, Emilie, Marek, Sergio, Samuel, Robbie, Gaia, Anham, Katie, Tayyaba, Sophie, and Prateek who assisted me in various activities during my PhD.

And finally, to my wife, Sana Tariq, your constant encouragement, love, and sacrifices have been a constant source of inspiration. Your boundless patience and understanding during late nights and busy days have allowed me to pursue this dream. And to our little Hashir Ali, your innocent laughter and joyful presence have brought light to even the most challenging moments. Your first year of life coincided with the completion of this thesis, reminding me that life's most precious moments are woven into every step of this journey. This work is a tribute to the love and joy you both bring to my life.

The Commonwealth Scholarship UK deserves the most significant gratitude for supporting my PhD and giving me this opportunity, and the University of Birmingham and John Innes Centre for providing the resources to complete this thesis. Again, I want to extend my gratitude to everyone who helped make this thesis possible.

Table of contents

Chapter 1: General Introduction	1
1.1 Wheat as a staple crop	2
1.1.1 Wheat production and consumption	4
1.1.2 Nutritional value	6
1.2 Micronutrients malnutrition	7
1.3 Plant iron and zinc nutrition	10
1.3.1 Iron	10
1.3.2 Zinc	13
1.4 An outlook of iron and zinc uptake from soil to grains	14
1.4.1 Uptake and distribution	14
1.4.2 Storage	17
1.5 Biofortification; A solution to fulfil the gap of micronutrient	18
1.5.1 Supplementation	18
1.5.2 Food fortification	19
1.5.3 Biofortification through agronomic approaches	20
1.6 New genomic resources for biofortification	25
1.5.1 Transgenic approaches	26
1.5.3 Genome selection approach	28
1.7 Thesis aims	29
Chapter 2: Identification of <i>ZIP</i> Genes and Their Functional Characterization in Wheat.....	30
2.1 Introduction	31
2.1.1 The <i>ZIP</i> gene family	31
2.1.2 Role of <i>ZIP</i> genes in model plants	32
2.1.3 Role of <i>ZIP</i> genes in wheat	33
2.1.3 The importance of TILLING population	34
2.2 Aims	37
2.3 Material and Methods	37
2.3.1 Nomenclature and expression of <i>ZIP</i> genes	37
2.3.2 TILLING mutant selection	38
2.3.3 Primers design	40
2.3.4 Genotyping	43
2.3.5 Plant growth and phenotyping	44
2.3.5.1 Germplasm development	44
2.3.5.2 Phenotypic characterisation	44

2.3.6 ICP-OES analysis	45
2.3.8 Data visualization and statistic analysis	46
2.4 Results	47
2.4.1 The nomenclature of <i>ZIP</i> family in wheat	47
2.4.2 The <i>ZIP</i> expressions in rice and wheat	51
2.4.3 Selecting Kronos TILLING mutants and generating double mutants	55
2.4.4 Agronomic traits of <i>TaZIP11</i>	61
2.4.4.1 Tiller numbers and plant height of <i>TaZIP11</i>	61
2.4.4.2 Grain numbers, total weight and thousand grain weight of <i>TaZIP11</i>	61
2.4.5 Agronomic traits of <i>TaZIP13</i> :.....	62
2.4.5.1 Tiller numbers and plant height of <i>TaZIP13</i>	62
2.4.5.2 Grain numbers, total weight and thousand grain weight of <i>TaZIP13</i>	63
2.4.6 Agronomic traits of <i>TaZIP14</i>	65
2.4.6.1 Tillers numbers and plant height of <i>TaZIP14</i>	65
2.4.6.2 Grain numbers, total weight and thousand grain weight of <i>TaZIP14</i>	66
2.4.7 Micronutrient quantification	68
2.4.7.1 Micronutrient quantification of <i>TaZIP11</i>	68
2.4.7.2 Micronutrient quantification of <i>TaZIP13</i>	69
2.4.7.3 Micronutrient quantification of <i>TaZIP14</i>	72
2.4.8 Functional complementation of <i>TaZIPs</i> in yeast	74
2.4.8.1 Yeast complementation of <i>zrt1/zrt2</i>	74
2.4.8.2 Yeast complementation of <i>fet3/fet4</i>	76
2.5 Discussion	77
2.5.1 TILLING mutants of <i>TaZIP11</i> , <i>TaZIP13</i> , and <i>TaZIP14</i> had no effect on agronomic traits and limited effects on micronutrients	78
2.5.2 Functional complementation shows the capacity of <i>TaZIP11</i> to transport Fe and Zn	80
2.5.3 Similarities and differences between <i>TaZIP11</i> , <i>13</i> and <i>14</i> and known <i>ZIPs</i> in wheat and other species	82
Chapter 3: Identifying Novel QTLs Involved in Controlling Grain Iron in Bread Wheat.....	85
3.1 Introduction	86
3.1.1 An Overview of iron metabolism in wheat.....	86
3.1.2 Limited understanding of the genetic basis of grain iron content	87
3.1.3 Known QTLs associated with grain iron	88
3.1.4 Bulk segregant analysis	89
3.2 Aim	91
3.3 Material and methods	92

3.3.1 Plant growth and population development	92
3.3.1.1 Screening of EMS population	92
3.3.1.2 Initial Perls staining and Visual scoring.....	92
3.3.1.3 Generating mapping population.....	93
3.3.2 Phenotyping.....	93
3.3.2.2 ICP-OES analysis.....	94
3.3.2.4 Computational scoring.....	95
3.3.3 Genetic analysis.....	95
3.3.3.1 DNA extraction	95
3.3.3.2 Sequence alignment.....	96
3.3.3.3 Bulked segregant analysis.....	96
3.4 Results	97
3.4.1 Initial screening presents three times higher grain iron.....	97
3.4.2 Parental lines have higher iron and zinc contents compared to WT	100
3.4.3 Computation vs personal scoring of Perls images.....	101
3.4.4 Generation of mapping population and selection of extreme bulks by computational scoring.....	105
3.4.5 QTLs identified by Bulk segregant analysis.....	113
3.4.5.2 BSA analysis using QTLseqr	117
3.4.5.3 Putative QTLs identified on Chr3B in population 7060.....	123
3.5 Discussions	125
3.5.1 EMS population shows variations in the grain iron content.....	125
3.5.2 Advantages of Perls staining vs ICP-OES	127
3.5.3 Computational scoring handles large datasets and standardise for complex traits like iron	128
3.5.4 Comparison of identified QTLs with previous studies	129
Chapter 4: General Discussion	131
4.1 Summary of the thesis.....	132
4.2 Nutrition as a complex trait and its demand to increase in wheat grain.....	133
4.3 Unveiling the <i>TaZIP</i> family for Fe and Zn content	134
4.4 Perls staining and image analysis help to localize the grain Fe content.....	137
4.5 Bulk segregant analysis offers cost-effective and rapid QTLs detection.....	139
4.6 Future Directions and Recommendations.....	141
4.6.1 <i>TaZIP</i> lines.....	142
4.6.2 EMS populations.....	142
4.6.3 Wheat improvement plans	143

4.7 Conclusion	146
References:	147

List of Figures

Figure 1.1: Evolution and domestication of bread wheat.....	4
Figure 1.2: Basic pathway for iron and zinc distribution in wheat.....	12
Figure 1.3: A visual depiction of iron and zinc biofortification using modern genomic resources.....	26
Figure 2.1: A phylogenetic tree of <i>ZIP1</i> in rice and wheat.....	38
Figure 2.2: Plant Ensembl gene tab.....	39
Figure 2.3: Plants Ensembl variant image.....	39
Figure 2.4: Plants Ensembl variant table.....	40
Figure 2.5: The expression level (RMA; Robust Multiarray Averaging) of <i>ZIP</i> genes in rice.....	52
Figure 2.6: The expression (TPM) level of 14 <i>ZIP</i> genes in bread wheat.....	53
Figure 2.7: The specific grain tissue expression (TPM) level of candidate.....	54
Figure 2.8: Crossing scheme to generate double mutants.....	56
Figure 2.9: Agronomic traits for <i>TaZIP11-1</i> (K3178 X K0417).....	62
Figure 2.10: Agronomic traits for <i>TaZIP13-1</i> (K0373 X K2425).....	64
Figure 2.11: Agronomic traits for <i>TaZIP13-2</i> (K2425 X K3714).....	65
Figure 2.12: Agronomic traits for <i>TaZIP14-1</i> (K3269 X K4450).....	66
Figure 2.13: Agronomic traits for <i>TaZIP14-2</i> (K3269 X K4275).....	67
Figure 2.14: Agronomic traits for <i>TaZIP14-3</i> (K3191 X K4275).....	68
Figure 2.15: Micronutrient quantification of <i>TaZIP11</i>	69
Figure 2.16: Micronutrient quantification of <i>TaZIP13-1</i>	71
Figure 2.17: Micronutrient quantification of <i>TaZIP13-2</i>	72
Figure 2.18: Micronutrient quantification of <i>TaZIP14-1</i>	73
Figure 2.19: Micronutrient quantification of <i>TaZIP14-2</i>	74
Figure 2.20: <i>TaZIP</i> genes complementation of the yeast Zn uptake mutant <i>zrt1/zrt2</i>	75
Figure 2.21: <i>TaZIP</i> genes complementation of the yeast Fe uptake mutant <i>fet3/fet4</i>	77
Figure 3.1: A basic scheme of BSA as applied to wheat grain Fe content.	91
Figure 3.2: A schematic representation of Perls staining.....	93
Figure 3.3: Perls staining of EMS lines and WT.....	98
Figure 3.4: Dissection of wheat grains for Perls staining.....	99
Figure 3.5: Visual scoring of longitudinal dissected of 100 EMS lines.....	100

Figure 3.6: Fe and Zn contents of wholemeal (A) and white meal (B) dry flour of EMS parental lines.....	101
Figure 3.7: Visual score comparison of 50 lines of BC ₁ F ₂ for 7077.....	102
Figure 3.8: Representation of Perls iron staining of EMS line 7077 parent and WT.....	103
Figure 3.9: Spyder image analysis.....	104
Figure 3.10: Perls image scoring correlation of F ₂ population.....	105
Figure 3.11: Agronomic traits of all three populations.....	107
Figure 3.12: This graph shows the computational (Spyder) score for whole F ₂ population (200 lines) made with parent 7077.....	109
Figure 3.13: This graph shows the computational (Spyder) score for whole F ₂ population (200 lines) made with parent 7060.....	110
Figure 3.14: This graph shows the computational (Spyder) score for whole F ₂ population (200 lines) made with parent 7054.....	111
Figure 3.15: Perls staining images of bulks for BSA 7077.....	112
Figure 3.16: This figure shows the data of population 7077 before filtering.....	114
Figure 3.17: This figure shows the data of population 7077 after filtering.....	115
Figure 3.18: These histograms show the G' value distribution with a threshold of 0.01 for P7077.....	118
Figure 3.19: Genome-wide distribution of number of SNPs of 7060.....	119
Figure 3.20: The tricube-smoothed Δ (SNP-index) of 7060.....	120
Figure 3.21: G' values distribution of 7060 of all chromosomes.....	121
Figure 3.22: <i>p-value</i> (-log ₁₀) distribution of 7060 of all chromosomes.....	122
Figure 3.23: The tricube-smoothed Δ (SNP-index) of 7060.....	124

List of Tables

Table 1.1: Micronutrients essential for human, their function and effect of deficiency...	9
Table 2.1: KASP primers for <i>TaZIP</i> TILLING mutants.....	41
Table 2.2: Details of ZIP genes identification in wheat.....	49
Table 2.3: Selected candidate genes to investigate the rule of these genes in Zn and Fe biofortification.....	55
Table 2.4: Location and characterization of the <i>TaZIP</i> mutation.....	57
Table 2.5: TILLING lines to characterise the <i>ZIP</i> genes.....	60
Table 3.1: Pearson's correlation coefficients between Fe content and agronomic traits of 7077.....	108
Table 3.2: Pearson's correlation coefficients between Fe content and agronomic traits of 7060.....	108
Table 3.3: Pearson's correlation coefficients between Fe content and agronomic traits of 7054.....	108
Table 3.4: SNPs filter options for 7077.....	116

List of Abbreviations

AA	Amino acids
AAS	Atomic absorption spectroscopy
ANOVA	Analysis of variance
At	<i>Arabidopsis thaliana</i>
BC	Backcross
BSA	Bulk segregant analysis
Cd	Cadmium
Chr	Chromosome
DH	Doubled haploid
DMA	2'-deoxymugineic acid
DNA	Deoxyribonucleic acid
EDTA	Ethylene diaminetetraacetic acid
EGTA	Ethylene glycoltetraacetic acid
ENA	Efflux transporter of NA
ER	Endoplasmic reticulum
EV	Empty vectors
FAO	Food and Agricultural Organization of the United Nations
Fe	Iron
Filt	Filter
FRO	Ferric reduction oxidase
FRDL	Ferric reductase defective like
GMO	Genetically modified organism
Gpc-B1	Grain protein content B1 locus
GUS	β -glucuronidase
HMA	Major heavy metal-associated family
Hv	<i>Hordeum vulgare</i>
ICP-OES	Inductively coupled plasma optical emission spectrometry
IRT	Iron regulated transporter
KASP	Kompetitive Allele Specific PCR
KWT	Kronos wild-type
MAS	Marker-assisted selection
Mn	Manganese
MTP	Metal tolerance protein
NA	Nicotianamine
Nano-SIMs	Nanoscale secondary ion mass spectrometry
NG	Number of grains
NGS	Next generation sequence
NT	Number of tillers
NRAMP	Natural resistance-associated macrophage protein
OPT	Oligo peptide transporter
Os	<i>Oryza sativa</i>
P	Plastids
PCR	Polymerase chain reaction
PH	Plant height
PS	Phytosiderophores
QTL	Quantitative trait loci/locus

RAP-IDs	Rice annotation project gene IDs
REF	Reference allele frequency
RILs	Recombinant inbred lines
RMA	Robust multiarray averaging
RNA	Ribonucleic acid
RNA-seq	RNA-sequencing
RNI	Reference nutrient intake
ROI	Region of interest
ROS	Reactive oxygen species
SD	Standard deviation
SEM	Scanning electron microscopy
SHW	Synthetic hexaploid wheat
SNP	Single nucleotide polymorphism
SP	Small proteins
ssp.	Subspecies
Ta	<i>Triticum aestivum</i>
TAE	Tris acetate EDTA
TF	Transcription factor
TGAC	The Centre for Genome Analysis
TGW	Thousand grain weight
TILLING	Targeting Induced Local Lesions IN Genomes
TOM	Transporter of mugineic acid
TPM	Transcripts per million
Tris	Tris (hydroxymethyl) aminomethane
TW	Total weight
UD	Undiluted
UK	United Kingdom
URA	Uracil
US	United States
V	Vacuoles
VIT	Vacuolar iron transporter
WHO	World Health Organisation
WT	Wild-type
XRF	X-ray fluorescence
YPD	Yeast peptone dextrose
YSL	Yellow-stripe like proteins
ZIP	ZRT/IRT-like protein
Zm	<i>Zea mays</i>
Zn	Zinc
ZRT	Zn-regulated transporter

Chapter 1: General Introduction

1.1 Wheat as a staple crop

Wheat is the most significant cereal crop in the planet as it is consumed in range of traditional and modern foods. Collectively, the three major worldwide staple cereals (wheat, rice, and maize) cover a key part of the daily human food, account for nearly 60% of the world's food calories (Dixon, 2007). Globally, only wheat plays a key role in ensuring worldwide nutrition security, supplying 20% of human calories and protein (FAO, 2017). More than 170 countries consume more than 50 kg of wheat per person each year (FAO, 2020). The final goal of current agriculture is to make healthy food in adequate quantities for the growing world. It is forecast that the population will be in surplus of 9 billion people by 2050 (Godfray et al., 2010). The existing land for crop farming could not increase and more pressures from restricted water resources and climate change will only aggravate the challenge of providing food safety for the global population (Foley et al., 2011). Though, people whose diets consist primarily of cereals like wheat can suffer micronutrient deficiencies due to low amounts of micronutrients like Fe and Zn in wheat grain. Because of this, enhancing nutrition quality, such as raising the levels of micronutrients in staple crops, is just as important as increasing food supply in terms of quantity.

1.1.1 Origin and evolution of wheat

The history of wheat from around 10,000 B.C. is a significant part of the history of farming (Venske et al., 2019). Wheat is supposed to have first been cultivated in the Middle East spreading from Lebanon, Jordan, and Palestine to Syria, Iran, Turkey, and Iraq that area called Fertile Crescent (Arzani & Ashraf, 2017). The initial cultivated varieties are hulled and contain all polyploidy levels known in *Triticum spp.*, diploid, tetraploid, and hexaploid (Arzani & Ashraf, 2017). These species are einkorn (*Triticum*

monococcum L.), emmer (*Triticum dicoccum*), and spelt (*Triticum spelta*). The corresponding wild relatives are still located in these countries (Harlan & Zohary, 1966; Shewry, 2009). However, the domestication caused huge genetic erosion that has been strengthened through modern breeding with the undesirable consequence of improved susceptibility to climate changes, and diseases (Peng et al., 2011).

Wheat, the *Poaceae* family (Hawkesford et al., 2013), which contains the *Triticeae* tribe, the division with the utmost efficiently important cereals. The fourteen genera that make up the *Triticeae* tribe are divided into the *Triticinae* and *Hordeinae* subtribes, and the development of amphiploids and interspecific hybrids suggests that the different genera may be compatible genetically or cytoplasmically. The widely cultivated wheat group of this tribe are hexaploid *Triticum aestivum* L., tetraploid *Triticum turgidum* L, and diploid einkorn *Triticum monococcum* L. (Peng et al., 2011). A similar domestication of wild tetraploid emmer wheat resulted in the sequential appearance of domesticated emmer wheat (*Triticum dicoccum*) and large-seeded, free-threshing durum wheat (*Triticum durum*) (Avni et al., 2017; Dubcovsky & Dvorak, 2007). Presently, the most efficiently important species are tetraploid pasta wheat (*Triticum turgidum* subsp.) and hexaploid bread wheat (J. H. Peng et al., 2011). The latter two wheat species came into existence as a result of two polyploidization occurrences. The first of these occurred about 500,000–150,000 years BP (before present) with the link of the genomes of diploid species: one was the wild species *Triticum urartu* providing the A genome and the other species from the *Sitopsis* providing the B genome (Figure 1.1). This produced the allotetraploid wild emmer wheat (*Triticum dicoccoides*; AABB; $2n = 4x = 28$) (IWGSC, 2014, 2018; Petersen et al., 2006). By the genetic resources of ancestral diploids, these planted allotetraploid wheat is normally more vigorous,

improving productions and adjusting to a broader range of ecological conditions compared to its family (Feuillet et al., 2008). The second event happened about 8,000–9,000 years BP between *Triticum turgidum* subsp. *dicoccum* and *Aegilops tauschii*, a wild diploid species, which generated the *Triticum aestivum*. (IWGSC et al., 2014; Peng et al., 2011).

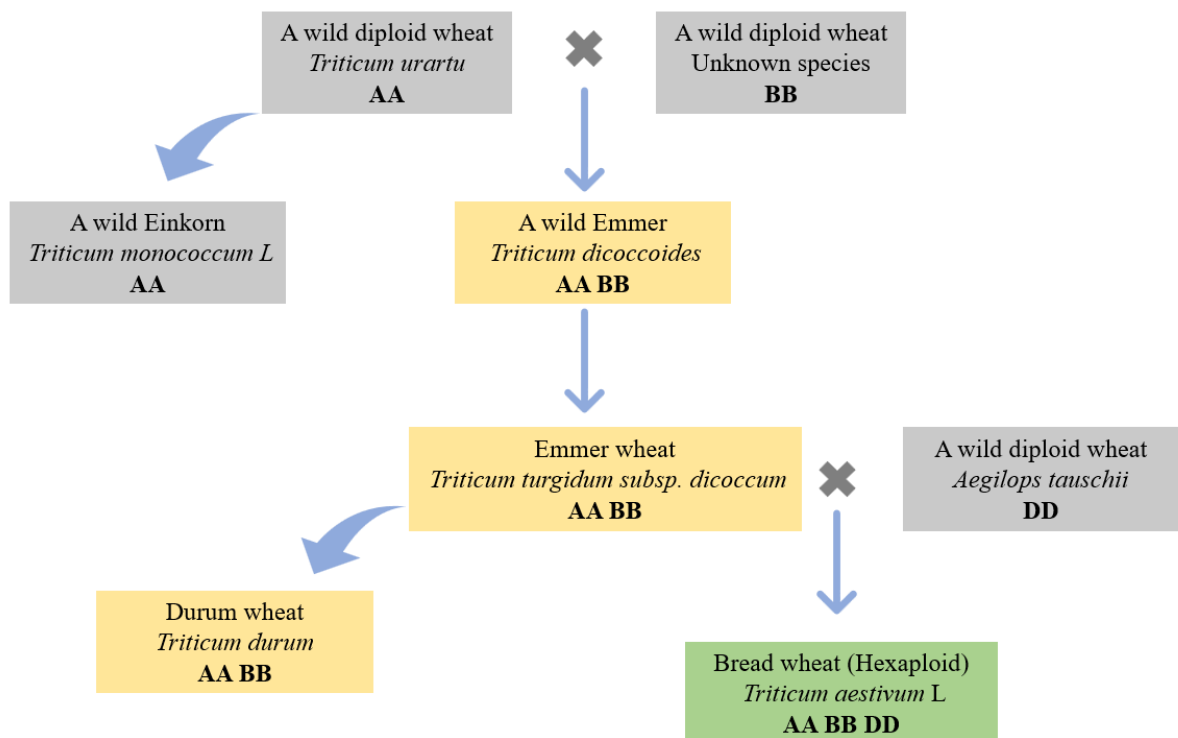


Figure 1.1: Evolution and domestication of bread wheat. The grey, yellow and green colours show diploid, tetraploid and hexaploidy in wheat.

1.1.2 Wheat production and consumption

The capability of world to compact with the growing population and demands was uncontrolled in the 1960s, especially in low income countries however this phenomenon activated a dramatic rise in cereal productions in various countries. The massive hunger and the related social and economic turmoil were prevented (Evans

& Lawson, 2020). Numerous genomic traits were nominated to enhance the production, constancy, and compliance of corn, wheat and rice (Khush, 2001). Introducing high-yielding varieties of wheat were come with by massive applying chemical composts and pesticides. These developments was so massive that it was known as the Green Revolution (Hedden, 2003).

The conventional old wheat varieties were tall with very hard stems and leafy. The Green Revolution increased wheat productivity, mainly due to the introducing cereals dwarfing genes (Zhang et al., 2014). The dwarfing genes addition from the Japanese variety 'Norin 10' increased the yield, harvest rate, resistance to environmental stresses and had better response to fertilizers (Khush, 2001). In fact, the "Norin 10" dwarfing genes are present in the genomes of more than 70% of commercially cultivated industrial wheat types. 'Norin 10' has *Rht1* and *Rht2* (dwarfing genes), which are semi-dominant alleles on chromosomes 1B and 1D, respectively (Hedden, 2003). Each gene has similar effect on plant and its combined effect is improver. This derives that these genes act as transcription factors (TF) in gibberellin signalling. Gibberellin is a crucial endogenous regulator of plant (Hooley, 1994) and the alleles which control dwarf genes that decrease plant height and reduce reaction to gibberellin levels. These genes also have disadvantage such as reduce the length of the coleoptile which decreases the seedling growth rate and also population density (Allan, 1989).

Bread wheat, which makes up over 95% of all wheat farmed worldwide, is primarily used to produce whole and refined flour for a variety of flat and fermented breads as well as a wide range of bakery items. Pasta wheat, which is used to manufacture semolina (coarse flour), the main component of a variety of other baking items, makes up the majority of the remaining 5% (Dubcovsky & Dvorak, 2007). Numerous strategies

have been employed to meet the needs as a result of the widespread consumption of wheat and the significant effects of the growing global population. Making frozen dough goods is one of the options because they have a much longer shelf life. However, the gluten network undergoes structural changes as a result of freezing (Meziani et al., 2011). According to certain research, these differences mostly influence the antiparallel-sheet structures, helices, and turns, whereas the sheet contents are unaffected by the length of time that materials are kept frozen (Chen, et al., 2014; Xu, et al., 2014). Further research has led to the conclusion that protein structural alterations are mostly caused by protein aggregation, which in turn causes gluten quality to degrade (Zhao et al., 2017). Dough and bread quality are thus significantly influenced by decreased yeast viability, decreased bread volume, increased stiffness of the bread crumb, and mass weight loss brought on by freezing and temperature variations during storage (Phimolsiripol et al., 2008). To overcome this problem in frozen storage different compounds are often added to expand the quality of the frozen dough. For instance, the adding NaI in wheat dough leads to regulate the β -turns at the expense of intra and intermolecular β -sheets. This helps to reduce protein interactions and raise in water protein interactions and consequently improve the property of frozen dough (Loveday et al., 2012; Xu, et al., 2014).

1.1.3 Nutritional value

Wheat can provide a range of protein content depending on wheat genetic and fertilizer inputs. However, Pasta wheats have a higher protein content than the majority of other cereals, and they have an equally good or better distribution of the essential amino acids (Cauvain, 2012). In general, the protein contents of wheat can be vary between 9-18% of the grain weight (Shewry, 2009). For instance, wheat used to make high

volume loaf bread normally needs a 12% protein or higher level, wheat used to make cakes and biscuits should ideally have a protein concentration of 7% to 11%. Given that modern wheat grains are larger and heavier than traditional wheat grains, which results in a greater starchy endosperm and, in turn, lower protein levels, modern wheat may have lower protein contents. In fact the protein contents in einkorn are 15.5–22.8% and the amylose is 23.8%, however, the protein contents and amylose in bread wheat are 12.9–19.9% and 28.4%, respectively (Arzani & Ashraf, 2017). Wheat is an important source of vitamins, antioxidants, macro and micronutrients, phytochemicals, and other elements that are crucial for human health in addition to its primary components, proteins, carbs, and lipids.

1.2 Micronutrients malnutrition

In general, the world population relies on the cultivation of the edible grains wheat (*Triticum aestivum*), barley (*Hordeum vulgare*), maize (*Zea mays*), and rice (*Oryza sativa*) as staple foods. Whereas cereals provide a valuable source of energy, but they are found deficiency of nutrients. Zinc, iron, and manganese tend to be underrepresented in cereal grains (Cakmak, 2008b). These elements are known as micronutrients because they are needed in relatively less concentrations (5 to 100 mg / kg) in plant tissues (Alloway, 2008). Humans need more than twenty-two mineral elements which are provided in adequate quantities when taking a diverse and nutritionally balanced diet (White & Broadley, 2005) A main problem comes when people rely on food sources with inadequate micronutrient contents like cereal grains for their everyday diet intake. The FAO (Food and Agricultural Organization of the United Nations) has calculated that 35% of world populations obtain their daily diet from wheat (Alloway, 2008). The percentage of this population is likely to be higher in

low income countries especially in rural areas (Cakmak, 2008b). Micronutrient malnutrition is widely spread in areas where populations have less dietary diversity.

The WHO (World Health Organization) initially created the term 'hidden-hunger' to explain the effects of micronutrient deficiencies have on humans that are not clear to the naked eye immediately (Parr & Fjeld, 1994). Millions of people worldwide lack access to the necessary micronutrients that they need from their daily diet and the most affected populations are in the developing countries. Micronutrient shortcomings lead to increase vulnerability to various diseases, and some are mentioned in the **Table 1.1**. Eventually these diseases can cause severe issues, but the origin of the issue is frequently the deficiency of micronutrients in the daily diets. Zn, Fe and vitamin A deficiencies have been ranked as the 5th, 6th and 7th respectively the most important contributors to diseases in the developing countries (WHO, 2018). Micronutrient deficiency affects two billion people worldwide with insufficient use of Fe and Zn in daily diet (Beal et al., 2017). The WHO estimated that one out of three women in reproductive time are anaemic, that is commonly affected by Fe deficiency (WHO, 2018). A lack of zinc intake affects about 17% of the world's population, stunting growth and raising the risk of infant mortality (Wessells & Brown, 2012). These micronutrient shortages are commonly found in the developing countries (Middle East, South Asia and North Africa).

Table 1.1: Micronutrients essential for human, their function and effect of deficiency.

Micronutrients	Recommended nutrient intakes per day	Role in humans	Deficiency effects in humans	References
Zinc	7-9.5 mg	Essential component for enzymes, alleviates molecular structure and membrane transporters	Increased susceptibility to malaria pneumonia and diarrhoea, reduced immune system, stunting, delayed sexual and bone maturation, impaired neonatal development.	(Caulfield et al., 2004; Liping Huang, 2015)
Iron	8.7-15 mg	Oxygen carrier in blood cells, electron acceptor in many metabolic enzymes	Anaemia, impaired immune functions, reduced work capacity	(Joann M. McDermid, 2012)
Iodine	90-120 µg	Maintain thyroid hormone production and weight losses	Goiter, Intensified susceptibility of the thyroid gland	(Trumbo, 2013)
Selenium	60-75 µg	Thyroid hormone and production, component in selenoproteins with roles including stress, and defence against oxidative	Cardiomyopathy and Kashin-Beck (arthritis)	(Rayman, 2000)
Sodium	≤2000 mg	Maintain normal cellular homeostasis, regulation of	Diarrhea, vomiting, diabetic ketoacidosis,	(Pasquale Strazzullo, 2014; WHO, 2012)

		fluid and blood pressure, involve in the transport of nutrients	continuous gastric suction, lose electrolytes	
Boron	1–13 mg	Bone formation, maintenance, cardiovascular health (CVH), and neurological role	Oxidative and inflammatory stress, osteoporosis,	(Forrest H Nielsen, 2020; Nielsen & Meacham, 2011)
Manganese	>1.4 mg	Component of several enzymes required in metabolism, lipid, amino acid, protein and carbohydrate	Skeletal abnormalities, and impaired growth, Reproductive function, Interference of lipid and carbs metabolism	(Aschner & Aschner, 2005)
Copper	1.2 mg	Required for normal consumption of dietary iron Importance in bone, brain and blood cells development	Myelodysplastic syndrome, and bone abnormalities, anaemia,	(Collins & Klevay, 2011)
Fluoride	3-4 mg	Stimulate bone cell, prevent tooth decay and bones	Dental caries, osteoporosis	(Palmer & Gilbert, 2012)

1.3 Plant iron and zinc nutrition

1.3.1 Iron

Iron (Fe) is the most versatile elements in the Planet's crust. It is abundant and widely distributed, making up a significant portion of the Earth's outer layer. One of its key roles is in photosynthesis, where Fe-containing enzymes facilitate the synthesis of

chlorophyll, enabling plants to harness light energy and produce their food. Additionally, Fe plays a crucial part in the electron transport chain during respiration, generating the necessary energy for metabolic activities. In its uptake, transport, and chemical reaction inside plant cells, it mixes with other transition metals including zinc and copper (Rout & Sahoo, 2015). Iron deficiency is a frequent nutritional condition that affects numerous crop plants, reducing yields and the quality of the feed (McLean et al., 2009). Fe is exhibit in unsolvable forms as Fe (III) hydroxides, oxides and phosphates, and free iron levels are abundant. Therefore, mostly plants face Fe deficiency. Fe contents in cells usually vary between 50-250 µg / g of dry mass (Welch & Shuman, 1995). Since plants are main sources of iron for humans, Fe deficiency anaemia in humans is frequently linked to plants low bioavailability of Fe. (McLean et al., 2009). Bioavailability of Fe refers to the proportion of Fe from ingested food/supplements that the body can absorb and utilize effectively. As a result, boosting the Fe content of staple foods is seen to be a useful strategy for reducing human Fe shortage. Notably, effective soil fortification approaches require a thorough comprehension of Fe uptake in plants. The oxidation state of the minerals in the shared rhizosphere and the relative concentration of other metals affect the acquisition of Fe.

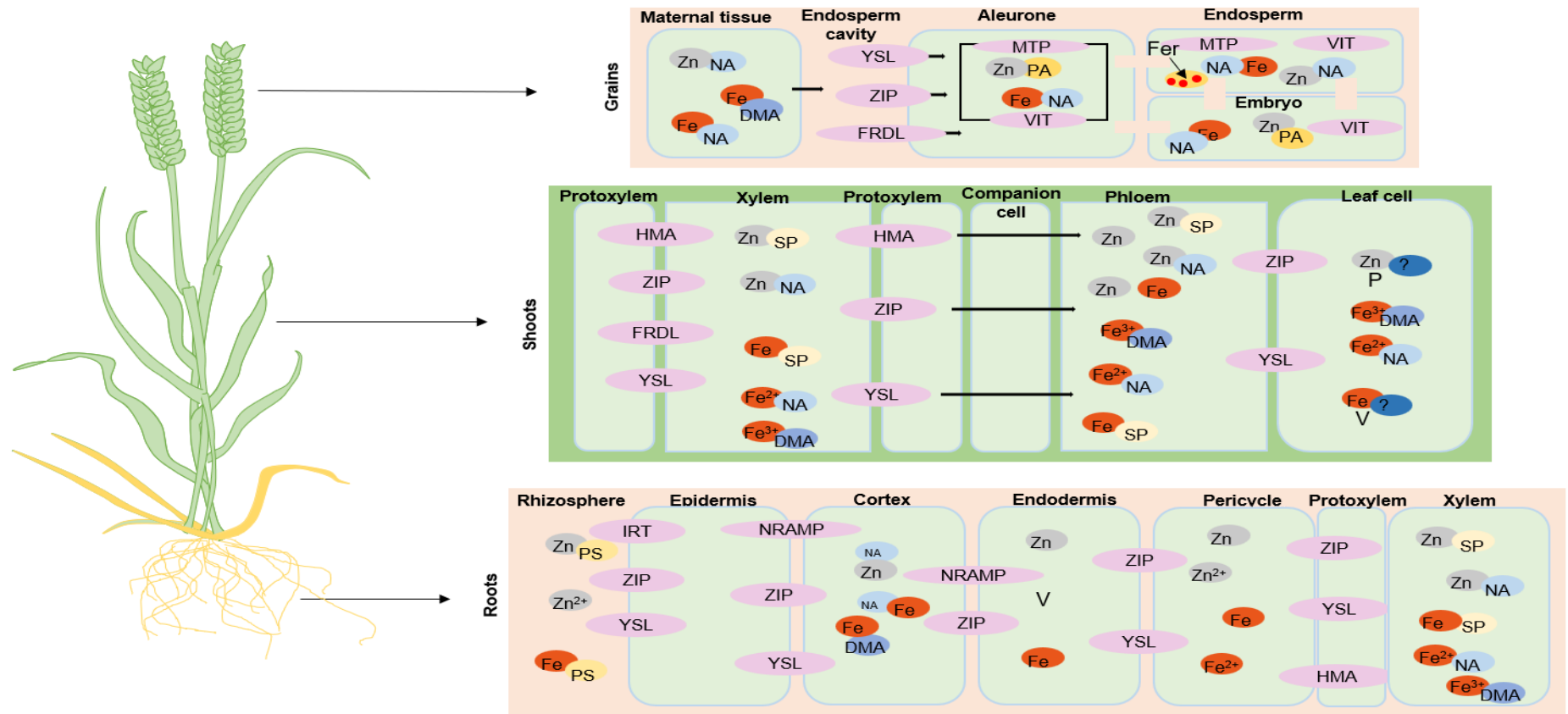


Figure 1.2: Basic pathway for iron and zinc distribution in wheat. Free Zn^{2+} and (PS) phytosiderophore-bound iron and zinc are absorbed from the soil into roots. Iron and zinc may be contained in vacuoles when travelling via the apoplast and symplast to the pericycle. The xylem carries iron and zinc before transferring it to the phloem. In order to transfer iron and zinc to the ear, they are remobilized from leaf cell plastids (P) and vacuoles (V). From the maternal tissue, iron and zinc are exported into the endosperm cavity. Most iron and zinc are stored in protein storage vacuoles bonded to phytic acid after uptake into the aleurone layer. Iron and zinc may enter the endosperm in trace amounts and are then stored as ferritin-bound amyloplasts. *ZIP*, *ZRT*-, *IRT*-like protein, *YSL*, *HMA*, major heavy metal-associated family, *YSL*, yellow stripe 1-like; *MTP*, metal tolerance protein, *FRDL*, ferric reductase defective like 1; *NRAMP*, natural resistance-associated macrophage protein, *VIT*, vacuolar iron transporter; *NA*, nicotianamine; *SP*, small proteins. Some of this information was taken from other grass species i.e., rice.

1.3.2 Zinc

Zinc (Zn) is important to the regular functioning, plant physiological paths and is essential for maintaining the structural and functional integrity of plant cellular membranes (Cakmak & Marschner, 1988). Zn functions in a variety of enzymes and regulatory proteins as a structural or catalytic cofactor. Numerous enzymes required in protein, DNA transcription, nucleic acid, carbs, and lipid metabolism benefit from zinc as a cofactor (Coleman, 1998; Hajiboland, 2012). Alcohol dehydrogenase, carbonic anhydrase, phospholipase, alkaline phosphatase, and RNA polymerase are just a few examples of the key Zn components found in plant enzymes. Zn is also involved in the reaction of other enzymes where it is not the main component (Hajiboland, 2012). Zn, unlike iron, is safe around sensitive biomolecules like DNA because it maintains a stable-redox state in cells once it has been absorbed. Zn is recognised as a key component of proteins involved in DNA and RNA synthesis, including transcription factors, reverse transcriptase, and phytohormone activity, because of its great propensity to form tetrahedral complexes (Cakmak & Marschner, 1986), fertility and seed production, photosynthesis (Sharma et al., 1990), as well as defence against disease. If Zn is not available in enough quantities to a plant, a decrease in development, yield and quality can occur (Randall & Bouma, 1973).

Zn is involved in three processes that are necessary to the making of photo-assimilates; (Ohki, 1976), carbonic anhydrase activity, chloroplast structure (Chen et al., 2008) and chlorophyll content (Hu & Sparks, 1991). Wheat has demonstrated the significance of Zn in photo-assimilate synthesis, with higher Zn levels leading to an increased final yield (Yilmaz et al., 1998). Zn has been demonstrated through experiments to be important for maintaining production when plants are under drought

stress (Bagci et al., 2007). Due to the widespread irregularity in rainfall across a large portion of the world's crop-growing regions, the drought resistance provided by elevated Zn levels in the plant is very significant for yield protection (Sadeghzadeh & Rengel, 2011). It is believed that Zn plays a role in preventing photooxidative loss caused by ROS (reactive oxygen species), which form inside the plant when there is dryness (Wenzel & Mehlhorn, 1995). Zn is a fundamental component of anti-oxidant enzymes like Zn superoxide dismutase that detoxify these ROS. Additionally, Zn is required for the synthesis of Zn-finger proteins, which act as transcription factors and activate a number of genes involved in the response to stress and drought (Davletova et al., 2005).

1.4 An outlook of iron and zinc uptake from soil to grains

Numerous studies have been published in order to comprehend the absorption and transfer of both zinc and iron from roots to grain in diploid plants including maize, barley, and rice. These pathways in wheat crops are not fully understood, however diploid crops can help anticipate the presence of Fe/Zn in wheat (Borrill et al., 2014). In this section, we will go over the main genes involved in iron and zinc transport as well as important steps wheat crops take to accumulate the elements from the roots to the grains.

1.4.1 Uptake and distribution

Iron and zinc are nutrients that are crucial for growth and development and delivered over a considerable distance in plants from roots to grains by xylem and phloem. The method referred to as the reduction strategy I, is used by the majority of non-grass plants and is classed in the model plant *Arabidopsis*. The H⁺ ATPase AHA2 in the rhizosphere releases protons in low iron conditions. The soil pH is lowered by the

released protons, which also increase Fe^{3+} solubility. Then, ABCG37 transporter-exported coumarin-family phenolics chelate soluble Fe^{3+} when it enters the apoplast (Mladěnka et al., 2010). With the help of high-affinity, *IRT1* (Iron-Regulated Transporter1) iron is transported into the root epidermal cells (Marschner, 1995). Strategy II occurs in grasses similarly used by different microbes like bacteria and also characterised as a chelation (Morrissey & Guerinot, 2009). This technique might have developed as a coping mechanism for alkaline soils where rhizosphere acidification is challenging to achieve. Its foundation is the manufacture and secretion of phytosiderophores (PS), which chelate Fe^{3+} and form the PS-Fe (III) complex in the rhizosphere (Figure 1.2). Then, *YSL* (Yellow Strip Like) gene family helps to transport into the root. The mass of PS produced and resistance to Fe deficient soils that are strongly correlated (Morrissey & Guerinot, 2009). Interestingly, graminaceous species for example rice has both strategies to optimize iron levels.

Metal-chelated forms of iron and zinc move in plants; nicotianamine (NA) and its derivative are carried in the phloem and are accelerated by *YSL2* (Deinlein et al., 2012; Ishimaru et al., 2010; Rellán-Álvarez et al., 2010). The transport of divalent metals is particularly important to biofortification, and the generation of *NA* requires enzymes that are mediated by *NAS*, which is employed as a substrate (Clemens et al., 2013; Connorton & Balk, 2019). In grasses, *NAAT* converts *NA* into *DMA*, and *DMA* makes it easier for roots and leaves to absorb iron (Banakar et al., 2017; Bashir et al., 2006). *YSLs*, *ZIPs* and *MTPs* are played their role for the transfer of Fe/Zn from xylem to phloem that happens in the roots, shoots, and throughout grain-fillings from leaves to grains (Borg et al., 2009; Borrill et al., 2014). Xylem is intermittent therefore all elements uptakes into grains via phloem in wheat plants (Zee and O'Brien, 1970).

Wheat grains aleurone layer that are displaced during milling has the highest concentrations of iron and zinc. Iron is stored in protein storage vacuoles in these organs and binds to phytate, which reduces its availability to people (Borg et al., 2009). Before entering at the stele for loading into the vascular, iron and zinc have to be outward transferred across various layers of root tissues such as epidermis, cortex and endodermis. Iron and zinc are combined in the symplast with chelators, to make Fe (II)–NA, Fe (II)–DMA, and Zn–NA complexes to improve transport efficiency. *YSL9* in rice and *MTP2* in Arabidopsis are heavily involved in this process (Senoura et al., 2017; Sinclair et al., 2018). Fe (III)-citrate is the predominant form of iron in the apoplast gap of the xylem, and the citrate transporters *FRD3* in Arabidopsis and *FRDL1* in rice plants are assumed to be crucial for iron loading into the pericycle cells (Durrett et al., 2007; Sinclair et al., 2018). *FPN1* in Arabidopsis also contributes to loading iron into the xylem (Morrissey et al., 2009). Members of the HMA family P1B-type ATPases, notably *HMA2* and *HMA9* in rice, mediate zinc loading into the xylem (Lee et al., 2007; Yamaji et al., 2013). In Arabidopsis, *MTP2* aids in the inward transport of zinc from the epidermis to the xylem across the root, and *HMA2* then supplies zinc to the apoplastic xylem (Sinclair et al., 2018). Moreover, *OsZIP4* is probably involved in phloem zinc load in rice (Ishimaru et al., 2005).

Iron and zinc can then be transported from the xylem to the phloem to undergo additional transport and remobilization to the sink tissues. Zinc is carried in both the form of free ions and metal chelates in the xylem, which has a pH range of between 5.0-6.5 (Yoneyama et al., 2015). Although the precise mechanisms governing the long-distance transportation of Fe/Zn from the xylem to the phloem are not fully understood, their remobilization at the source tissues via the phloem has been generally uncovered.

OPT3 (oligo peptide transporter) helps *Arabidopsis* regulate the movement of iron signals from shoots to roots and the redistribution of iron to growing organs through the phloem (Mendoza-Cózatl et al., 2014; Zhai et al., 2014). The predominant iron in rice chelates in the phloem are Fe(II)–NA and Fe(II)–DMA (Kyriacou et al., 2014). *YSL2* may be related to Fe(II)–NA translocation, through the phloem in rice (Ishimaru et al., 2010). *YSL18* and *YSL16* in rice plant are responsible for Fe (II)–DMA translocation through the phloem. *YSL9* transports both Fe(II)–NA and Fe(II)–DMA in the phloem of rice (Senoura et al., 2017). In graminaceous family, stem nodes are of significance as a hub for the distribution of zinc and also iron from xylem to phloem to different stem tissues. *OsZIP3*, *OsHMA2*, *OsHMA9*, and *YSL* are important for zinc from xylem to phloem and phloem to tissues and remobilization in rice (Lee et al., 2007; Sasaki et al., 2015; Yamaji et al., 2013).

1.4.2. Storage

Plants have two major methods for iron storage, one is confiscation into vacuoles and second into ferritin mostly in the shape of ferrous iron complexes (Connorton, Balk, et al., 2017). The total iron stored into vacuoles and ferritin varies among plant species (Zielińska-Dawidziak, 2015). In *Arabidopsis*, about 50% of the total iron is present into endodermal cells, however ferritin is deposited in seeds fewer than 5% (Ravet et al., 2009). On the other hand, seeds of legume species such as lentils, soybean and chickpea are full in ferritin. In the cereal crops such as wheat and rice, iron is mostly present in the seed-coat and also in vacuoles of alurone-layer. *YSL1* and *YSL3* helped to transport Fe–NA complexes into *Arabidopsis* seeds (Chu et al., 2010; Waters et al., 2007). The storage of iron in vacuoles is facilitated by vacuolar iron transporter (*VIT1*) transporter (Kim et al., 2006). *NRAMP3* and *4* help to transfer of iron from the vacuole

to the cytosol that is essential for germination (Segond et al., 2009; Thomine et al., 2003). Similarly, *VIT* gene family including *VIT1* and *VIT2* in rice grains play a vital role in iron appropriation into vacuoles (Zhang, Xu, et al., 2012) and Fe uptake from the vacuoles is facilitated by *NRAMPs* (Nevo & Nelson, 2006). In the alourone and sub-alourone layer of wheat grains, iron and zinc are assembled where they localize with P (phosphorus) in the shape of phytic acid. Some iron and zinc are also localized in starchy endosperm (Moore et al., 2012a). So, a possible way for wheat biofortification is to instantaneously (Raboy, 2001) increase iron and zinc levels and their bioavailability (Beasley, Bonneau, Sánchez-Palacios, et al., 2019).

1.5 Biofortification; A solution to fulfil the gap of micronutrient

In past years, scientists were worked on rising agricultural production. This was the reason behind malnourishment, and nutrient deficiencies. Now researchers are focussing towards nutrition rich and increase crop production by applying various approaches and managements including biofortification (Garg et al., 2018). Biofortification is applied to improve the nutrient value of cultivated crops. It is a technique to enhance the nutrition of cereal grains by agronomical and biotechnological methods. Biofortification is one of the possible approaches to overcome the malnutrition in the world.

1.5.1 Supplementation

In order to address micronutrient deficiencies, more direct methods like dietary supplementation, food fortification, and dietary diversity have been adopted (White & Broadley, 2005). Dietary supplementation entails giving a person a needed micronutrient in a pill form that is easily absorbed. Despite the fact that numerous clinical trials have demonstrated the effectiveness of direct nutrient supplementation,

many human factors still play a role in this strategy. Unfortunately, many of the major places where malnutrition is prevalent lack these. Many impacted locations lack the infrastructure to administer supplements in pharmaceutical form, and it's possible that there won't be enough ongoing funding to create and maintain such a plan (Timmer, 2003). Governments that are unstable are unlikely to allow for adequate distribution in their respective regions.

1.5.2 Food fortification

Food fortification is another strategy to address the vitamin shortages. It entails directly incorporating healthy elements into commonly consumed meals during processing to raise the concentration of a specific element. In the past, food augmentation initiatives for several micronutrients, particularly iron, have had considerable effectiveness (Hurrell, 1997). Since the 1970s, iron deficiency has steadily decreased in Sweden and America because to effective food fortification schemes implemented at the time (Cook et al., 1986). White bread, pasta, breakfast cereals, and newborn formula milk are all fortified with iron in several nations. Several bulk flour fortification initiatives with the inclusion of zinc are now in place (Brown et al., 2010). There is little information on these fortification projects' efficacy, however preliminary results from a Chinese programme to fortify cereals indicate that it is not very effective. when compared to similar women who weren't given the fortified flour, exposed women of reproductive age to the zinc-enriched flour saw statistically significant increases in zinc serum levels (Brown et al., 2010). While this achievement seems promising and food fortification are not as much effective in the low income countries especially in countryside. This can be due to poor infrastructure, such as roads and transportation, or a lack of availability of fortified foods in local markets. Fortified foods can be more expensive

than non-fortified foods, which can be a barrier for people in rural areas who may have limited financial resources (Tontisirin et al., 2002).

The ultimate solution is dietary diversification to overcome the micronutrient malnutrition. In the developed world, the diversification of nutritional intake to contain a diverse range of food groups to offer all required micronutrients is an effective strategy. However, this has very small chance of application to rural areas of developing countries where dependence on a few staple crops is high and therefore micronutrient deficiency rates are high. If pharmaceutical supplements or fortified flour cannot get the access in these areas then there is no hope of providing balanced foods with full of micronutrients such as dairy, meat and fish. In the existing state of world's development, not any of the above-mentioned approaches to improve worldwide nutrition. Researchers must discover other solutions such as agronomic and genomic biofortification.

1.5.3 Biofortification through agronomic approaches

The agronomical approach of biofortification is a technique used by researchers for several decades to address the micronutrient deficiencies. In that approach, the uses of Fe/Zn containing fertilizers have been applied. Agronomic biofortification is an easy method of increasing minerals availability in crops and soil microbes (Cakmak, 2008a). This method affects plant functions and improves productions. Agronomical approaches are being employed for different crops to increase the certain micronutrients (De-Valença et al., 2017). In 2008 worldwide programs known as Harvest Plus were conducted to improve the zinc levels in major Poaceous family such as wheat, rice and maize. There were various countries participating in this program, including China, Pakistan, Brazil, India and Thailand (Zhang, Sun, et al., 2012).

HarvestPlus had successfully bred and disseminated biofortified crop varieties with enhanced levels of zinc, iron, and other micronutrients. These improved crop varieties had been released to farmers, and their cultivation had spread to various countries. They introduced iron and zinc enhanced wheat in India, Pakistan, and Bangladesh. Similar to this, iron was applied topically to wheat and rice to increase their iron levels (De-Valença et al., 2017; Shahzad et al., 2014). Thus, applying agronomic biofortification, food crops can be improved with essential micronutrients such as iron and zinc, which improves nutrients in everyday diet to cope malnutrition.

Fertilisers are frequently used in agriculture to increase the crop's access to macronutrients including nitrogen, phosphorus, and potassium. Utilising these minerals promotes total plant growth in both the root and shoot, which improves the uptake of soil-available elements, including Zn (Sadeghzadeh & Rengel, 2011). Additionally, microelement fertilisers can be utilised as a handy method of supplying extra micronutrients that might not be easily accessible in the soil. Fertiliser applications could remedy a Zn shortage in the soil, assuring optimal yields and raising the zinc content of the edible grains. Fertilisers can be sprayed on a crop's soil or foliage. Zinc sources are utilised in $ZnSO_4$, $ZnCO_3$, $ZnCl_2$, ZnO , and $Zn(NO_3)_2$ fertilisers (Shuman, 1998). Zinc can be improved by adding fertilisers by coating it on granular compound fertiliser during manufacture, embedding it into granules during granule formation, or simply bulk combining zinc fertilisers in granular form. Depending on the stage of crop development (Ozturk et al., 2006), zinc application efficiency varies, site of the plants and the form in which zinc is integrated into fertiliser (Martens & Westermann, 1991). The cost-benefit assessments have demonstrated the potential macroeconomic advantage of applying zinc fertiliser; the costs of application are offset

by savings from decreased healthcare expenses and increased productivity (Kumssa et al., 2015).

Agronomic biofortification is necessary for temporary solutions, however for long term iron and zinc improved grains to the globe is questionable (Cakmak, 2008a). Every two to three years, the soil must be fertilised with zinc. Farmers in low income countries do not have the access to iron and zinc-enriched fertilisers because of financial/logistical limitations, which is an issue. If enhanced fertilisers are used year after year, there is even a chance that zinc toxicity will develop in the soil. The examination of long-term studies may offer the most convincing arguments against agronomic fortification as the best single strategy. Over the past 160 years the grain zinc levels have reduced, with the initiation of semi-dwarf elite varieties (Fan et al., 2008). Conversely, because of the zinc included in the higher rates of fertilisers being sprayed, the soil micronutrients have stayed stable. This decrease in grain zinc content is partly brought on by what is known as the "dilution effect" (Oury et al., 2006). Dilution effect is the decrease in micronutrient content of grain as a result of the larger grain size brought on by the use of cultivars with higher yields. Diluting impact of a rising grain yield does not entirely account for the declining grain zinc content seen in wheat. Plotting iron and zinc content trends against the year of cultivar registration revealed negative trends (Zhao et al., 2009). These micronutrient losses become more apparent after the introduction of semi-dwarf wheat cultivars. Researchers have hypothesised that the semi-dwarf phenotype probably directly affects the mineral status through either a diminished root system or a decreased ability to accumulate elements in the tissues before redistribution to the grain (Shewry et al., 2016). These findings demonstrate that the essential breeding techniques employed in the past to boost yield were done so at the

price of the concentration of micronutrients in the grain. It is obvious that agronomic methods of preserving soil zinc concentration will be required, but it is unlikely that they will result in the dramatic increase required to sustain the required improvement in grains. A more sophisticated and genetic approach is expected to be supplemented by agronomic biofortification techniques.

1.5.4 Biofortification through genetic approach

Genetic biofortification involves using genetic engineering techniques to enhance the nutrients of crops. This approach can be used to develop crops that are enriched in specific micronutrients, such as iron and zinc. Wheat germplasm varies genetically in terms of the amounts of iron and zinc in the grain. For instance, the range of grain zinc concentrations measured in bread wheats was 25.2 to 53.3 mg / kg in 132 samples (Graham et al., 1999). Wild wheat accessions gathered from the Fertile Crescent have also revealed a notable diversity. These were found to have grains with zinc contents ranging from 14 to 190 mg per kg (Cakmak et al., 2004). This cross-line adaptation demonstrates the ability to increase the zinc content of wheat grains through genetics rather than agronomic techniques.

A worldwide initiative HarvestPlus is established to increase iron and zinc content in various cereal crops. By 2006-7 the zinc with different genotypes have been applied to develop wheat cultivars with an 8 to 12 mg per kg increase in grain zinc contents through conventional approaches. Seven wheat varieties with grain zinc (33 mg/kg) concentrations above the baseline have been developed as a result of multi-location testing in target locations (Velu et al., 2016). One of these varieties, called "ZincShakthi," underwent extensive testing across multiple locations in India through the distribution of 1,000 mini-kit seed packets to farmers, and is now sold and made

available across the entire nation. (Tiwari et al., 2016). This will make it possible to evaluate how well these biofortified cultivars will work in practise to treat the micronutrient deficits that affect the entire population.

Multiple quantitative trait loci (QTLs) experiments have been shown the chromosomal region of genes that are involved to enhance grain Fe and Zn contents. The goal of an initial QTL analysis using wild emmer wheat (*Triticum diccocooides*) was to identify a locus controlling grain protein content. On chromosome 6B, a region known as *Gpc-B1* (Grain Protein Content B1) was shown to be a potential candidate (Distelfeld et al., 2007). This locus in ancestral wheat, which speeds up senescence and enhances nutrient remobilization from leaves to the early grains, encodes a NAC transcription factor that also raises iron and zinc levels (Distelfeld et al., 2007; Uauy et al., 2006). Using a DH (double haploid) population resulting from a hybrid between RAC875-2 and Cascades, another QTL analysis analysing grain zinc concentration found QTLs on 3D, 4B, 6B, and 7A and mapped well for grain Zn levels. (Genc et al., 2009). It may be possible to boost the micronutrient content of the grain by incorporating the genes underlying these loci into commercial wheat cultivars. It is evident that there are significant differences in grain iron and zinc levels both across and within ancient and contemporary wheat cultivars. There is less genetic variation in iron compared to zinc. This could be a potential limitation for iron, as it may be more difficult to breed for higher iron content in crops due to the limited genetic variation. On the other hand, there appears to be more genetic variation in zinc, which could make it easier to breed for higher zinc content in crops (Gorafi et al., 2018). The reasons why some cultivars partition more nutrients to the grain and are more effective at absorbing micronutrients than others are not well understood at the molecular level, though. Future cultivars with

higher grain nutrient contents may be bred using a more focused, genetic approach if the molecular mechanisms underlying these changes in grain Fe or Zn content were better understood. By filling in the knowledge gap about the controlling mechanisms that regulate grain nutrient contents, a complementing genetic solution for the production of crop types that are biofortified may be explored.

1.6 New genomic resources for biofortification

Biofortification have been considered since years and demonstrated challenging for biofortify cereals using traditional breeding programmes apart due to higher costs of calculating micronutrient concentration that required for a conventional phenotype approach. MAS (Marker-assisted selection) approach could be a lower-cost way to improve micronutrient concentration however, this method has been obstructed by the lack of wheat genome sequence, that was hard to assemble, because of the large size (16 Gb) of the wheat genome, and its extension repetitions (>85%) and polyploid in nature. It has been difficult without a genome sequence to plan genetic markers, to map locus regulating Fe/Zn contents or apply gene-targeted methods based on data from model plants. Current developments offer an opportunity in genomic resources to get control of these obstacles and increase the chances to develop biofortified wheat varieties (Figure 1.3). These resources include genome sequences, gene models, mutant resources, and gene expression atlases. These resources can be applied to biofortification, which involves developing crops with higher nutrient content. For example, genomic resources can be used to identify QTL and GWAS to accelerate genetic marker development. Additionally, having access to genome sequences and gene models facilitates biofortification techniques like transgenics, gene editing, or the usage of sequenced mutants.

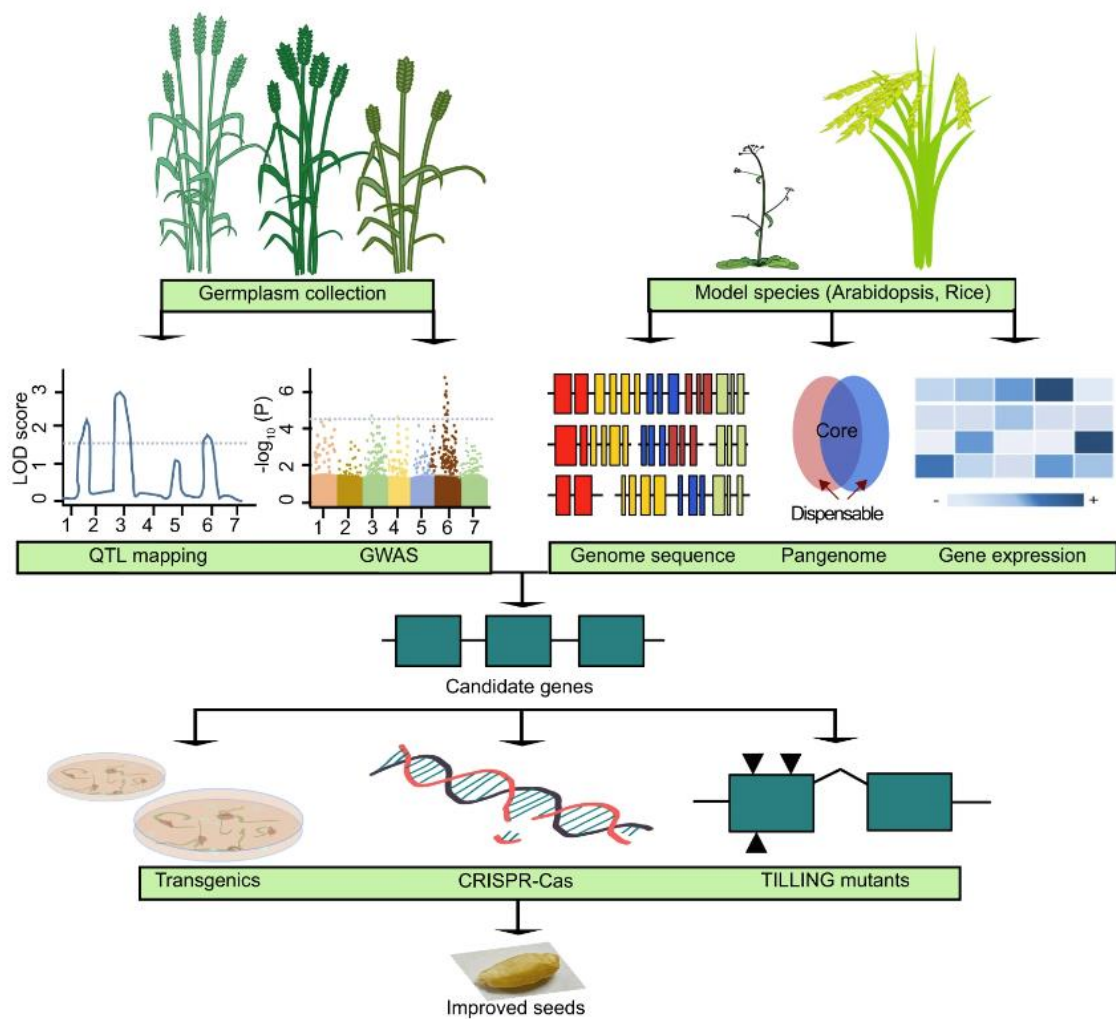


Figure 1.3: A visual depiction of iron and zinc biofortification using modern genomic resources. There are two ways to find potential biofortification candidate genes. It is possible to check germplasm collections for lines that have high iron and zinc. By utilising GWAS/QTL mapping to identify the genetic loci controlling iron and zinc content, new genome sequences will make it easier to find candidate genes within these loci. A second method finds orthologous candidate genes in the wheat genome using knowledge about gene function from model species. Candidate genes can be improved with the use of gene expression, sequencing, or presence/absence variation from pangenomes. Before being incorporated into breeding programmes, candidate genes can be confirmed using transgenic, CRISPR-Cas, or TILLING methods. This figure is from our published review article (Ali & Borrill, 2020).

1.5.1 Transgenic approaches

Many genes have been identified in rice and Arabidopsis that are involved in iron and zinc uptake, storage, and regulation. Ferric reductases, proton ATPases, and NA/DMA

synthases are crucial in the process of iron and zinc uptake, and the related candidate genes need to be validated and employed to increase plant iron and zinc contents. Numerous important transporters, including *FRD3*, *FPN1*, *ZIP* gene family, and the *YSL*, are primarily in charge of maintaining homeostasis for the translocation of iron and zinc.

White flour already contains more iron and zinc than whole-grain flour, but endosperm-expressed ferritin, *VIT*, and the *NRAMP* family genes could also be used to enhance iron and zinc content in white wheat (Connorton et al., 2017). Alternately, certain transcription factors (TFs) and other regulators of iron and zinc can also be thought of as potential candidate genes for biofortification, provided that they impose no yield penalty. Using a promoter unique to the endosperm, two ferritin genes (*Fer1/Fer2*), which encode Fe-binding proteins, were expressed in the transgenic method to improve iron concentration in wheat. This led to an elevated level grain iron, which was 50 to 85% greater than in WT plants in both crops (Borg et al., 2012). In a more recent study, when *TaVIT2* was produced via an endosperm-specific promoter, wheat flour's iron content doubled compared to control lines (Connorton et al., 2017). Due to a lack of genomic data for wheat, transgenic studies have been impeded. Though it is anticipated that transgenic research will play a big role in figuring out the activities of the genes that are involved in Fe/Zn transport in wheat given the accessibility of high-quality sequences and rising transformation efficiency.

1.5.2 Gene editing approach

Gene editing may be a more effective method than the transgenic strategy for predicting modifications to be made in targeted genes by switching off, producing functional alleles, substituting mutant alleles, and developing site-specific transgene

integration (Petolino et al., 2016). There are no reports of editing in iron- and zinc-related genes regardless of a range of efforts, including yield attributes and pre-harvesting sprouting resistance (Hao et al., 2020; Lin et al., 2020). Tools for gene editing, particularly the newly developed plant prime editing, allow for precise gene alteration, such as base substitution and base insertion/deletion. Thus, it offers potential for wheat iron and zinc biofortification (Li et al., 2020). Since *Gpc-B1* can be used as a starting view for candidate genes editing and because larger levels of iron and zinc have been found in grains, it may be possible to restore NAC predicted function by removing 1-bp from its exon in some wheat genotypes.

1.5.3 Genome selection approach

Transgenic and genes editing methods can be effectively and indeed increase essential grain iron and zinc contents but their applications are very limited due to public acceptance and government laws (Callaway, 2018). Genome selection could aid as a potential technique for iron and zinc biofortification except one significant factor affecting genomic selection accurateness is whether markers of candidate genes are incorporated in the model plants (Heffner et al., 2010). Genome selection, which has been employed extensively in wheat breeding schemes, is reliant on the legacy of a high Fe/Zn phenotype along with a specific genetic marker. It is possible to further corroborate the nearby relationship of markers for the genetic loci, regardless of whether marker trait associations result from large natural populations or from biparental hybrid populations. The confirmed molecular markers and, preferably, functional gene markers can then be utilised in MAB (marker-assisted breeding) for grains with high levels of iron and zinc. For example, *Gpc-B1* has been exploited for wheat grain iron and zinc enrichment following MAB. Remarkably the *Gpc-B1* showed

drastically higher iron and zinc contents (Tabbitta et al., 2017). The genomic selection uses genomically calculated breeding values created by all markers rather than including only relevant markers into a selection model in breeding. This can be done everywhere, even in non-target conditions, and it can speed up the breeding programme effectively and cheaply (Xu et al., 2017). Thus, a systematic effort in iron and zinc genes and marker development would not only accelerate the breeding for iron and zinc contents but also enhance accuracy of molecular techniques for future wheat development. In this thesis, we tried to understand the molecular mechanisms controlling iron and zinc contents in wheat grains using reverse and forward genetics approaches.

1.7 Thesis aims

The main objective of this research is to explore molecular mechanism of iron and zinc transportation into wheat grains. The specific objectives are:

1. To identify the *ZIP* gene family, present in wheat and its expressions
2. To determine the role of *TaZIP* in Fe and Zn transportation
3. To identify the genomic regions associated with Fe contents using bulk segregant analysis
4. To establish a computational method to quantify the Fe contents in wheat grains

Chapter 2: Identification of *ZIP* Genes and Their Functional Characterization in Wheat

2.1 Introduction

2.1.1 The *ZIP* gene family

Plants exhibit remarkable adaptability and resilience, enabling them to thrive in diverse environmental conditions. This ability is intricately linked to the complex molecular mechanisms operating within their cells. One group of genes that plays a crucial role in regulating various aspects of plant growth, development, and stress responses is the *ZIP* gene family. The *ZIP* (Zinc-regulated Transporter/Iron-Regulated Transporter-like Protein) gene family encodes a class of metal ion transporters that facilitate the uptake and distribution of essential metals, such as zinc, iron, and manganese, in plants (Bashir et al., 2012). Metal ions are vital for numerous physiological processes in plants, including photosynthesis, respiration, DNA replication, and enzyme catalysis. However, the availability of these essential metals can be limited in the soil, posing a challenge to plant's ability to acquire and utilize them efficiently (Ramesh et al., 2003). This is where the *ZIP* gene family steps in, acting as key players in metal homeostasis by facilitating the transport of metals across cellular membranes.

The *ZIP* gene family is characterized by a conserved domain called the *ZIP* domain, which forms a transmembrane structure responsible for metal ion transport. Members of this gene family have been identified in various plant species, including *Arabidopsis thaliana*, rice, maize, and soybean, indicating their evolutionary significance and widespread distribution across the plant kingdom (Guerinot, 2000). The *ZIP* transporters exhibit diverse expression patterns and are found in different plant tissues and organs, suggesting their involvement in distinct physiological processes. For instance, certain *ZIP* genes are predominantly expressed in the roots, where they play a crucial role in metal uptake from the soil. Others are expressed in aerial parts of the

plant, participating in metal transport within the plant and regulating metal distribution to different organs (Bouis & Saltzman, 2017; Li et al., 2013).

In addition to their role in metal transport, *ZIP* genes have been implicated in responses to abiotic and biotic stresses. Environmental challenges such as nutrient deficiencies, heavy metal toxicity, and pathogen attacks can disrupt metal homeostasis in plants (Quarshie et al., 2021). *ZIP* transporters contribute to the plant's defence mechanisms by modulating metal ion concentrations, thereby influencing stress tolerance and overall plant health (Moore et al., 2012b). Understanding the functions and regulatory mechanisms of the *ZIP* gene family is of great importance for unravelling the intricate interplay between metal homeostasis, plant growth, and stress responses (Guerinot, 2000). Studying *ZIP* genes provides valuable insights into plant adaptation strategies and offers potential avenues for enhancing crop productivity, nutrient biofortification, and stress resistance in agricultural systems.

2.1.2 Role of *ZIP* genes in model plants

The *ZIP* family plays a vital role in model species like *Arabidopsis thaliana* and rice. A total of 15 *ZIP* genes had been identified and characterized in *Arabidopsis*. These genes are part of the *ZIP* family and are involved in metal ion transport and homeostasis (Lee et al., 2021). *IRT1* is a *ZIP* family gene involved in iron uptake from the soil. It is highly expressed in roots under iron-deficient conditions and plays a crucial role in iron acquisition (Eng et al., 1998). *ZIP1* and *ZIP2* are zinc transporters in *Arabidopsis*. They are responsible for zinc uptake from the soil and are expressed in the roots. These genes are essential for maintaining zinc homeostasis in the plant (Lee et al., 2021). *ZIP3* and *ZIP4* are additional members of the *ZIP* family involved in zinc transport. They are expressed in different tissues, including roots, shoots,

reproductive organs, and play the role in zinc translocation within the plant (Assunção et al., 2010). *ZIP5* and *ZIP6* are copper transporters in Arabidopsis. They are involved in copper uptake from the soil and are expressed in the roots. These genes are critical for copper homeostasis in the plant (Wu et al., 2009). Similarly, several *ZIP* genes have been studied in rice for their roles in metal ion transport. *ZIP1* is a zinc transporter in rice that is involved in zinc uptake and translocation. It plays a crucial role in maintaining zinc homeostasis in the plant. *ZIP3* is a manganese transporter in rice. It is responsible for manganese uptake from the soil and its subsequent translocation within the plant (Ramesh et al., 2003). *ZIP4* is a zinc transporter that facilitates zinc uptake in rice. It is expressed in both roots and shoots and contributes to zinc homeostasis (Ishimaru et al., 2007). *ZIP5* is a member of the *ZIP* family involved in iron and zinc transport in rice. It participates in iron uptake from the soil and is expressed in roots (Lee et al., 2010). *ZIP8* is a manganese transporter in rice like Arabidopsis that plays a role in manganese uptake and translocation. It is expressed in both roots and shoots (Lee et al., 2010). Understanding the functions of the *ZIP* gene family in both Arabidopsis and rice provides valuable insights into the mechanisms underlying metal ion transport, homeostasis, and nutrient balance in these plants. The continued study of these genes enhances our understanding of plant nutrition, growth, and responses to environmental stresses.

2.1.3 Role of *ZIP* genes in wheat

Wheat (*Triticum aestivum*) is one of the most important cereal crops worldwide, serving as a staple food for a significant portion of the global population. As a critical source of calories, protein, and essential nutrients, ensuring the productivity and nutritional quality of wheat is of utmost importance (Peng et al., 2011). The efficient uptake,

distribution, and utilization of essential metals by wheat plants play a fundamental role in their growth, development, and stress responses (Li et al., 2019). In this context, the *ZIP* gene family has emerged as a key regulator of metal homeostasis in wheat, influencing its overall performance and adaptability.

The *ZIP* gene family in wheat consists of multiple members, each with specific functions and expression patterns. Several *ZIP* genes have been identified and characterized in wheat, including *TaZIP1*, *TaZIP3*, *TaZIP5*, *TaZIP7*, *TaZIP8*, and *TaZIP9*. These genes exhibit distinct tissue-specific expression patterns and respond to various developmental and environmental cues (Evens et al., 2017). In wheat, the *ZIP* genes are involved in the uptake of metals from the soil. For example, Yeast complementation of *TaIRT2*, *TaZIP13*, and *TaZIP14* showed that they have the ability to transport iron and zinc (Song 2021). It is hypothesized that they can facilitate the transport of these metals across the plasma membrane of root cells, allowing their entry into the plant's vascular system. Once absorbed by the roots, metals need to be translocated to different plant tissues for proper distribution. *TaZIP5* and *TaZIP7* are expressed in the vascular tissues and the authors hypothesized, these genes may involve in the long-distance transport of zinc and manganese, respectively (Evens et al., 2017). These transporters play a crucial role in ensuring the delivery of these metals to various aerial parts of the plant, including leaves, stems, and grains.

2.1.3 The importance of TILLING population

The creation and utilization of Targeting Induced Local Lesions IN Genomes (TILLING) populations have significantly contributed to advancing wheat research and breeding efforts (Irshad et al., 2020). TILLING populations are invaluable resources that enable the identification and characterization of novel genetic variations, providing a platform

for functional genomics studies and targeted crop improvement strategies (Rawat et al., 2012).

Wheat is a complex crop with a large genome, making traditional breeding methods time-consuming and challenging. TILLING populations offer a targeted and efficient approach to screen and identify specific mutations in the wheat genome. This technique involves the chemical induction of random mutations in a population of wheat plants, followed by screening for desired traits or genes of interest (Chen et al., 2012). By harnessing the power of mutagenesis and high-throughput DNA sequencing technologies, TILLING populations allow researchers to systematically explore the wheat genome for beneficial genetic variations. The importance of TILLING populations in wheat research lies in their ability to provide a comprehensive catalog of genetic diversity. This diversity serves as a valuable resource for studying gene function, deciphering molecular pathways, and identifying novel alleles associated with desirable traits (Rawat et al., 2012). Researchers can exploit TILLING populations to identify and characterize mutations in specific genes or genomic regions, revealing insights into gene structure, regulation, and functional significance.

Moreover, TILLING populations facilitate the discovery of non-GM variants and the development of novel genetic resources for wheat breeding programs. By screening TILLING populations for desired traits, such as disease resistance, abiotic stress tolerance, yield-related traits, or nutritional quality, researchers can identify rare mutations that confer advantageous phenotypes (Uauy et al., 2015). These mutations can then be utilized in breeding programs through traditional breeding approaches or by utilizing advanced genome editing techniques for precise genetic modifications. TILLING populations also contribute to accelerating the development of improved

wheat varieties with enhanced traits. The identified mutations can be combined through traditional breeding methods or gene stacking approaches to create elite wheat lines with multiple desirable traits (Sestili et al., 2019). This enables the production of new wheat varieties that exhibit improved productivity, quality, nutritional value, and resilience to biotic and abiotic stresses.

Additionally, TILLING populations provide a valuable tool for validating gene function and establishing gene-trait associations in wheat. By generating specific mutations in candidate genes and studying the resulting phenotypic changes, researchers can confirm the functional role of these genes and understand their contribution to specific traits or biological processes. This knowledge aids in elucidating the underlying molecular mechanisms governing important agronomic traits in wheat. The establishment and utilization of TILLING populations in wheat research have revolutionized our understanding of the wheat genome and its functional elements (Krasileva et al., 2017). These populations serve as invaluable resources for studying gene function, discovering novel alleles, accelerating breeding efforts, and improving wheat varieties. By leveraging the genetic diversity within TILLING populations, researchers and breeders can make significant strides towards developing more productive, sustainable, and resilient wheat cultivars to meet the growing global demand for this essential crop.

There is the lack of knowledge on the *ZIP* gene family of the worldwide important cereal crops like wheat. In this chapter, we selected TILLING mutant lines to characterise the *ZIP11*, *13*, and *14* genes in tetraploid wheat.

2.2 Aims

- Identify *ZIP* (zinc-regulated, iron-regulated transporter protein) family from the literature (from rice).
- Select TILLING mutants for *ZIP* family, and cross to generate double mutants in Kronos background.
- Characterise TILLING mutant lines (agronomic traits and micronutrients quantification).
- Determine the ability of *TaZIPs* to transport iron and zinc through heterologous expression of the *TaZIPs* in the mutant yeast strains.

2.3 Material and Methods

2.3.1 Nomenclature and expression of *ZIP* genes

In Evens and collaborators (2017) used TGAC gene IDs for nomenclature of *ZIP* gene family in wheat. By taking this article as a reference source for *ZIP* genes, we converted TGAC IDs into RefSeq v1.1 gene IDs to get the expression through wheat-expression (<http://www.wheat-expression.com>) and eFP browsers. We explored *ZIPs* in rice as a correct source for getting phylogenetic tree on Ensembl Plants (<https://plants.ensembl.org/index.html>) Figure 2.1. We named the wheat *ZIP* genes according to the most closely related rice *ZIP* genes on phylogenetic tree. We found 14 *ZIP* genes in wheat according to Evens and collaborators (2017) but found a few differences in the nomenclature of *ZIP5*, *8*, *9*, *13* and *16*. We renamed these genes according to rice *ZIPs* and phylogenetic tree. We downloaded the expression in various plant tissues (different stages of roots, shoots and leaves) of all *ZIPs* in rice and wheat

browser (<http://bar.utoronto.ca/>) (Ramírez-González et al., 2018; Wang et al., 2014; Winter et al., 2007) .



Figure 2.1: A phylogenetic tree of *ZIP1* in rice and wheat. The *TaZIP1* has three homoeologs A, B and D. This figure is generated on plant ensemble using rice genes for *ZIP1*. The red text shows the main gene ID for rice and green highlights show the homoeologs of wheat.

2.3.2 TILLING mutant selection

We selected TILLING mutants using Ensembl Plants with RefSeqv1.1 gene IDs (Figure 2.2-2.4). We downloaded variants using the "variant table" tab. The variant

table contains the same information as variant image (Figure 2.3) but in table format. By default, the variant table includes details about variation in the gene of interest from multiple different sources, but we can display TILLING mutations only by selecting “EMS-induced mutation” in the source filter at the top of the table (Figure 2.4a).

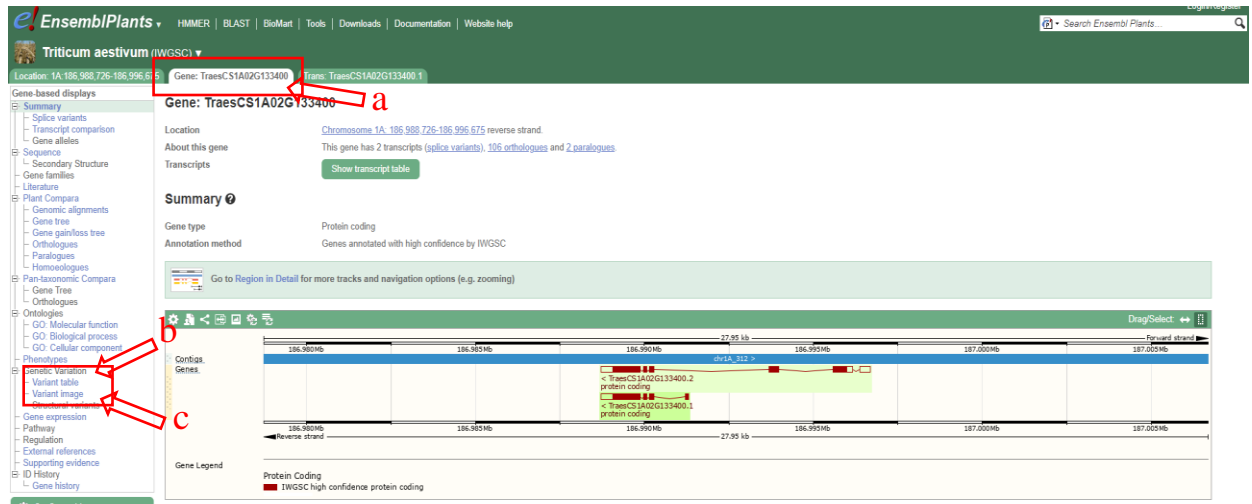


Figure 2.2: Plant Ensembl gene tab. To view the gene, click on Gene tab view (a), and TILLING mutants can be accessed using either the Variant table (b) or Variant image (c).

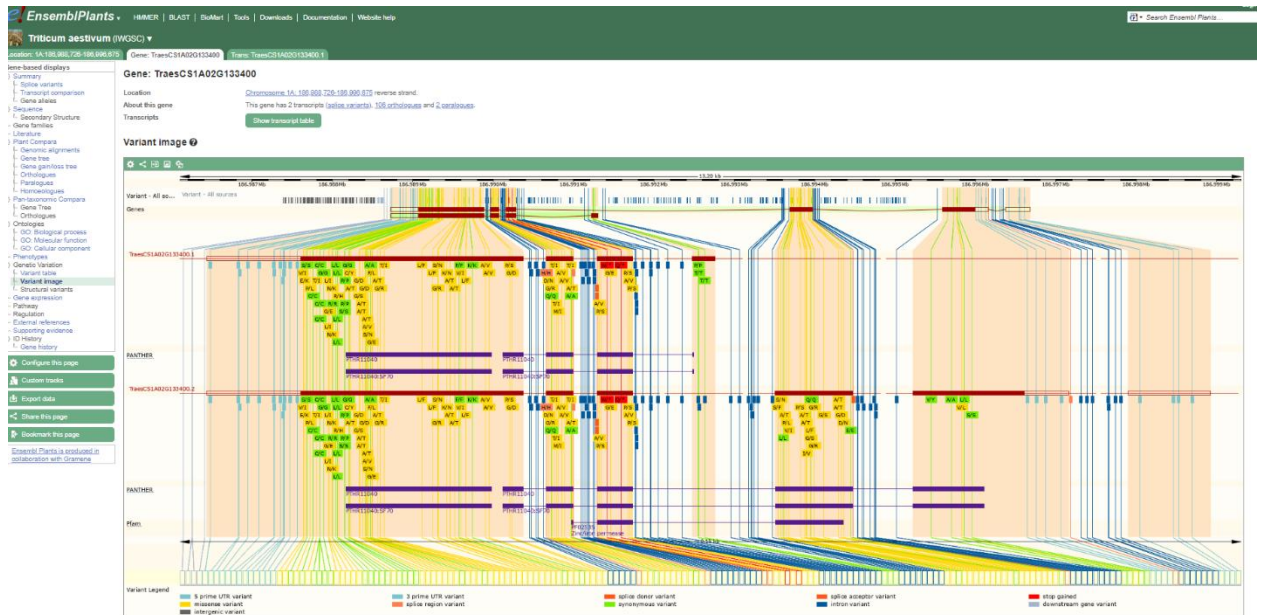


Figure 2.3: Plants Ensembl variant image.

Gene: TracesCS1A02G123400

Location: Chromosome 1A: 158,888,726-158,956,673 reverse strand

About this gene: This gene has 2 transcripts (sdpa.vacat5), 302 orthologues and 2 paralogs

Transcripts: [Show transcript table](#)

Variant table

Variant table

This table shows known variants for this gene. Use the 'Consequence' filter to view a subset of these.

Filter: SIFT-A Consequence: A Source: EMS-induced mutation Filter Other Columns

Variant ID	Chr. bp	Alleles	Class	Source	Evidence	Clin. Sig.	Conseq. Type	AA	AA coord	SIFT	Transcript
Celadon150 chr1A.18988971	1A:18988971	CT	SNP	EMS-induced mutation	-	-	3 prime UTR variant	-	-	-	TracesCS1A02G123400.1
Celadon151 chr1A.18988972	1A:18988972	CT	SNP	EMS-induced mutation	-	-	3 prime UTR variant	-	-	-	TracesCS1A02G123400.1
Celadon152 chr1A.18988973	1A:18988973	GTA	SNP	EMS-induced mutation	-	-	3 prime UTR variant	-	-	-	TracesCS1A02G123400.1
Celadon153 chr1A.18988974	1A:18988974	GTA	SNP	EMS-induced mutation	-	-	3 prime UTR variant	-	-	-	TracesCS1A02G123400.1
Celadon154 chr1A.18988975	1A:18988975	CT	SNP	EMS-induced mutation	-	-	missense variant	VII	373	B	TracesCS1A02G123400.1
Celadon155 chr1A.18988976	1A:18988976	CT	SNP	EMS-induced mutation	-	-	missense variant	EIK	371	B	TracesCS1A02G123400.1
Celadon156 chr1A.18988977	1A:18988977	GTA	SNP	EMS-induced mutation	-	-	missense variant	PL	364	B	TracesCS1A02G123400.1
Celadon157 chr1A.18988978	1A:18988978	GTA	SNP	EMS-induced mutation	-	-	synonymous variant	C	360	-	TracesCS1A02G123400.1
Celadon158 chr1A.18988979	1A:18988979	GTA	SNP	EMS-induced mutation	-	-	missense variant	TI	356	B	TracesCS1A02G123400.1
Celadon159 chr1A.18988980	1A:18988980	GTA	SNP	EMS-induced mutation	-	-	synonymous variant	C	352	-	TracesCS1A02G123400.1
Celadon160 chr1A.18988981	1A:18988981	CT	SNP	EMS-induced mutation	-	-	missense variant	GE	341	B	TracesCS1A02G123400.1
Celadon161 chr1A.18988982	1A:18988982	CT	SNP	EMS-induced mutation	-	-	synonymous variant	R	336	-	TracesCS1A02G123400.1
Celadon162 chr1A.18988983	1A:18988983	GTA	SNP	EMS-induced mutation	-	-	synonymous variant	L	331	-	TracesCS1A02G123400.1
Celadon163 chr1A.18988984	1A:18988984	GTA	SNP	EMS-induced mutation	-	-	synonymous variant	S	322	-	TracesCS1A02G123400.1
Celadon164 chr1A.18988985	1A:18988985	CT	SNP	EMS-induced mutation	-	-	synonymous variant	G	317	-	TracesCS1A02G123400.1
Celadon165 chr1A.18988986	1A:18988986	CT	SNP	EMS-induced mutation	-	-	missense variant	QY	316	B	TracesCS1A02G123400.1
Celadon166 chr1A.18988987	1A:18988987	CT	SNP	EMS-induced mutation	-	-	missense variant	AIT	315	B	TracesCS1A02G123400.1
Celadon167 chr1A.18988988	1A:18988988	CT	SNP	EMS-induced mutation	-	-	missense variant	GD	304	B	TracesCS1A02G123400.1
Celadon168 chr1A.18988989	1A:18988989	CT	SNP	EMS-induced mutation	-	-	missense variant	GS	304	B	TracesCS1A02G123400.1
Celadon169 chr1A.18988990	1A:18988990	CT	SNP	EMS-induced mutation	-	-	missense variant	AIT	301	B	TracesCS1A02G123400.1

Figure 2.4: Plants Ensembl variant table. The variant table will display information on variation by default in your gene of interest from a different source, but TILLING mutations can choose by selecting "EMS-induced mutation" in the source filter at the top of the table (a).

2.3.3 Primers design

The list of KASP (Kompetitive Allele Specific PCR) primers used for each of the TILLING lines used in this study is presented in Table 2.1. Where possible, KASP primers were designed using the PolyMarker tool (Ramirez-Gonzalez et al., 2015). In cases where suitable KASP markers could not be created automatically, we manually chose primer sets that guaranteed homoeolog and allele specificity. The HEX tail ("GAAGGTCGGAGTCAACGGATT") is present on all WT primers, whereas the FAM tail ("GAAGGTGACCAAGTTCATGCT") is present on all mutant (Mut) primers.

Table 2.1: KASP primers for *TaZIP* TILLING mutants.

Primer name	Sequence (5' - 3')	Comments
MA01_A	GAAGGTGACCAAGTTCATGCTggaagaacctctgcaataacaatC	TraesCS1A02G133400
MA01_B	GAAGGTCGGAGTCAACGGATTggaagaacctctgcaataacaatT	TraesCS1A02G133400
MA01_C	Tactggtttgctgcagggt	TraesCS1A02G133400
MA02_A	GAAGGTGACCAAGTTCATGCTctttgtgccgatgcatttC	TraesCS1A02G133400
MA02_B	GAAGGTCGGAGTCAACGGATTctttgtgccgatgcatttT	TraesCS1A02G133400
MA02_C	Cagaggctacttgagatggagtc	TraesCS1A02G133400
MA03_A	GAAGGTGACCAAGTTCATGCTggaagaacctctgcaataacaatcC	TraesCS1B02G150000
MA03_B	GAAGGTCGGAGTCAACGGATTggaagaacctctgcaataacaatcT	TraesCS1B02G150000
MA03_C	Tactggtttgctgcagggt	TraesCS1B02G150000
MA04_A	GAAGGTGACCAAGTTCATGCTcttctccatgttgctcaagaatC	TraesCS1B02G150001
MA04_B	GAAGGTCGGAGTCAACGGATTcttctccatgttgctcaagaatT	TraesCS1B02G150001
MA04_C	Gctcaggatgctagctgtgt	TraesCS1B02G150001
MA05_A	GAAGGTGACCAAGTTCATGCTctttgtacttattctgagctgcaG	TraesCS6A02G158700
MA05_B	GAAGGTCGGAGTCAACGGATTctttgtacttattctgagctgcaA	TraesCS6A02G158701
MA05_C	Cttcacggatccaagaaatacc	TraesCS6A02G158702
MA06_A	GAAGGTGACCAAGTTCATGCTgcacacaaCgcactcaactC	TraesCS6A02G158700
MA06_B	GAAGGTCGGAGTCAACGGATTgcacacaaCgcactcaactT	TraesCS6A02G158700

MA06_C	ctGcaagaaagatccaaccG	TraesCS6A02G158700
MA07_A	GAAGGTGACCAAGTTCATGCTGcaagaaagatccaaccCacG	TraesCS6B02G192600
MA07_B	GAAGGTCTGGAGTCAACGGATTGcaagaaagatccaaccCacA	TraesCS6B02G192600
MA07_C	tccattggcttcttgaaggcT	TraesCS6B02G192600
MA08_A	GAAGGTGACCAAGTTCATGCTtgcggtataacgaaaatgcaG	TraesCS6B02G192600
MA08_B	GAAGGTCTGGAGTCAACGGATTtgcggtataacgaaaatgcaA	TraesCS6B02G192601
MA08_C	tggtgcaatacatagctgcat	TraesCS6B02G192602
MA09_A	GAAGGTGACCAAGTTCATGCTcaccatcgctctcaGG	TraesCS3A02G120900
MA09_B	GAAGGTCTGGAGTCAACGGATTcaccatcgctctcaGA	TraesCS3A02G120900
MA09_C	gtgctAcgccacgAcacC	TraesCS3A02G120900
MA10_A	GAAGGTGACCAAGTTCATGCTtcagttgattttctgacaatgC	TraesCS3A02G120901
MA10_B	GAAGGTCTGGAGTCAACGGATTtcagttgattttctgacaatgT	TraesCS3A02G120901
MA10_C	ggctgtagttgaaaatttcaccA	TraesCS3A02G120901
MA11_A	GAAGGTGACCAAGTTCATGCTacgctaagcaactcAatgtgtG	TraesCS3B02G140400
MA11_B	GAAGGTCTGGAGTCAACGGATTacgctaagcaactcAatgtgtA	TraesCS3B02G140400
MA11_C	acgctaagcaactcAatgtgtA	TraesCS3B02G140400
MA12_A	GAAGGTGACCAAGTTCATGCTtgtgatcctaaaacggcttcC	TraesCS3B02G140400
MA12_B	GAAGGTCTGGAGTCAACGGATTtgtgatcctaaaacggcttcT	TraesCS3B02G140401
MA12_C	caatctacatactgactgccacata	TraesCS3B02G140402

2.3.4 Genotyping

In order to confirm the existence or absence of the anticipated ZIP mutations in the mutant and WT TILLING lines, respectively, KASP genotyping was used at all stages of the experiment. According to the instructions in (Pallotta et al., 2003), wheat leaf tissue was used to extract DNA for genotyping. In a 96-well plate (Fisher Scientific cat. no. AB0564), tissue samples (about 3 cm in length) were crushed in 500 mL of extraction buffer (0.1M Tris-HCl pH 7.5, 0.05 M EDTA pH 8.0, 1.25% SDS). Each sample received 250 μ L of 6 M ammonium acetate after the plates were cooled to room temperature following an hour at 65°C of incubation. The Eppendorf® 5810R, catalogue number 5810000017, was used to centrifuge the plates for 15 minutes at 4°C after cooling them for 15 minutes at 4°C. 250 μ L of ice-cold isopropanol was placed in each well of a fresh plate on which 600 μ L of the supernatant had been transferred. DNA precipitation was allowed to occur after the supernatant and isopropanol were combined and precipitated for five minutes. The DNA was then pelleted by centrifuging the plate for 15 minutes at 4000 rpm. The pellet was washed in 500 μ L of ethanol after the supernatant was removed, and it was then pelleted again (15 minutes, 4000 rpm). The DNA pellet was taken out of the supernatant, allowed to dry overnight, and then resuspended in 100 μ L of dH₂O. The primer assay mixtures for KASP genotyping contained 46 μ L of dH₂O, 30 μ L of the common primer (100 μ M), and 12 μ L of each tailed primer (100 μ M). Genotyping were performed using 384-well format with 2.5 μ L KASP-reaction volume consisting of 15 to 25 ng DNA, and 1.25 μ L PACE 2 \times Mastermix, 1.25 μ L dH₂O and 0.047 μ L primer assay mix. Using a thermocycler, KASP experiments were carried out. The cycling parameters were as follows: 15 min at 94°C, 10 cycles of 20 s at 94°C, 60 s at 65–57°C (decreasing by 0.8°C every cycle), followed

by 30-45 cycles of 20 s at 94°C, 60 s at 57°C. For several markers, the PCR cycle conditions needed to be optimised. A Pherastar plate reader was used to measure the fluorescence, and KlusterCaller software (version 4.1; LGC Genomics, UK) was used to evaluate the data.

2.3.5 Plant growth and phenotyping

2.3.5.1 *Germplasm development*

Kronos TILLING mutant lines which contained mutations in the *ZIP* genes were selected initially. The chosen TILLING lines seeds underwent pre-germination on wet filter paper for 48 hours at 4°C. Then, seeds were planted in P96 trays using a mixture of 85% fine peat and 15% horticultural grit. Individual seedlings were transplanted into 1 L round pots containing Petersfield Cereal Mix (Petersfield, Leicester, UK) when they had two to three leaves. These plants then backcrossed with Kronos WT to minimise the mutation in the glasshouse. After single backcross (BC₁F₂), we developed double mutants by crossing genome A mutant with genome B mutant and then selfing the progeny to obtain homozygous plants.

2.3.5.2 *Phenotypic characterisation*

After developing germplasm, these mutants were grown in standard control environment rooms, with 16:8 hours of light:dark cycles. At the seedling stage, they were genotyped to identify homozygous single and double mutants and WT lines. Before harvesting, we measured plant height and total number of tillers for each plant. We used Marvin to calculate the number of seeds, total weight and thousand grain weight (TGW)

2.3.6 ICP-OES analysis

After being dried at 60°C for 3 hours, the wheat grains were all coarsely pulverised in a coffee grinder before being processed into flour in a pestle and mortar. Three biological replicates and three technical replicates are included for each sample. Flour samples were first dried overnight at 55°C before being digested for one hour at 95°C in ultrapure nitric acid (55%, v/v) and hydrogen peroxide (6%, v/v). ICP-OES (Vista-PRO CCD Simultaneous ICP-OES; Agilent) was used to analyse the samples after diluting them 1:10 in ultrapure water and calibrating it with standards for Zn, Fe, Mn, P, Mg, and Ca. The reference material, soft winter wheat flour (RM 8438; U.S. National Institute of Standards and Technology), was examined concurrently with all experimental samples.

2.3.7 Transformation and expression of *TaZIPs* in yeast mutants

Coding DNA sequencing for *TaZIP11*, *TaZIP13* and *TaZIP14* were synthesised by Twist Bioscience and inserted into EcoR1 site of expression vector pYES2 (<https://www.thermofisher.com/order/catalog/product/V82520>) for *ZIP11* and *14* and Nco1 for *ZIP13*. The constructs were confirmed by sanger sequencing. The yeast *Saccharomyces cerevisiae* were provided by Rothamsted Research, West Common, Harpenden, Hertfordshire, UK. The following three strains were used in this study: wild-type DY1457 (MATa, ade1/+ can1, his3, leu2, trp1, ura3), *zrt1/zrt2* (DY1457 + *zrt1::LEU2*, *zrt2::HIS3*) and *fet3/fet4* (DY1457 + *fet3-2::HIS3*, *fet3-1::LEU2*). The constructs (pYES2*TaZIP*) were transformed into yeast cells (*zrt1/zrt2* and *fet3/fet4*) prepared with the instructions of Gietz and Schiestl 1995. Two wheat *ZIP* genes *ZIP6* and *ZIP7* already studied (Evens et al., 2017) were also transformed into yeast strains

as a positive control. The wild-type strain DY1457 was used as another positive control. The empty vector pYES2 was used as a negative control.

Following transformation, we confirmed pYES2TaZIP containing *zrt1/zrt2* colonies by PCR and inoculated in 10 ml of complete synthetic media -URA overnight at 30°C. Inoculums were centrifuged for 3 min and pellet suspended in complete synthetic media -URA. Then incubated for 4 h at 30°C to allow gene induction. Inoculums were pelleted and washed to remove excess Zn from the pellet. Inoculums were diluted to OD600 = 0.4 using complete synthetic media -URA minus Zn and serial dilutions (0.5, 0.1, 0.01 and 0.001) made. Seven microlitres of the dilutions plated onto complete synthetic media -URA plates containing either 200 µM ZnSO₄ (+Zn), 0 Zn + 0 mM, 2 mM, 5 mM and 7.5 mM EGTA, incubated at 30°C and photographed after 8 days.

Following transformation, colonies were confirmed using PCR and then inoculated in 10 mL complete synthetic media -URA + 10 µM FeCl₃ overnight at 30°C. Then inoculums pellet suspended in complete synthetic media -URA + 10 µM FeCl₃ and incubated for 4 h at 30°C to allow gene induction. Inoculums diluted to OD600 = 0.4 using complete synthetic media -URA + 10 µM FeCl₃ and serial dilutions (0.5, 0.1, 0.01 and 0.001) made. Seven microlitres of the dilutions plated onto complete synthetic media -URA with Fe supplemented with 0 µM, 0.74 µM or 10 µM FeCl₃, incubated at 30°C and photographed after 3 days.

2.3.8 Data visualization and statistic analysis

The heatmaps were made using R, principally with the ggplot2 (v 3.3.6) packages as well as pheatmap package. ANOVA was used for analysis of all data throughout this chapter. Following ANOVA, significant effects and interactions were investigated post-

hoc with Tukey HSD test at 5%. Microsoft Excel's (v 2019) built-in functions, including AVERAGE, MEDIAN, and STDEV were employed to calculate measures such as the mean, median, standard deviation, and frequency counts for agronomic traits and micronutrients.

2.4 Results

2.4.1 The nomenclature of *ZIP* family in wheat

The *ZIP* family proteins are essential membrane proteins that span numerous times through cellular membranes to produce channels or transporters that allow zinc and iron ions to pass more easily between membranes. We hypothesised that *ZIP* genes are essential for the transportation of zinc and iron in wheat. To investigate this hypothesis, we identified 14 *ZIP* genes in wheat based on orthologs of *ZIP* family known in rice.

Evens and collaborators (2017) used TGAC gene IDs for nomenclature of *ZIP* gene family in wheat. By taking this article as a reference source for *ZIP* genes, we converted TGAC IDs into RefSeq v1.1 gene IDs. Table 2.2 indicates the nomenclature used in this study as well as studied in Evens and collaborators (2017) and Tiong and collaboratore (2014) We explored ZIPs in rice as a correct source for getting phylogenetic tree on Ensembl Plants (<https://plants.ensembl.org/index.html>). We named the wheat *ZIP* genes according to the most closely related to rice *ZIP* genes on phylogenetic tree. Full homeolog complements were found for all these genes in each of the A, B and D genomes. Only one homeolog of each of the 11 wheat *ZIP* discovered by Tiong and collaboratore (2015) was described. We found 14 *ZIP* genes in wheat, consistent with Evens and collaborators (2017) but found a few differences in the nomenclature of *TaIRT5*, *TaZIP8*, *TaZIP9*, *TaZIP13* and *TaZIP16*. We renamed these

genes according to rice ZIPs and phylogenetic tree. We identified some extra genes in *TaIRT1*, *TaZIP2*, *TaZIP8*, *TaZIP9* and *TaZIP10* that were also closely related with rice orthologs. The wheat *ZIP* genes found and examined in this thesis (table 2.2) have the names of the wheat genes reported by Tiong and collaboratore (2015).

Table 2.2: Details of ZIP genes identification in wheat. Gene name shows nomenclature used throughout this thesis. RAP: Rice Annotation Project gene IDs.

Gene name	Gene IDs	Extra genes found in gene tree	TGAC gene ID	Accession no	Amino acid residues	Ref	Rice gene IDs (Tiong et al., 2014)	RAP ID
<i>TaIRT1</i>	TraesCS4A02G294300 TraesCS4B02G019300 TraesCS4D02G017600	TraesCS4A02G294200 TraesCS7D02G098100 TraesCS4A02G403300	4AL_TGACv1_290140_AA0982100 4BS_TGACv1_328611_AA1090980 4DS_TGACv1_361462_AA1168460		373	(Evens et al., 2017)	LOC_Os03g46470	Os03g0667500
<i>TaZIP1</i>	TraesCS3A02G527000 TraesCS3B02G595100 TraesCS3D02G532400		3AL_TGACv1_195235_AA0646850 3B_TGACv1_221732_AA0748740 3DL_TGACv1_250330_AA0866240	ABF55691.1	355	(Tiong et al., 2015)	LOC_Os01g74110	Os01g0972200 Os08g0533900 (orthlog)
<i>TaZIP2</i>	TraesCS6A02G099800 TraesCS6B02G128000 TraesCS6D02G082600	TraesCS5A02G256100	6AS_TGACv1_487184_AA1568790 6BS_TGACv1_513631_AA1646150 6DS_TGACv1_544682_AA1749140	CAJ19368.1	363		LOC_Os03g29850	Os03g0411800
<i>TaZIP3</i>	TraesCS2A02G424200 TraesCS2B02G443800 TraesCS2D02G422000		2AL_TGACv1_094530_AA0299310 2BL_TGACv1_129658_AA0391920 2DL_TGACv1_160080_AA0546500	AAW68439.1	360	(Tiong et al., 2015) (S. Li et al., 2019)	LOC_Os04g52310	Os04g0613000
<i>TaZIP4</i>	Missing						LOC_Os08g10630	Os08g0207500
<i>TaZIP5</i>	TraesCS4A02G025400 TraesCS4B02G278600 TraesCS4D02G277100 These gene IDs closed to ZIP9		4AS_TGACv1_306183_AA1003790 4BL_TGACv1_321083_AA1054990 4DL_TGACv1_342890_AA1124750		349	(Tiong et al., 2015)	LOC_Os05g39560	Os05g0472700
<i>ZIP5</i>	TraesCS1A02G297500 TraesCS1B02G306500 TraesCS1D02G293900							Os05g0472700
<i>TaZIP6</i>	TraesCS1A02G111000 TraesCS1B02G128800 TraesCS1D02G112500		1AS_TGACv1_019973_AA0073380 1BS_TGACv1_050073_AA0167090 1DS_TGACv1_082083_AA0263760	AK333945	395		LOC_Os05g07210	Os05g0164800
<i>TaZIP7</i>	TraesCS1A02G125500 TraesCS1B02G144500 TraesCS1D02G128000		1AS_TGACv1_018996_AA0057560 1BS_TGACv1_049369_AA0150920 T1DS_TGACv1_082535_AA0264750	ABF55692.1	386	(Tiong et al., 2015) (S. Li et al., 2019)	LOC_Os05g10940	Os05g0198400
<i>TaZIP8</i>	TraesCS1A02G297500 TraesCS1B02G306500 TraesCS1D02G293900 These gene IDs are closed to ZIP5		1AL_TGACv1_000915_AA0021780 1BL_TGACv1_030324_AA0086740 1DL_TGACv1_061188_AA0188250			(Evens et al., 2017)	LOC_Os07g12890	Os07g0232800

ZIP8	TraesCS2A02G505500 TraesCS2B02G533800 TraesCS2D02G506300	TraesCS2A02G143400 TraesCS2B02G168400 TraesCS2D02G146800 TraesCS2D02G506300 TraesCS6B02G201300						Os07g0232800
TaZIP9	TraesCS2A02G143400 TraesCS2B02G168400 TraesCS2D02G146800		2AS_TGACv1_112113_AA0330750 2BS_TGACv1_146518_AA0467340 2DS_TGACv1_177487_AA0578500				LOC_Os05g39540	Os05g0472400
ZIP9	TraesCS4A02G025400 TraesCS4B02G278600 TraesCS4D02G277100	TraesCS1A02G297400 TraesCS1B02G306400 TraesCS1D02G294000						Os05g0472400
TaZIP10	TraesCS7A02G361000 TraesCS7B02G266800 TraesCS7D02G362100	TraesCS7B02G321200 TraesCS7A02G420600 TraesCS7D02G413300 TraesCS7D02G412900 TraesCS7A02G420200 TraesCS7D02G413400	7AL_TGACv1_558847_AA1796430 7BL_TGACv1_577920_AA1886220 7DL_TGACv1_603327_AA1981040	AK334164	417	Tiong 2015	LOC_Os06g37010	Os06g0566300
TaZIP11	TraesCS1A02G133400 TraesCS1B02G150000 TraesCS1D02G124300		1AS_TGACv1_019215_AA0063260 1BS_TGACv1_049922_AA0164330 1DS_TGACv1_080155_AA0241650		577		LOC_Os05g25194	Os05g0316100
TaZIP13	TraesCS2A02G505500 TraesCS2B02G533800 TraesCS2D02G506300 These gene IDs are closed to ZIP8		2AL_TGACv1_098072_AA0325680 2BL_TGACv1_129838_AA0397670 2DL_TGACv1_159221_AA0534750	ABF55690.1	576		LOC_Os02g10230	Os02g0196000
ZIP13	TraesCS6A02G158700 TraesCS6B02G192600 TraesCS6D02G153800							Os02g0196000
TaZIP14	TraesCS3A02G120900 TraesCS3B02G140400 TraesCS3D02G123200		3AS_TGACv1_212290_AA0699680 3B_TGACv1_224841_AA0802240 3DS_TGACv1_273454_AA0931350	AK331623	497		LOC_Os08g36420	Os08g0467400
TaZIP16	TraesCS6A02G158700 TraesCS6B02G192600 TraesCS6D02G153800 These gene IDs are closed to ZIP13		6AS_TGACv1_485332_AA1543320 6BS_TGACv1_513963_AA1653060 6DS_TGACv1_542944_AA1733060		273		LOC_Os08g01030	Os08g0100200
ZIP16	TraesCS7A02G340000 TraesCS7B02G251700 TraesCS7D02G347700							Os08g0100200

2.4.2 The *ZIP* expressions in rice and wheat

We examined the expression of plant tissues (different stages of roots, shoots, and leaves) of all *ZIP*s in rice and wheat. We prioritised these genes on the expression levels of different roots, shoots and leaves stages. Based on expression level in rice, *OsZIP2*, *OsZIP6*, *OsZIP11*, *OsZIP13*, and *OsZIP14* showed the highest expression in different stages of roots, shoots, leaves, and grain (Figure 2.5). *OsIRT1*, and *OsZIP1* are highly expressed only in root tissues.

The expressions of 14 *ZIP* genes in wheat are shown in Figure 2.6. The genes *TaZIP11*, *TaZIP13*, and *TaZIP14* are highly expressed in most of the tissues. The expression pattern of *TaZIP2* is quite different from *TaZIP11*, *TaZIP13*, and *TaZIP14* and it is highly expressed in flag leaf. Most of the *ZIP* genes in rice and wheat are expressed and they are tissue specific in general. *TaZIP11*, *TaZIP13*, and *TaZIP14* showed almost same expression in rice and wheat in most of the tissues. In wheat, these genes only have 3 homoeologs and no closely related paralogs which makes them good candidates for a TILLING approach. Considering that *TaZIP11*, *TaZIP13*, and *TaZIP14* are highly expressed in both rice and wheat, we considered them strong candidate genes that may be involved in micronutrient transport in wheat.

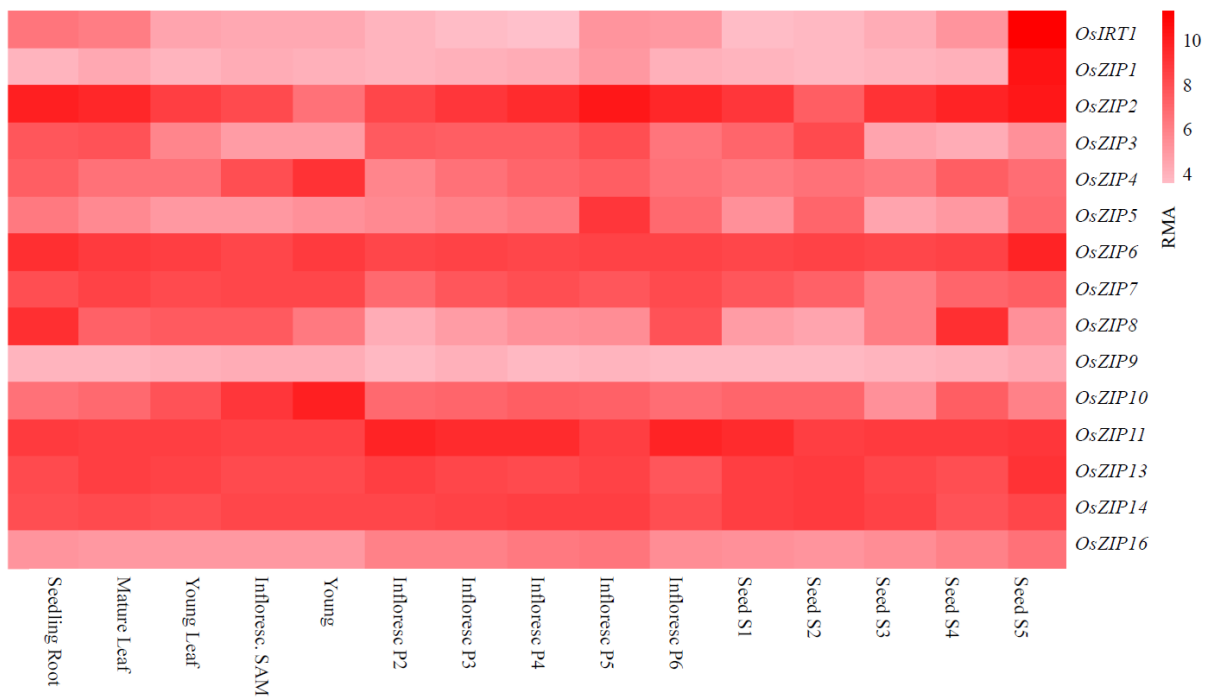


Figure 2.5: The expression level (RMA; Robust Multiarray Averaging) of *ZIP* genes in rice (data from Jain et al., 2007). X-axis shows the different plant tissue and y-axis shows rice *ZIP* genes. Red colour shows the highest expression. Raw data is taken from eFP browser (<http://bar.utoronto.ca>) and this figure generated on R using pheatmap package. S1; early globular embryo, S2; late globular embryo, S3; embryo morphogenesis, S4; embryo maturation, S5; dormancy and desiccation tolerance, P2 and P3; meiotic stage, P4; young microspore stage, P5; vacuolated pollen stage, P6; mature pollen stage, SAM; shoot apical meristem and rachis meristem.

We also investigated the expression of candidate genes in the grain tissues (Figure 2.7). The expression shows that the *TaZIP11* is highly expressed in seed coat, aleurone layer and grain compared to *TaZIP13* and *TaZIP14*. For further characterisation of these candidate genes, we selected TILLING mutant lines.

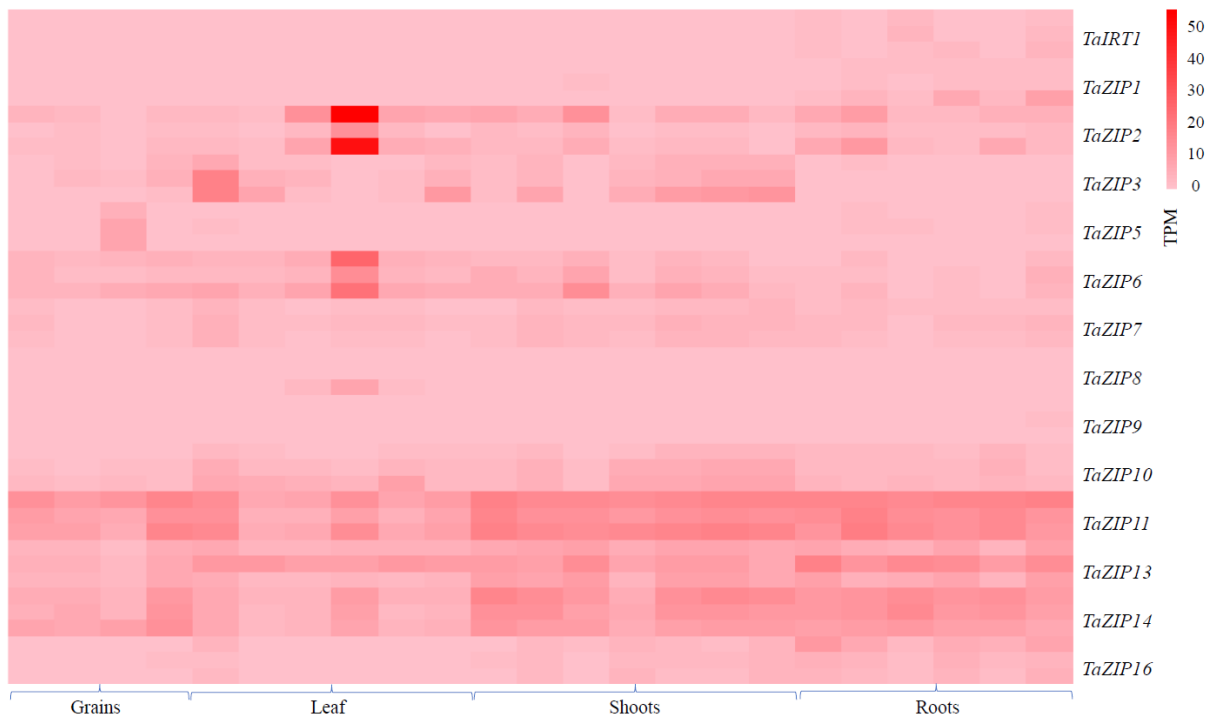


Figure 2.6: The expression (TPM) level of 14 *ZIP* genes in bread wheat. The major plant tissues (Different stages of roots, shoots, and grains) are included for comparing these 14 *ZIP* genes (Ramírez-González et al., 2018) and this figure generated on R using pheatmap package. Each gene shows the expressions of A, B and D genomes. TPM (Transcripts Per Million) is a normalization method for RNA-seq.

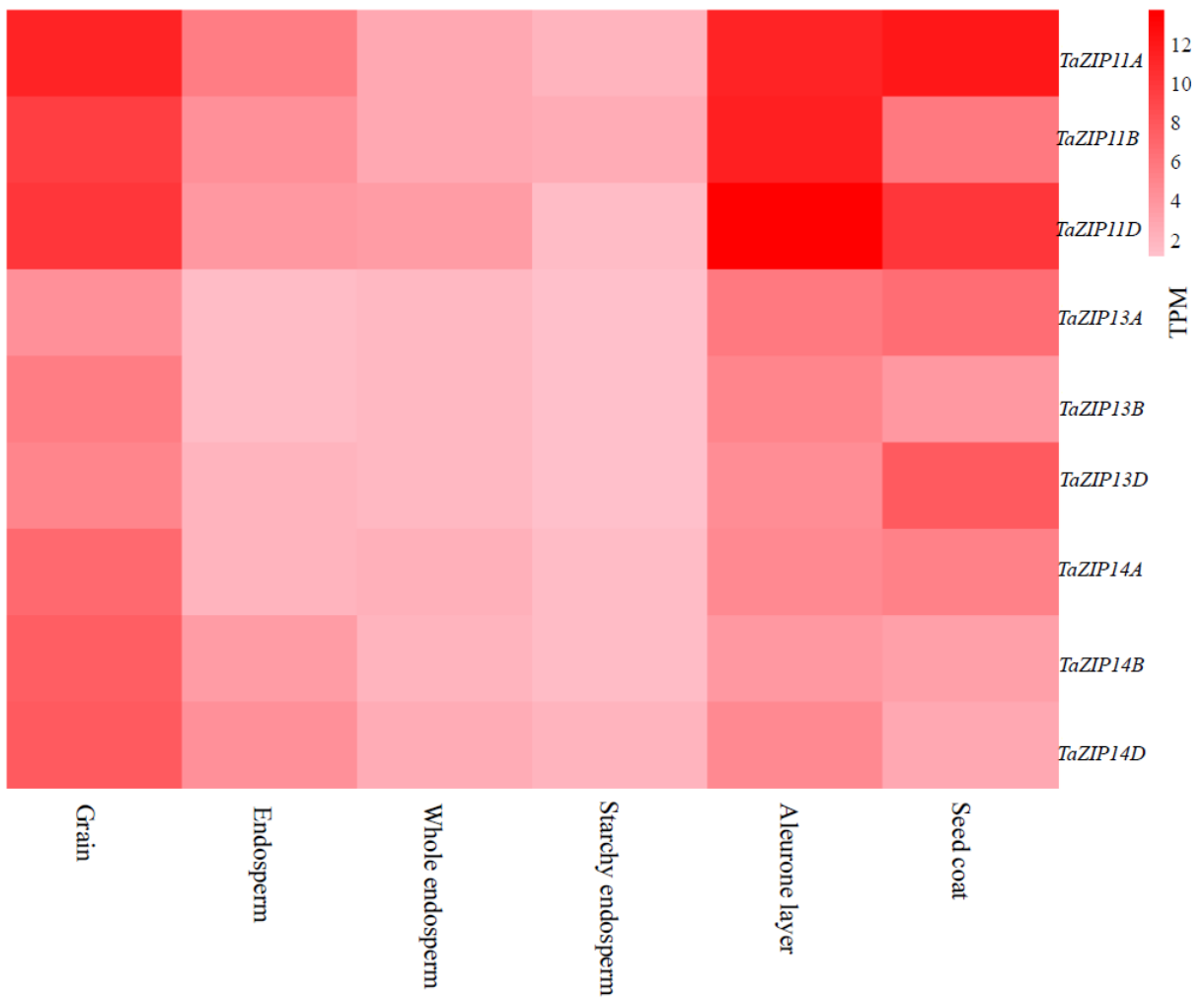


Figure 2.7: The specific grain tissue expression (TPM) level of candidate *ZIP* (*TaZIP11*, *TaZIP13*, and *TaZIP14*) genes in bread wheat with all three genomes A, B and D (Ramírez-González et al., 2018). The red colour shows the highest expression and blue for the lowest expression. TPM (Transcripts Per Million) is a normalization method for RNA-seq.

Table 2.3: Selected candidate genes to investigate the rule of these genes in Zn and Fe biofortification. Transcripts of wheat are selected using rice gene IDs on Ensembl Plants (<https://plants.ensembl.org/index.html>).

Gene name	RefSeq v1.1 gene IDs	Transcript IDs for wheat	Transcript IDs for rice
<i>TaZIP11</i>	TraesCS1A02G133400 TraesCS1B02G150000 TraesCS1D02G124300	TraesCS1A02G133400.2 TraesCS1B02G150000.2 TraesCS1D02G124300.1	Os05g0316100-02
<i>TaZIP13</i>	TraesCS6A02G158700 TraesCS6B02G192600 TraesCS6D02G153800	TraesCS6A02G158700.1 TraesCS6B02G192600.1 TraesCS6D02G153800.1	Os02g0196000-01
<i>TaZIP14</i>	TraesCS3A02G120900 TraesCS3B02G140400 TraesCS3D02G123200	TraesCS3A02G120900.3 TraesCS3B02G140400.2 TraesCS3D02G123200.1	Os08g0467400-03

2.4.3 Selecting Kronos TILLING mutants and generating double mutants

Most wheat genes have knock-out mutations, which are a priceless tool for characterizing gene functions. We used the plant ensembl website to identify the mutations present in *ZIP* genes in the Kronos population and checked the presence and effect of these mutations. We selected Kronos (tetraploid) population to investigate a complete knockout of the gene. Kronos population is faster to reach a complete knockout by crossing because it has two homoeologs (A and B). Initially, we selected four mutant lines for each candidate gene and documented variant IDs, position of the mutation, SNPs, class, consequence type, amino acid affect and zygosity. We then prioritised each line based on the mutation type (Table 2.4) and zygosity. We selected stop gained, splice acceptor variant, and missense variant of all candidate genes (Table 2.5) We ordered two Kronos mutant lines for each candidate gene. After getting the seeds, we grew these lines in the uniform condition and did a backcross. Then we crossed lines

mutated in genome A with lines mutated in genome B to generate double mutants (Figure 2.8). At the end, we got one cross for *TaZIP11* (K3178 X K0417) and two for *TaZIP13* (K0373 X K2425 and K2425 X K3714) and three for *TaZIP14* (K3269 X K4450, K3269 X K4275, and K3191 X K4275). We used these final mutant lines to functionally characterize the candidate genes.

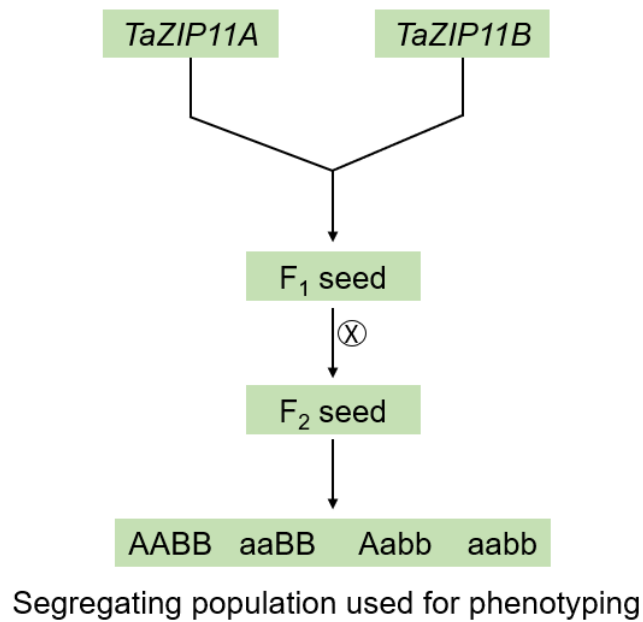


Figure 2.8: Crossing scheme to generate double mutants.

Table 2.4: Location and characterization of the TaZIP mutation. Details on the individual ZIP gene in Kronos population are provided.

Gene name/ RefSeq v1.1 gene IDs	Variant ID	SNPs	Consequence	AA	AA co- ord	Protein	Transcript	Zygoty	Ranking
<i>ZIP11-A/</i> TraesCS1A02G133400	Kronos3178.chr1A.186990190	C/T	stop gained	W/*	262	577aa	TraesCS1A02G133400.2	Homozygous	1 st
<i>ZIP11-A/</i> TraesCS1A02G133400	Kronos2402.chr1A.186990240	G/A	stop gained	Q/*	246	577aa	TraesCS1A02G133400.2	Heterozygous	2 nd
<i>ZIP11-A/</i> TraesCS1A02G133400	Kronos3588.chr1A.186993972	C/T	splice acceptor variant	-	-	577aa	TraesCS1A02G133400.2	Heterozygous	3 rd
<i>ZIP11-A/</i> TraesCS1A02G133400	Kronos2695.chr1A.186993830	C/T	missense variant	G/R	184	577aa	TraesCS1A02G133400.2	Heterozygous	4 th
<i>ZIP11-B/</i> TraesCS1B02G150000	Kronos417.chr1B.228171601	C/T	stop gained	W/*	262	577aa	TraesCS1B02G150000.2	Heterozygous	1 st
<i>ZIP11-B/</i> TraesCS1B02G150000	Kronos3214.chr1B.228175425	C/T	splice acceptor variant	-	-	577aa	TraesCS1B02G150000.2	Heterozygous	2 nd
<i>ZIP11-B/</i> TraesCS1B02G150000	Kronos890.chr1B.228175306	C/T	missense variant	G/D	176	577aa	TraesCS1B02G150000.2	Heterozygous	3 rd
<i>ZIP11-B/</i> TraesCS1B02G150000	Kronos3092.chr1B.228175312	C/T	missense variant	G/D	174	577aa	TraesCS1B02G150000.2	Heterozygous	4 th

<i>ZIP13-A/</i> TraesCS6A02G158700	Kronos2425.chr6A.150229234	G/A	splice acceptor variant	-	-	276aa	TraesCS6A02G158700.1	Heterozygous	1 st
<i>ZIP13-A/</i> TraesCS6A02G158700	Kronos3168.chr6A.150228734	C/T	missense variant	S/F	63	276aa	TraesCS6A02G158700.1	Heterozygous	2 nd
<i>ZIP13-A/</i> TraesCS6A02G158700	Kronos1232.chr6A.150231463	G/A	missense variant	G/D	193	276aa	TraesCS6A02G158700.1	Heterozygous	3 rd
<i>ZIP13-A/</i> TraesCS6A02G158700	Kronos364.chr6A.150229256	C/T	missense variant	P/L	137	276aa	TraesCS6A02G158700.1	Heterozygous	4 th
<i>ZIP13-B/</i> TraesCS6B02G192600	Kronos3714.chr6B.226870440	C/T	stop gained	W/*	72	277aa	TraesCS6B02G192600.1	Homozygous	1 st
<i>ZIP13-B/</i> TraesCS6B02G192600	Kronos373.chr6B.226869719	C/T	splice acceptor variant			277aa	TraesCS6B02G192600.1	Homozygous	2 nd
<i>ZIP13-B/</i> TraesCS6B02G192600	Kronos3878.chr6B.226870643	C/T	splice donor variant	-	-	277aa	TraesCS6B02G192600.1	Homozygous	3 rd
<i>ZIP13-B/</i> TraesCS6B02G192600	Kronos3173.chr6B.226870439	C/T	splice donor variant			277aa	TraesCS6B02G192600.1	Homozygous	4 th
<i>ZIP14-A/</i> TraesCS3A02G120900	Kronos3269.chr3A.95029821	C/T	stop gained	W/*	120	494aa	TraesCS3A02G120900.3	Homozygous	1 st
<i>ZIP14-A/</i> TraesCS3A02G120900	Kronos3191.chr3A.95018162	C/T	missense variant	G/R	483	494aa	TraesCS3A02G120900.3	Homozygous	2 nd

<i>ZIP14-A/</i> TraesCS3A02G120900	Kronos2803.chr3A.95022759	C/T	missense variant	G/E	369	494aa	TraesCS3A02G120900.3	Heterozygous	3 rd
<i>ZIP14-A/</i> TraesCS3A02G120900	Kronos4368.chr3A.95021496	C/T	missense variant	G/E	400	494aa	TraesCS3A02G120900.3	Heterozygous	4 th
<i>ZIP14-B/</i> TraesCS3B02G140400	Kronos4450.chr3B.126578372	G/A	stop gained	Q/*	476	494aa	TraesCS3B02G140400.2	Homozygous	1 st
<i>ZIP14-B/</i> TraesCS3B02G140400	Kronos4275.chr3B.126582174	C/T	splice acceptor variant	-	-	494aa	TraesCS3B02G140400.2	Homozygous	2 nd
<i>ZIP14-B/</i> TraesCS3B02G140400	Kronos3231.chr3B.126578351	C/T	missense variant	G/R	483	494aa	TraesCS3B02G140400.2	Heterozygous	3 rd
<i>ZIP14-B/</i> TraesCS3B02G140400	Kronos2712.chr3B.126580568	C/T	missense variant	G/E	426	494aa	TraesCS3B02G140400.2	Heterozygous	4 th

Table 2.5: TILLING lines used to characterise the *ZIP* genes for micronutrients and agronomic traits.

Gene name	Mutant line	Consequence	Preference
<i>ZIP11-A</i>	Kronos3178	stop gained	1 st
	Kronos2402	stop gained	2 nd
<i>ZIP11-B</i>	Kronos417	stop gained	1 st
	Kronos3214	splice acceptor variant	2 nd
<i>ZIP13-A</i>	Kronos2425	splice acceptor variant	1 st
	Kronos3168	missense variant	2 nd
<i>ZIP13-B</i>	Kronos3714	stop gained, splice region variant	1 st
	Kronos373	splice acceptor variant	2 nd
<i>ZIP14-A</i>	Kronos3269	stop gained	1 st
	Kronos3191	missense variant	2 nd
<i>ZIP14-B</i>	Kronos4450	stop gained	1 st
	Kronos4275	splice acceptor variant	2 nd

2.4.4 Agronomic traits of *TaZIP11*

2.4.4.1 Tiller numbers and plant height of *TaZIP11*

To investigate the phenotypic effects, we evaluated the single and double mutants of selected TILLING lines. We generated a double mutant of *TaZIP11* (K3178 X K0417) following single backcross. Number of tillers and plant height are shown in the Figure 2.9A and 2.9B respectively. It can be observed that KWT (Kronos wild type) has the highest number of tillers (8) and tallest plant height (73 cm). The AABB genotype has the second highest number of tillers, but A mutant has the second highest number of tillers. In terms of plant height, AABB has the second highest height (68 cm). Statistical analysis revealed a no significant difference in both the number of tillers and plant height between the KWT and mutants.

2.4.4.2 Grain numbers, total weight and thousand grain weight of *TaZIP11*

We also measured grain numbers, total dry weight and TGW. The KWT has the highest total number of grains with 136, followed by B mutant with 99 grains, A mutant with 77 grains, double mutant with 66 grains, and AABB with the lowest number of grains at 59 (Figure 2.9C, D, and E). The KWT also has the highest total weight with 6.9 g, followed by AAbb with 3.0 g, aaBB with 2.9 g, aabb with 2.5 g, and AABB with the lowest total weight at 2.4 g. There is no significant difference in grain number and total weight.

The thousand-grain weight (TGW) is an important agronomic trait that influences crop yield and quality. In this study, we also evaluated the TGW of KWT, single and double mutants. In terms of TGW, the KWT has the highest value with 60.2, followed by AABB with 42.6, aabb with 37.7, and AAbb with the lowest TGW at 30.9. There is significant

difference between KWT and mutants ($p < 0.05$, one-way ANOVA with post-hoc Tukey HSD) and no significance difference in single and double mutants.

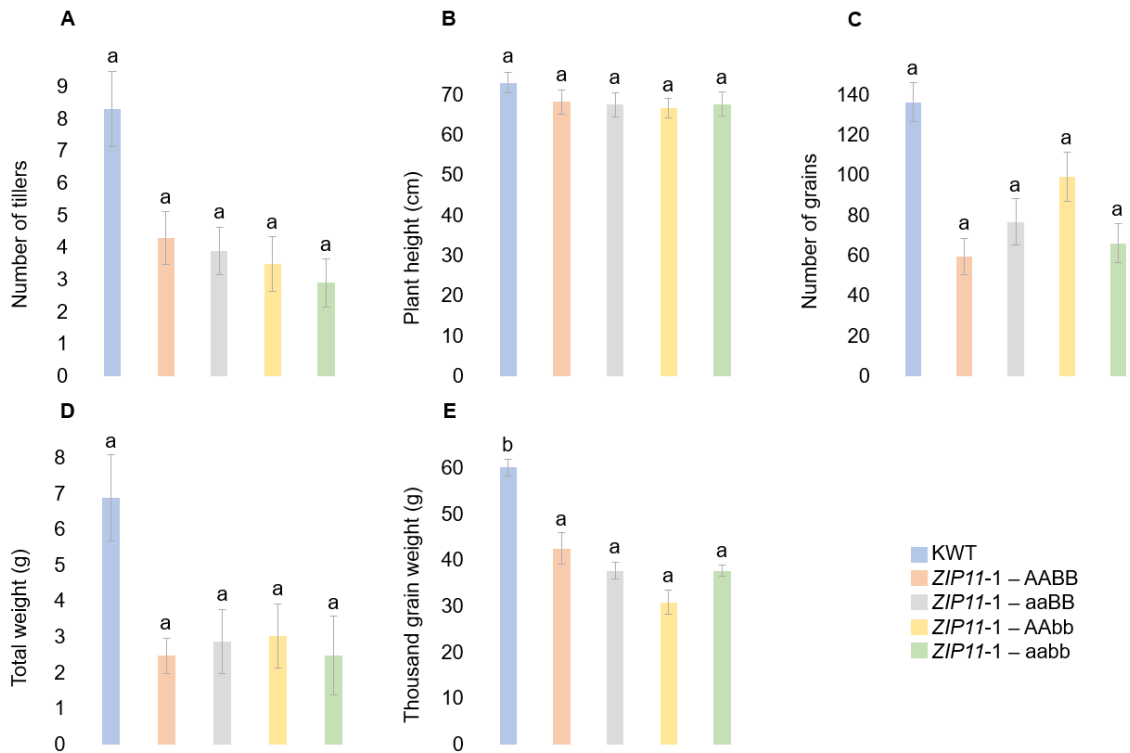


Figure 2.9: Agronomic traits for *TaZIP11-1* (K3178 X K0417). (A) Number of tillers per plant, (B) Plant height, (C) Number of grains, (D) Total weight and (E) Thousand grain weight. Error bars represent standard error of the mean, n=10. Lower case letters indicate statistically significant differences ($p < 0.05$, one-way ANOVA with post-hoc Tukey HSD).

2.4.5 Agronomic traits of *TaZIP13*:

2.4.5.1 Tiller numbers and plant height of *TaZIP13*

We got two double mutant lines after a single backcross for *TaZIP13*. The tiller numbers for *TaZIP13-1* (K0373 X K2425) are shown in Figure 2.10A. The KWT consistently produced the highest number of tillers. The mutants produced lower numbers of tillers than KWT. However, the differences in mean tiller numbers between the lower-tiller genotypes are generally small, and in all cases, the differences are not statistically significant.

Comparing the plant height data between the *TaZIP13-1*, we observe that there is no statistically significance difference in the mean plant heights for each genotype (Figure 2.10B). Similarly, *TaZIP13-2* (K2425 X K3714) also has the same trend in number of tillers and plant height. The overall trend is similar for most of the genotypes, with some minor differences.

2.4.5.2 Grain numbers, total weight and thousand grain weight of *TaZIP13*

The grain numbers, total weight and TGW are also investigated in the two different *TaZIP13* crosses (Figure 2.10-2.11C, D, and E). The KWT genotype produce 136 grains. For the AABB genotype, there is a reduction in grain yield from 97 to 68 grains. For the A mutant, there is also a reduction in grain yield from first cross (107 grains) to second cross (75 grains). For the B mutant, there is a moderate reduction in grain yield from first cross (111.8 grains) to second cross (97 grains). Similarly, double mutant also has a reduction in grain yield. Overall, these results suggest that there are no significant differences in the number of grains produced by different genotypes in the *TaZIP13-1* and *TaZIP13-2*.

In the *TaZIP13-1*, the KWT has the highest total weight of 6.9 g, which are higher than the total weight of all other genotypes (Figure 2.10D). The AABB and AAbb genotypes have similar total weights of 5.2 g and 5.7 g, respectively, while the single mutants have the lowest total weights of 4.6 g and 4.7 g, respectively. These differences in total weight among the genotypes are not statistically significant ($p < 0.05$, one-way ANOVA with post-hoc Tukey HSD). In the *TaZIP13-2*, the B mutant has a higher total weight of 5.3 g and double mutant has the lowest total weight of 2.6 g Like *TaZIP11*, there is no significance difference in number of grains and total weight in both *TaZIP13-1* and *TaZIP13-2*.

The TGW is also measured for *TaZIP13-1* and *TaZIP13-2*. In the *TaZIP13-1*, the KWT has the highest TGW of 60.2 g, while the A mutant has the lowest TGW of 42.3 g (Figure 2.10E). The AABB and AAbb genotypes have intermediate TGW values of 56.1 g and 44.6 g, respectively, while the double mutant has a TGW of 49.9 g. The differences in TGW among the genotypes are statistically significant ($p < 0.05$, one-way ANOVA with post-hoc Tukey HSD).

In *TaZIP13-2*, the results are different from the first cross. The AABB and A mutant have almost the same TGW (Figure 2.11E). The B mutant and double mutant has TGW values of 56.11 g and 45.22 g, respectively. The differences in TGW among the KWT and genotypes are statistically significant ($p < 0.05$).

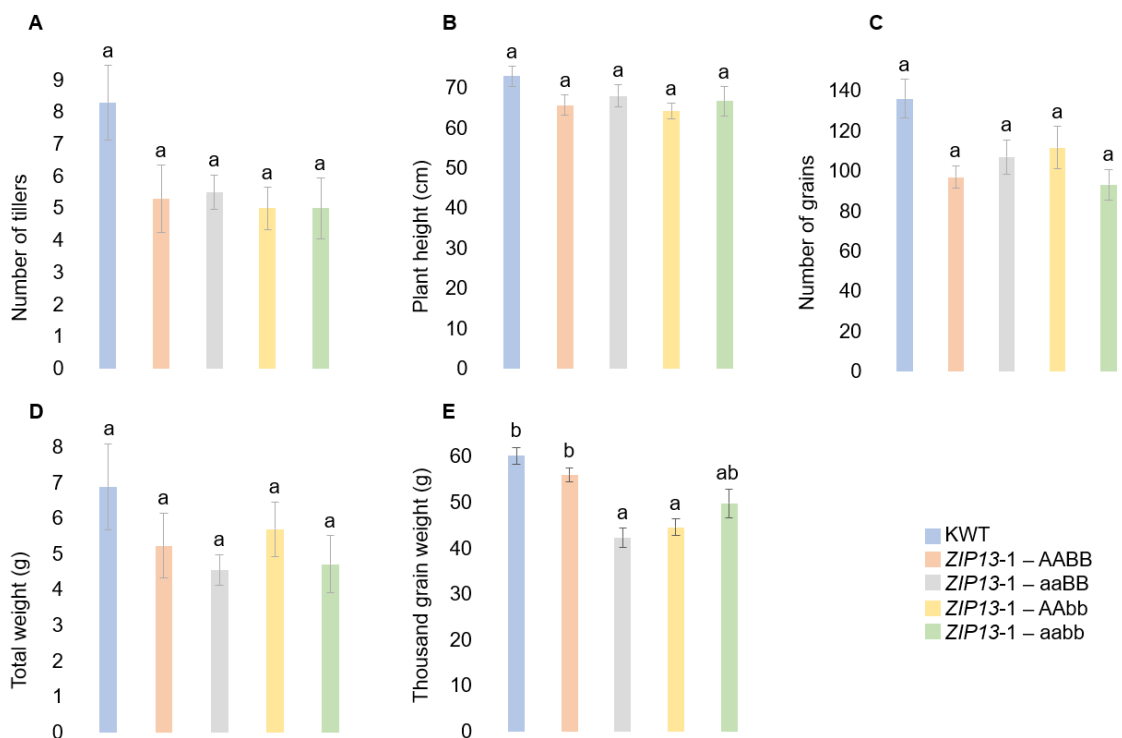


Figure 2.10: Agronomic traits for *TaZIP13-1* (K0373 X K2425). (A) Number of tillers per plant, (B) Plant height, (C) Number of grains, (D) Total weight and (E) Thousand grain weight. Error bars represent standard error of the mean, $n=10$. Lower case letters indicate statistically significant differences ($p < 0.05$, one-way ANOVA with post-hoc Tukey HSD).

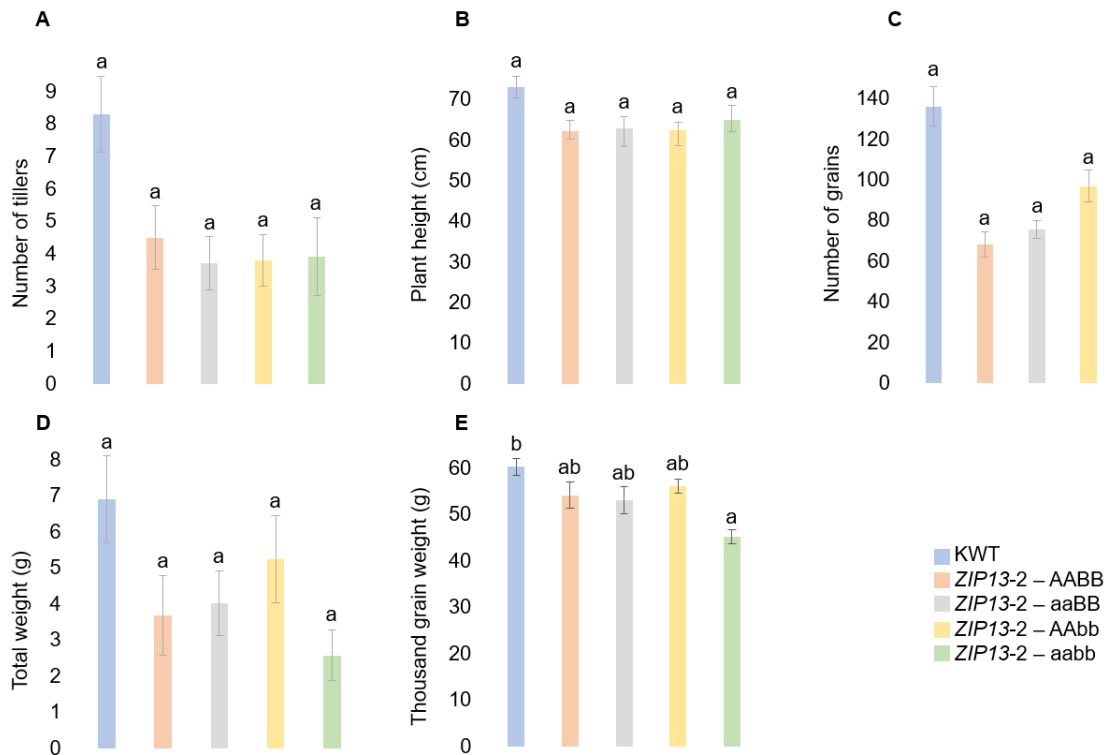


Figure 2.11: Agronomic traits for *TaZIP13-2* (K2425 X K3714). (A) Number of tillers per plant, (B) Plant height, (C) Number of grains, (D) Total weight and (E) Thousand grain weight. Error bars represent standard error of the mean, n=10. Lower case letters indicate statistically significant differences ($p < 0.05$, one-way ANOVA with post-hoc Tukey HSD).

2.4.6 Agronomic traits of *TaZIP14*

2.4.6.1 Tillers numbers and plant height of *TaZIP14*

We crossed all possible mutant's lines to generate the double mutants and successfully, we got three double mutant's combinations (K3269 X K4450, K3269 X K4275, and K3191 X K4275) for *TaZIP14* (Figure 2.12, 2.13 and 2.14). K3269 and K4450 have stop gained mutations, while K3191 and K4275 have missense variant and splice acceptor variant respectively. Unfortunately, there were no significant differences in tiller numbers and plant height in *TaZIP14* lines.

2.4.6.2 Grain numbers, total weight and thousand grain weight of *TaZIP14*

The total number of grains for different genotypes in three different *TaZIP14* crossed are shown in Figure 2.12C, 2.13C, and 2.14C. There were no significant differences in total grain number and total weight in all three *TaZIP14* lines. The results show that the TGW of the genotypes varied significantly between KWT and mutants in all *TaZIP14-1*, *TaZIP14-2*, and *TaZIP14-3*. In *TaZIP14-1*, the TGW of KWT and AABB, ranging from 60.23 g to 61.03 g and has a significance difference compared to single and double mutants ($p < 0.05$, one-way ANOVA with post-hoc Tukey HSD). However, in *TaZIP14-2*, the TGW of AABB, and single mutants are significantly lower than the KWT. There was not a consistent difference of TGW between AABB, single and double mutants. Therefore, these results indicate that *TaZIP14* does not affect TGW.

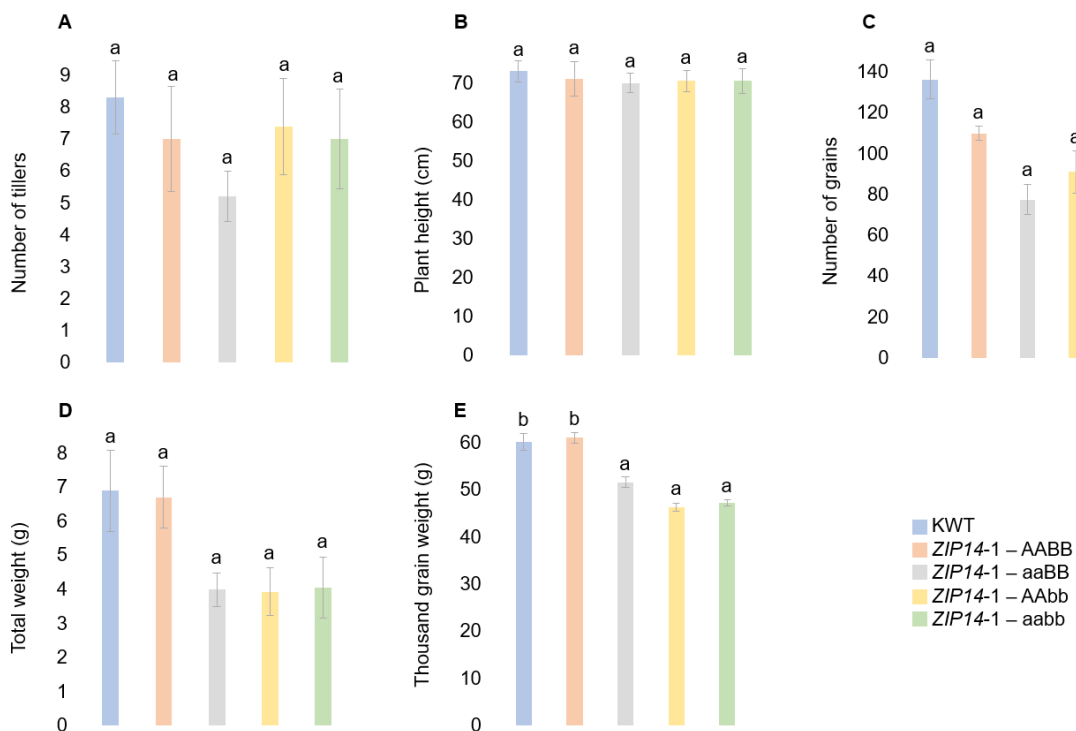


Figure 2.12: Agronomic traits for *TaZIP14-1* (K3269 X K4450). (A) Number of tillers per plant, (B) Plant height, (C) Number of grains, (D) Total weight and (E) Thousand grain weight. Error bars represent standard error of the mean, $n=10$. Lower case letters indicate statistically significant differences ($p < 0.05$, one-way ANOVA with post-hoc Tukey HSD).

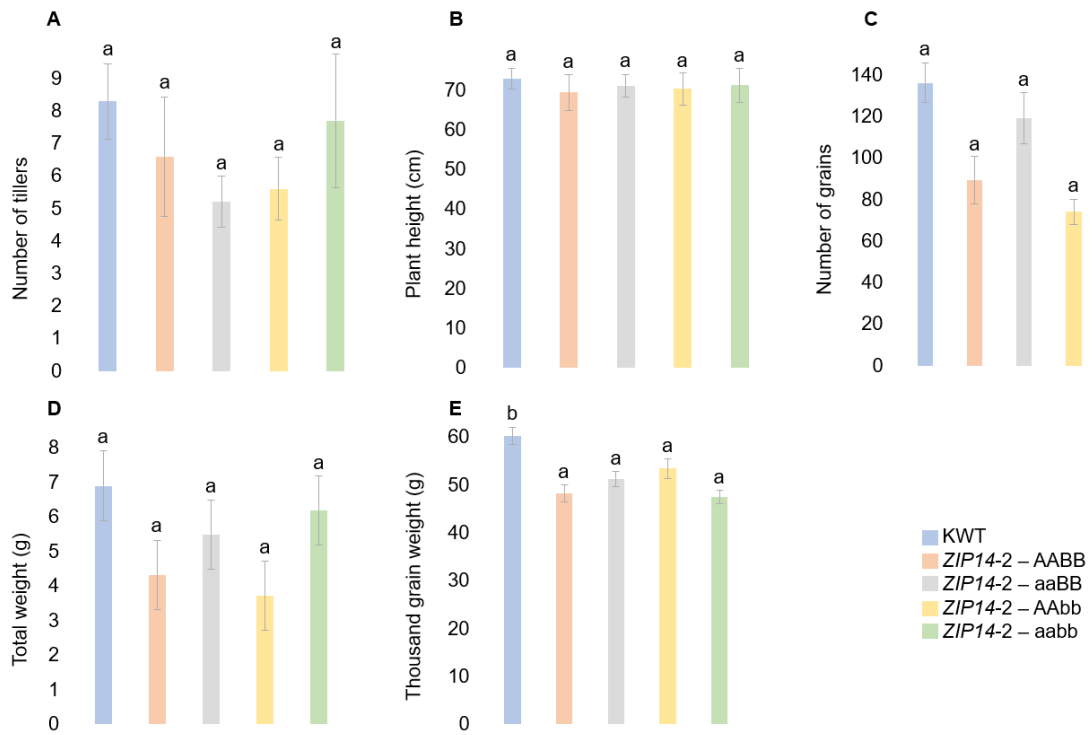


Figure 2.13: Agronomic traits for *TaZIP14-2* (K3269 X K4275). (A) Number of tillers per plant, (B) Plant height, (C) Number of grains, (D) Total weight and (E) Thousand grain weight. Error bars represent standard error of the mean, n=10. Lower case letters indicate statistically significant differences ($p < 0.05$, one-way ANOVA with post-hoc Tukey HSD).

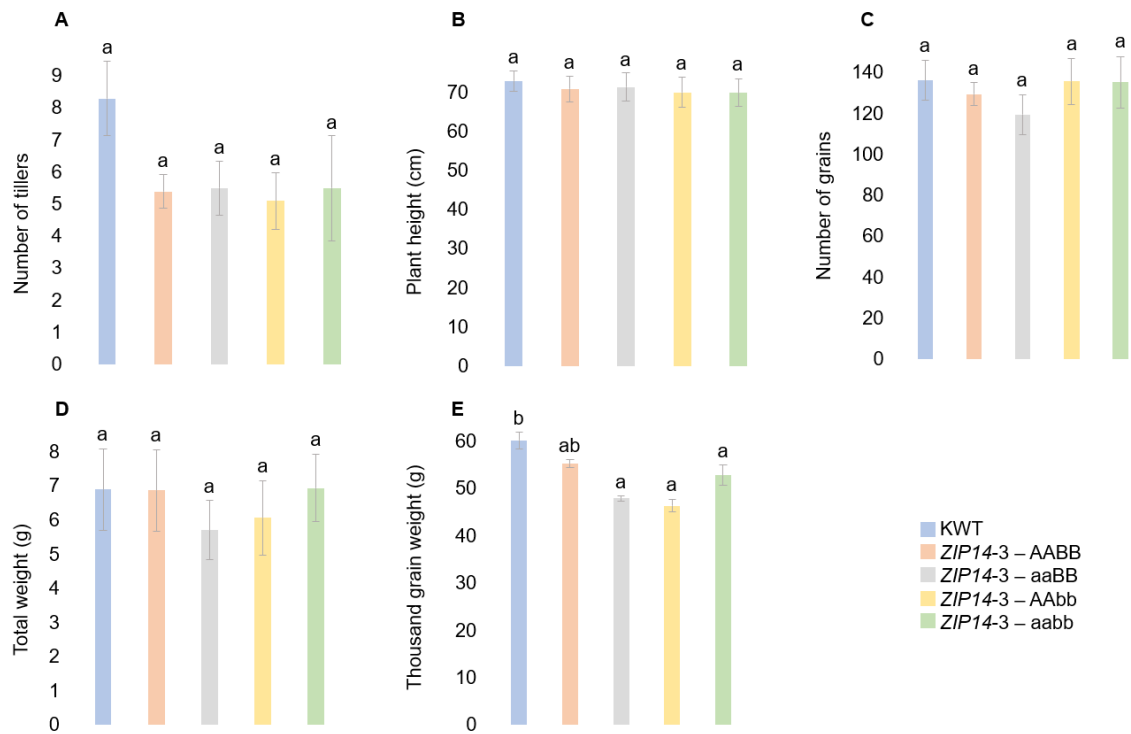


Figure 2.14: Agronomic traits for *TaZIP14-3* (K3191 X K4275) (A) Number of tillers per plant, (B) Plant height, (C) Number of grains, (D) Total weight and (E) Thousand grain weight. Error bars represent standard error of the mean, n=10. Lower case letters indicate statistically significant differences ($p < 0.05$, one-way ANOVA with post-hoc Tukey HSD).

2.4.7 Micronutrient quantification

The micronutrients of wholemeal flour of grains were analysed using ICP-OES. We selected KWT, WT (AABB) and double mutant (aabb) of *TaZIP11-1*, *TaZIP13-1*, *TaZIP13-2*, *TaZIP14-1*, and *TaZIP14-2* and measured Fe, Zn, Mn, P, Mg, and Ca content.

2.4.7.1 Micronutrient quantification of *TaZIP11*

The micronutrients quantification of *TaZIP11* is shown in Figure 2.15. There were no significant differences ($p < 0.05$, one-way ANOVA with post-hoc Tukey HSD) in any measured minerals between the AABB and double mutant for *TaZIP11*. The AABB and

aabb had higher Fe, Zn and Mn contents compared to KWT but again there were no significant difference between AABB and aabb.

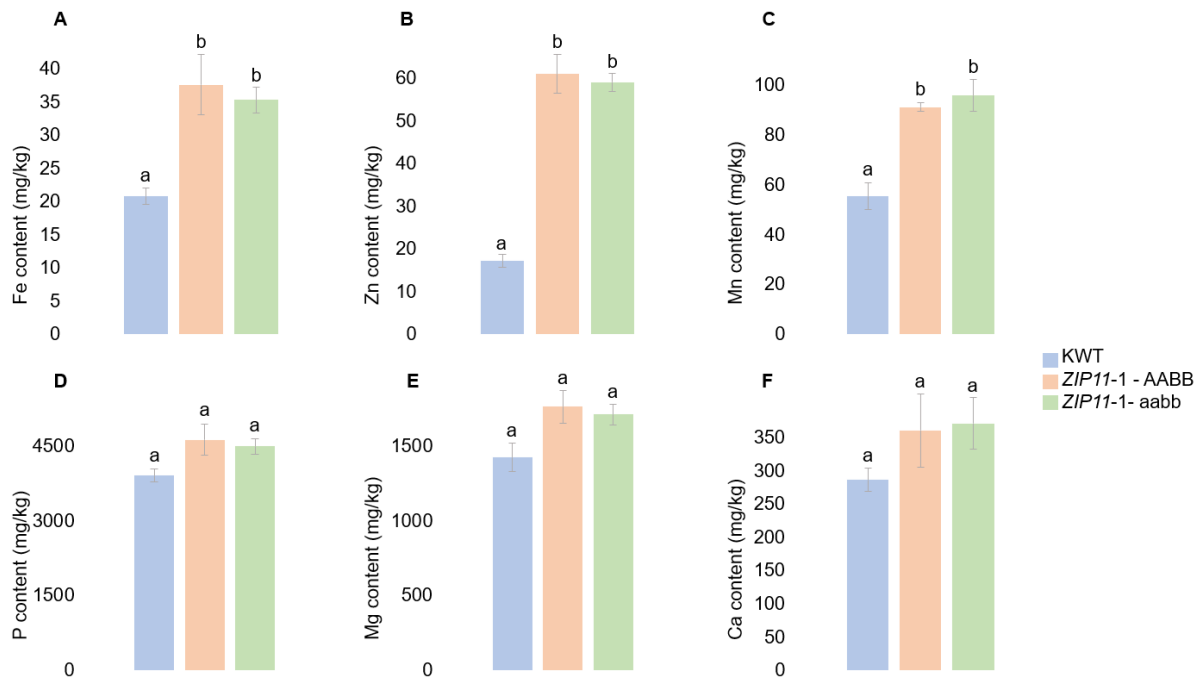


Figure 2.15: Micronutrient quantification of *TaZIP11*. (A) Fe content, (B) Zn content (C) Mn content (D) P content (E) Mg content and (F) Ca content (mg/kg). Bars denote means of three biological replicates \pm SD. Lower case letters indicate statistically significant differences and significance ($p < 0.05$) tests with post-hoc Tukey HSD using one-way ANOVA.

2.4.7.2 Micronutrient quantification of *TaZIP13*

The micronutrients were measured for *TaZIP13-1* and *TaZIP13-2* and shown in Figure 2.16 and 2.17 respectively. In terms of Fe levels for *TaZIP13-1*, the AABB genotype had the highest concentration at 27.8 mg/kg, followed by the aabb genotype at 22.2 mg/kg and has a significant difference ($p < 0.05$, one-way ANOVA with post-hoc Tukey HSD). For Zn, the AABB genotype displayed the highest value of 35.4 mg/kg, followed by the aabb genotype at 26.2 mg/kg. The KWT genotype had the lowest Zn level. In the case of Mn, the AABB genotype had the highest concentration at 91.4 mg/kg and

had no significant difference between AABB and double mutants. Regarding P content, the AABB genotype showed the highest concentration at 4431.1 mg/kg, followed closely by the aabb genotype at 4211.2 mg/kg. The KWT had the lowest P level and significantly difference. In term of Mg, there was no significant difference among KWT, AABB, and aabb. Interestingly, for Ca levels, the aabb displayed the lowest content at 211.8 mg/kg, followed by the AABB genotype at 265.5 mg/kg. The aabb was significantly lower than AABB and KWT ($p < 0.05$, one-way ANOVA with post-hoc Tukey HSD).

In case of *TaZIP13-2*, the aabb had the highest content of Fe levels, at 33.9 mg/kg, followed by the AABB genotype and KWT and had a significant difference between AABB and aabb. Similarly, aabb had the highest contents of Zn and Mn and had no significant difference between AABB and aabb in term of P, Mg and Ca, we found no significant difference among KWT, AABB and aabb. In summary, we found interesting results for Zn levels in *TaZIP13-1* and Fe levels in *TaZIP13-2* where we had a significant difference between mutants.

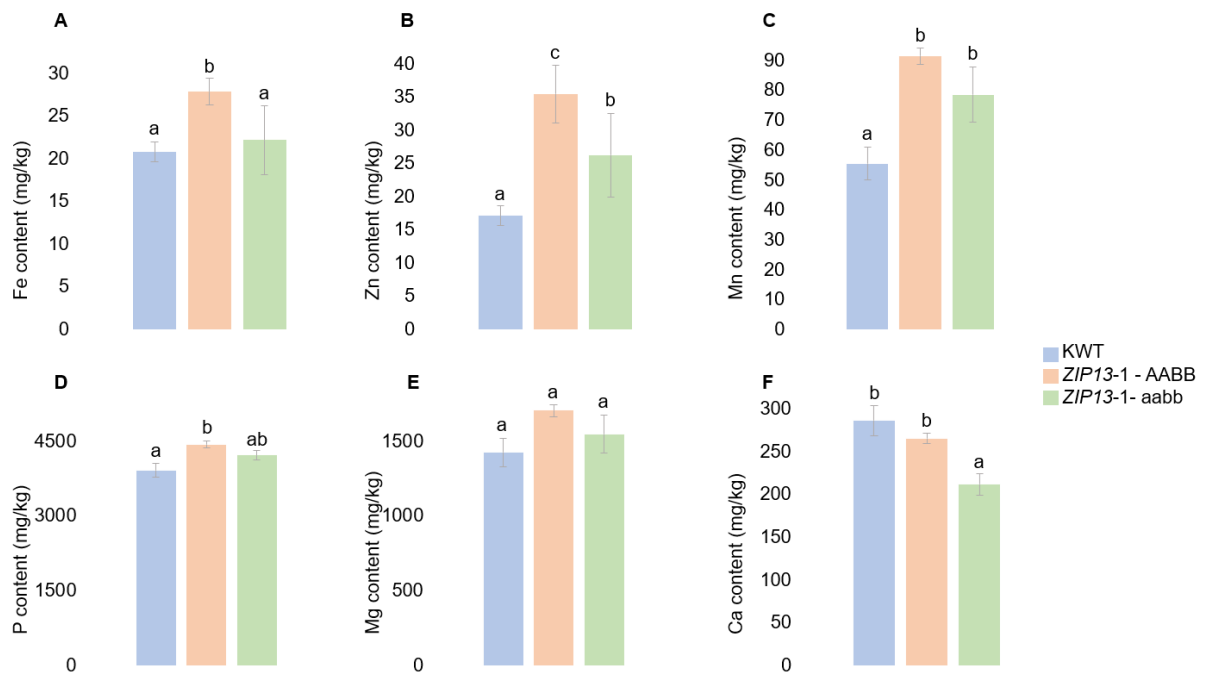


Figure 2.16: Micronutrient quantification of *TaZIP13-1*. (A) Fe content, (B) Zn content (C) Mn content (D) P content (E) Mg content and (F) Ca content (mg/kg). Bars denote means of three biological replicates \pm SD. Lower case letters indicate statistically significant differences and significance ($p < 0.05$) tests with post-hoc Tukey HSD using one-way ANOVA.

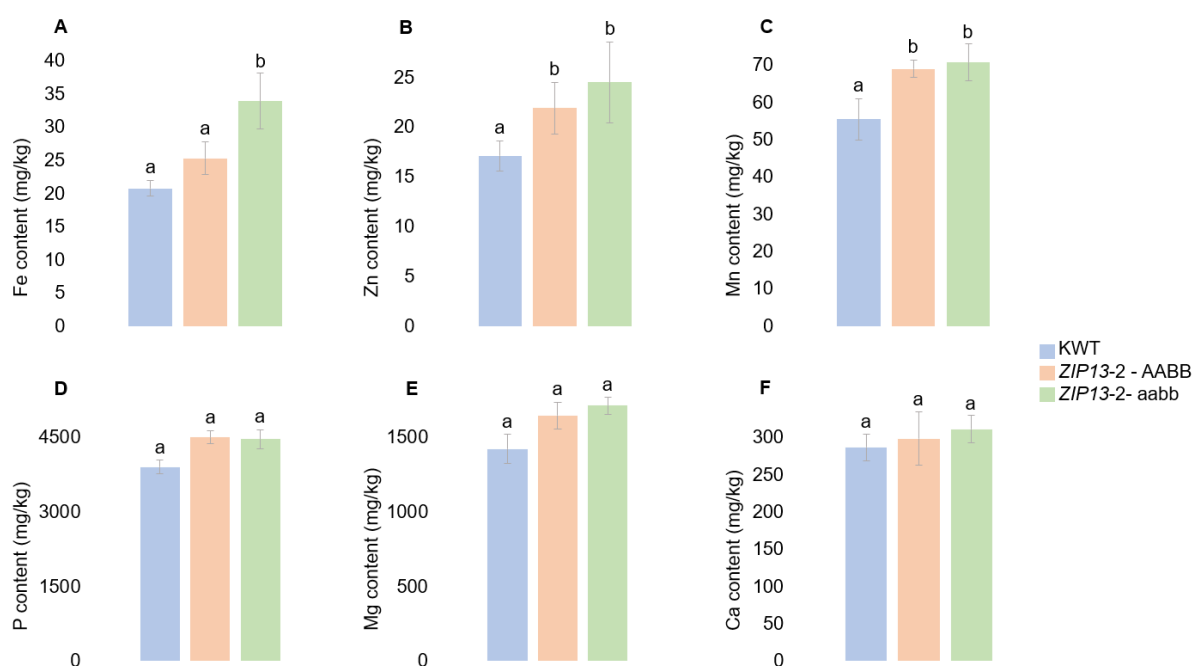


Figure 2.17: Micronutrient quantification of *TaZIP13-2*. (A) Fe content, (B) Zn content (C) Mn content (D) P content (E) Mg content and (F) Ca content (mg/kg). Bars denote means of three biological replicates \pm SD. Lower case letters indicate statistically significant differences and significance ($p < 0.05$) tests with post-hoc Tukey HSD using one-way ANOVA.

2.4.7.3 Micronutrient quantification of *TaZIP14*

We generated two double mutants for *TaZIP14* (*TaZIP14-1* and *TaZIP14-2*) after one backcross and measured the micronutrients shown in Figure 2.18 and 2.19. Like *TaZIP11* and *TaZIP13*, we got similar results for *TaZIP14-1*. The AABB genotype showed the content of 36.5 mg/kg Fe and had no significant difference between AABB and aabb ($p < 0.05$, one-way ANOVA with post-hoc Tukey HSD). The KWT displayed the lowest content of Zn at 17.1 mg/kg, while the AABB genotype exhibited the highest Zn level, measuring 44.7 mg/kg and had no significant difference between AABB and aabb. Similarly, Mn and P also had the same trend and had no significant difference between AABB and aabb. In contrast to *TaZIP14-1*, *TaZIP14-2* had only significant differences in P and Ca ($p < 0.05$, one-way ANOVA with post-hoc Tukey HSD) (Figure

2.19). The P contents in *TaZIP14-2* was higher and Ca was lower in double mutants compared to WT. In summary, we got a significant difference in P content in both *TaZIP14-1* and *TaZIP14-2* and Ca content only in *TaZIP14-2* between AABB and aabb.

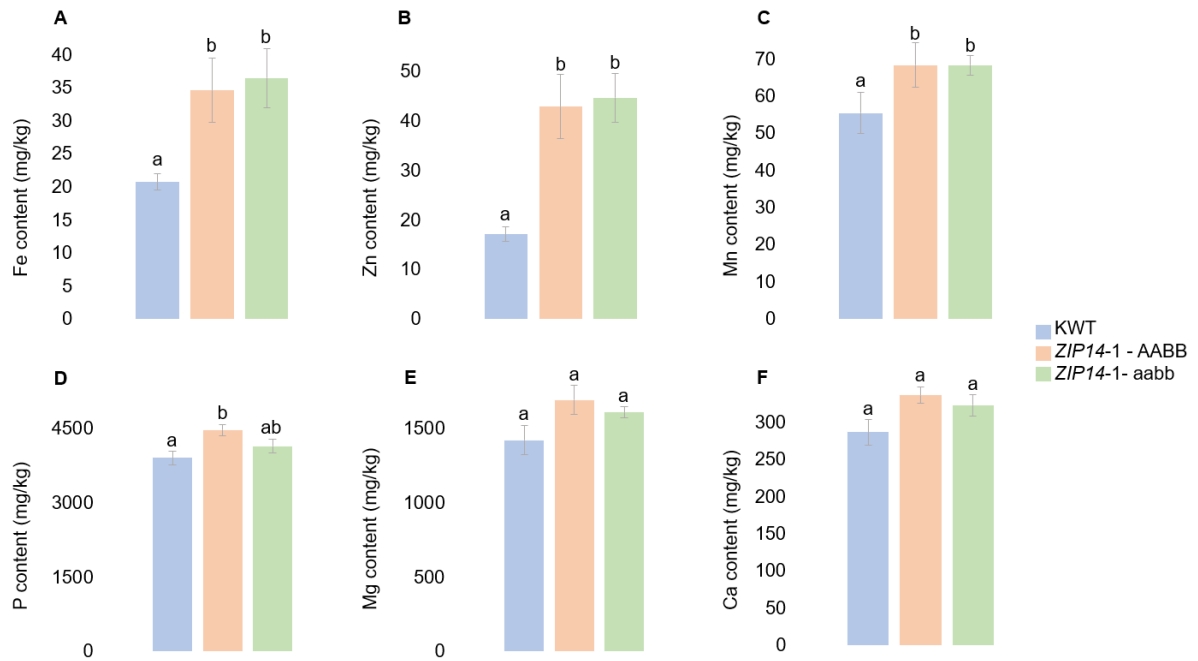


Figure 2.18: Micronutrient quantification of *TaZIP14-1*. (A) Fe content, (B) Zn content (C) Mn content (D) P content (E) Mg content and (F) Ca content (mg/kg). Bars denote means of three biological replicates \pm SD. Lower case letters indicate statistically significant differences and significance ($p < 0.05$) tests with post-hoc Tukey HSD using one-way ANOVA.

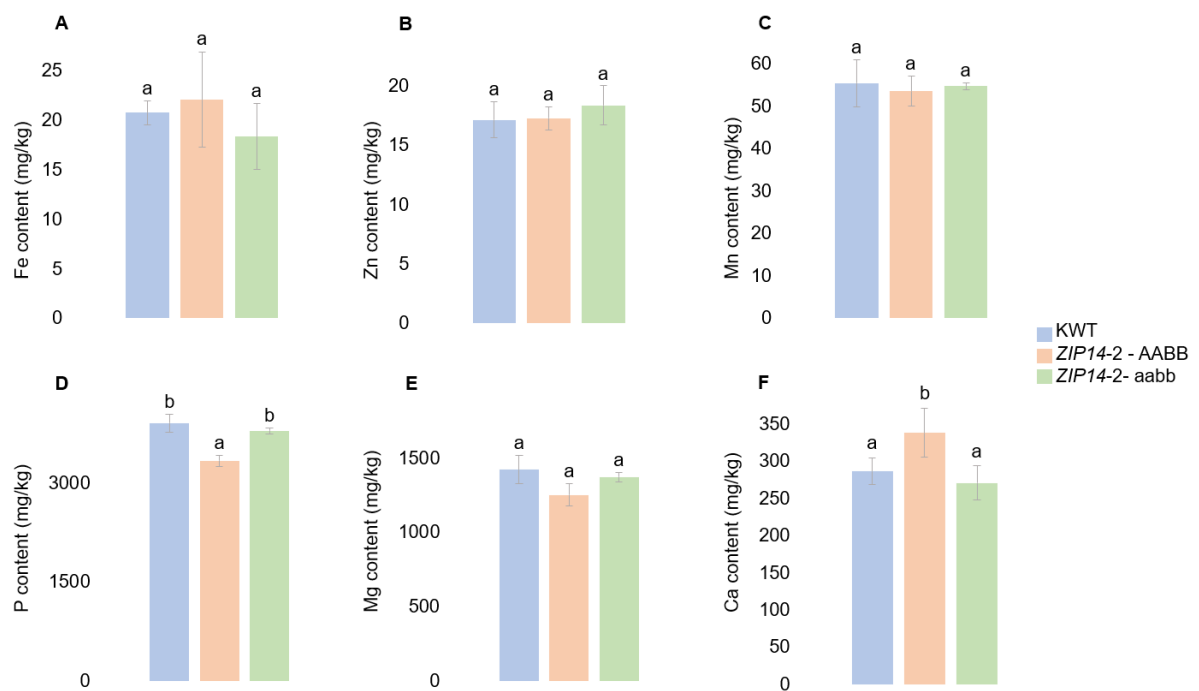


Figure 2.19: Micronutrient quantification of *TaZIP14-2*. (A) Fe content, (B) Zn content (C) Mn content (D) P content (E) Mg content and (F) Ca content (mg/kg). Bars denote means of three biological replicates \pm SD. Lower case letters indicate statistically significant differences and significance ($p < 0.05$) tests with post-hoc Tukey HSD using one-way ANOVA.

2.4.8 Functional complementation of *TaZIPs* in yeast

2.4.8.1 Yeast complementation of *zrt1/zrt2*

Using yeast complementation, a subset of the wheat *ZIPs* (*TaZIP11*, *TaZIP13* and *TaZIP14*) was examined for a functional involvement in Zn transport. Each of the three *TaZIPs* cloned was evaluated to see if it could complement the *zrt1/zrt2* mutant yeast strain in order to determine its Zn transport capacity. The *zrt1/zrt2* mutant yeast strain and the wild type of this strain (DY1457) were transformed with the pYES2-*ZIP* vectors and an empty pYES2 vector as a control. Colony PCR with pYES2 backbone primers was used to confirm transformations. pYES2 has a GAL1 promoter upstream of the multiple cloning site, and *TaZIP* expression was induced prior to plating of the drop

spot experiment by growing the transformed yeast in galactose-containing conditions. After *TaZIP* induction, drops of culture serial dilutions were plated on medium that included 200 μM Zn, which is required for the mutant yeast strain to thrive, and media that did not contain Zn but did contain increasing concentrations of the Zn chelator EGTA (0 mM to 5.0 mM EGTA), which is used to bind Zn. According to Figure 2.20A, the *zrt1/zrt2* strain was less grow at Zn levels of 200 μM comparable to that demonstrated by the wild type of strain DY1457. The growth of this mutant yeast strain was however slowed down by the addition of EGTA chelator Figure 2.20C.

The *zrt1/zrt2* strain with the *TaZIP*-containing pYES2 vectors including positive controls (*TaZIP6* and *TaZIP7*) grew at greater rates in the Zn-deficient medium (0 μM , 5 mM EGTA) than the empty pYES2 vector. The mutant *TaZIP11* had great rescue capacity when linked to the other *TaZIP* genes at the 5.0 mM EGTA concentration The expression of any of the *TaZIPs* did not completely restore growth levels and wild type growth was still larger than that of the empty pYES2 carrying *TaZIP* genes.

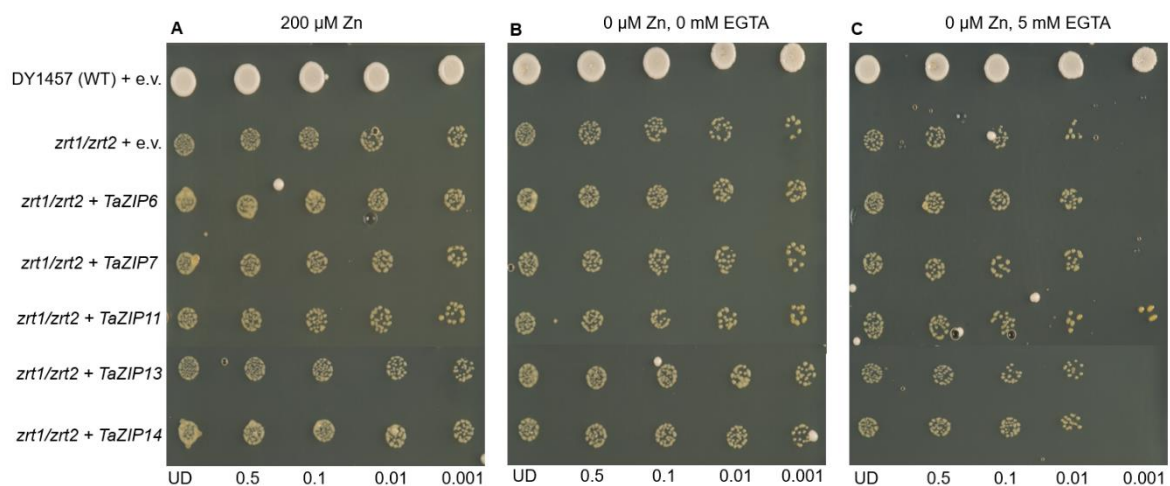


Figure 2.20: *TaZIP* genes complementation of the yeast Zn uptake mutant *zrt1/zrt2*. *TaZIP11*, *TaZIP13*, and *TaZIP14* genes were used to transform the yeast mutant *zrt1/zrt2*, and they are displayed here with empty vector as controls (e.v.) in both the mutant and wild type. *TaZIP6* and *TaZIP7* used as a positive control. Each spot

represents a dilution of the culture starting on the left of each plate (undiluted, 0.5, 0.1, 0.01, 0.001). Following eight days of growth, complementation is displayed, and to the top of each plate, the contents of the selective media are listed. Undiluted=UD, EGTA=aminopolycarboxylic acid, a chelating agent.

2.4.8.2 Yeast complementation of *fet3/fet4*

The Fe transport capacity of the cloned *TaZIP* genes was examined by transformation and testing in the *fet3/fet4* mutant yeast strain. The pYES2-*TaZIP* vectors and empty pYES2 controls, as previously stated in Section 2.8.1, was transformed the *fet3/fet4* and the WT DY1457 strains. By colony PCR and pYES2 backbone primers, transformations were verified.

Before plating the drop spot test, *TaZIP* expression was activated by growing the transformed yeast in a galactose controlling culture. Following *ZIP* induction, drops at successively lower concentrations were plated onto medium with different Fe contents. Fe concentrations ranged from 10 μM for highest levels to 0.75 μM , which is often seen in yeast growth media, and Fe completely missing (0 μM Fe). The *fet3/fet4* mutant yeast strain displays a Fe-deficient phenotype at higher Fe levels than the WT strain because it lacks both the *FET4* low affinity Fe uptake transporter and *FET3* high affinity iron uptake transporter. The *fet3/fet4* was cultivated on plate media with a pH of 4 to allow for the observation of the Fe-deficient phenotype. The growth of *fet3/fet4* was comparable to that of the WT (DY1457) at 10 μM Fe, but at baseline concentrations of 0.75 μM and without Fe media, growth was drastically diminished (Figure 2.21A-C). All *TaZIP* genes were heterologously produced, but none of them were able clearly to reverse the Fe-deficient phenotype that the *fet3/fet4* strain presented except *TaZIP11*. The findings of the yeast complementation experiments of all *TaZIP* genes reveal only *TaZIP11* could transport Fe and Zn.

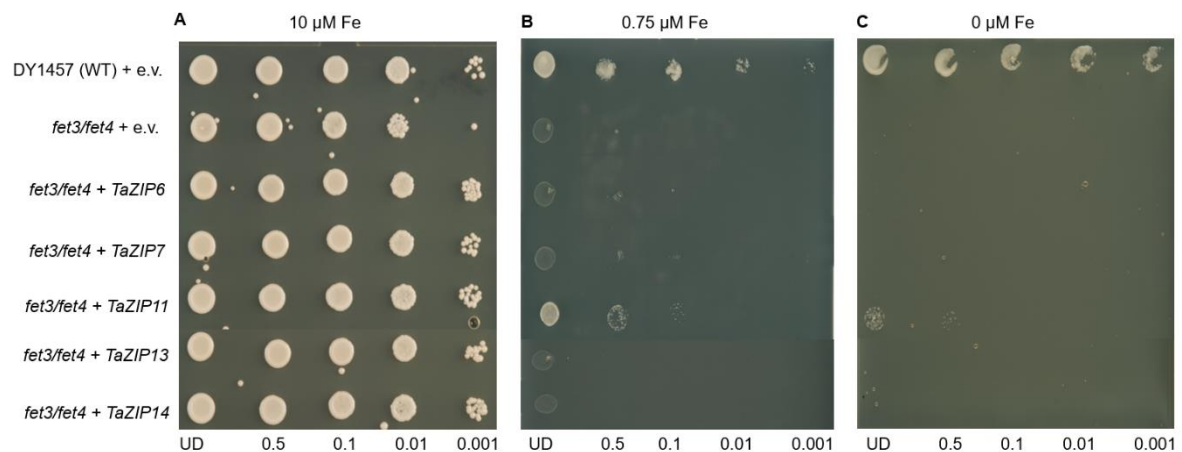


Figure 2.21: *TaZIP* genes complementation of the yeast Fe uptake mutant *fet3/fet4*. *TaZIP11*, *TaZIP13*, and *TaZIP14* genes were used to transform the yeast mutant *fet3/fet4*, and they are displayed here with empty vector controls (e.v.) in both the mutant and wild type. *TaZIP6* and *TaZIP7* used as a negative control. Each spot represents a dilution of the culture starting on the left of each plate (undiluted, 0.5, 0.1, 0.01, 0.001). After three days of growth, complementation is displayed, and to the top of each plate, the contents of the selective media are listed. Undiluted=UD.

2.5 Discussion

The agronomic data of selected TILLING lines shows *TaZIP* genes are not affecting the overall biomass of plants. ICP-OES results indicate, only *TaZIP13-1* has a significant difference in Fe, Zn and Ca accumulation in AABB and aabb, while *TaZIP13-2* has only for Fe content. *TaZIP13-1* and *TaZIP13-2* had opposite results for Fe contents. *TaZIP13-A* has a splice acceptor and missense variant mutation and *TaZIP13-B* has stop gained and splice acceptor variant mutations. In *TaZIP13-1*, mutant had lower Fe level than WT and in *TaZIP13-2* mutant had higher Fe level than WT. Yeast complementation of *TaZIP* genes shows only *TaZIP11* has the ability to transport Fe and Zn. Overall, these results suggest a further investigation is required to fully understand the role of these *TaZIP* genes.

2.5.1 TILLING mutants of *TaZIP11*, *TaZIP13*, and *TaZIP14* had no effect on agronomic traits and limited effects on micronutrients

In this study, we investigated the functional role of *TaZIP11*, *TaZIP13*, and *TaZIP14*, in relation to agronomic traits and micronutrient content in wheat. By utilizing TILLING technique, we generated *TaZIP* mutant lines for each transporter and characterized their phenotypic and biochemical traits. Surprisingly, our findings reveal that the disruption of *TaZIP11*, and *TaZIP14* had no discernible effect on agronomic traits or micronutrient levels except *TaZIP13*.

The *ZIP* family of transporters has been implicated in the uptake and transport of divalent metal ions, such as zinc, iron, and manganese, across cellular membranes in plants. These transporters play critical roles in regulating metal homeostasis, which is essential for various physiological processes, including growth, development, and micronutrient acquisition (Lin et al., 2009). Therefore, it was anticipated that perturbing the function of *TaZIP11*, *TaZIP13*, and *TaZIP14* would lead to observable phenotypic changes and altered micronutrient accumulation in wheat plants. Previous studies in other plant species have reported significant alterations in agronomic traits and micronutrient content upon manipulating *ZIP* family transporters. For instance, in *Arabidopsis thaliana*, loss-of-function mutants of *AtZIP4* displayed severe growth defects and exhibited zinc-deficient phenotypes, including reduced biomass and altered leaf morphology (Grotz et al., 1998). Similarly, disruption of *OsZIP1* in rice led to stunted growth and reduced iron uptake, resulting in iron deficiency symptoms (Ishimaru et al., 2005). Interestingly, *TaZIP13-1* displayed higher Fe and Zn contents in AABB compared to aabb while in *TaZIP13-2* has higher Fe contents in aabb. These results are not consistent in both crosses might be due to different mutation types in A

and B genomes in selected TILLING lines. Given these precedents, our unexpected findings regarding the lack of phenotypic and nutritional changes in the *TaZIP11*, *TaZIP13*, and *TaZIP14* mutants are intriguing. It could be due to differences in the mutant alleles, or due to background mutations.

Several factors may account for the observed lack of phenotypic and biochemical alterations in our study. First, redundancy within the *ZIP* transporter family could compensate for the loss of function of *TaZIP11*, *TaZIP13*, and *TaZIP14* in wheat. It is possible that other closely related transporters with overlapping substrate specificities might have been able to complement the disrupted transport activity, thereby maintaining normal growth and nutrient status in the mutant lines. Additionally, compensatory mechanisms involving other transporters or regulatory pathways might have come into play to ensure the adequate uptake and distribution of metals in the absence of *TaZIP11*, *TaZIP13*, and *TaZIP14*. Furthermore, the complex interactions between plants and their rhizosphere, including the soil microbial community, might influence nutrient availability and uptake, thereby modulating the phenotypic and nutritional responses to transporter perturbations.

It is also worth noting that the lack of observable phenotypic changes in the *TaZIP11*, *TaZIP13*, and *TaZIP14* mutants after single backcross does not necessarily imply their dispensability under all conditions. It is possible that these transporters play more significant roles under specific stress conditions or in specific tissues or developmental stages that were not addressed in our study. Future investigations targeting these aspects could provide further insights into the functional relevance of *TaZIP11*, *TaZIP13*, and *TaZIP14* in wheat.

In summary, our study demonstrates that the disruption of *TaZIP11*, *TaZIP13*, and *TaZIP14* through TILLING mutants after one backcross had no apparent effect on agronomic traits or micronutrient levels in wheat. These findings suggest the presence of compensatory mechanisms or alternative transporters that enable the maintenance of normal growth and nutrient status in wheat.

2.5.2 Functional complementation shows the capacity of *TaZIP11* to transport Fe and Zn

We conducted functional complementation assays to investigate the Zn and Fe transport capacities of *TaZIP11*, *TaZIP13*, and *TaZIP14* in wheat. Our findings revealed that only *TaZIP11* exhibited the ability to transport Fe and Zn (Figure 2.19-20). The *ZIP* family of transporters is known for its role in metal ion uptake and transport in plants, and members of this family often exhibit substrate specificity. Therefore, understanding the specific metal transport capabilities of *TaZIP11*, *TaZIP13*, and *TaZIP14* is crucial for unravelling their roles in Zn and Fe homeostasis in wheat. Consistent with their classification as *ZIP* transporters involved in Zn homeostasis, *TaZIP11* demonstrated the capacity to transport Zn in our complementation assays. This aligns with previous studies on *ZIP* transporters in other plant species, where members of the *ZIP* family have been shown to transport Zn. The Zn transport activity of *TaZIP11* confirms their involvement in Zn uptake and distribution in wheat.

Intriguingly, our results also unveiled a unique characteristic of *TaZIP11*, as it exhibited functional complementation and demonstrated the ability to transport Fe. This suggests that *TaZIP11* may possess a broader substrate specificity compared to *TaZIP13* and *TaZIP14*, extending its role beyond Zn transport to include Fe uptake as well. The transport of Fe by *TaZIP11* is of particular significance, as Fe is another

essential micronutrient required for various physiological processes in plants, including photosynthesis and enzyme activity. Although *TaZIP11* transported Fe in yeast, while we did not see any effect in wheat mutants. This may be due to background mutation in TILLING lines. However, the mechanisms underlying the Fe transport activity of *TaZIP11* remain to be fully elucidated and warrant further investigation.

The differential metal transport capacities observed among *TaZIP11*, *TaZIP13*, and *TaZIP14* highlight the functional diversity within the *ZIP* transporter family. These findings are consistent with previous studies, where distinct members of the *ZIP* family have been shown to exhibit different substrate specificities and transport capabilities (Li et al., 2019). The functional complementation assays conducted in this study provide valuable insights into the metal ion transport abilities of the individual transporters and contribute to our understanding of their roles in metal homeostasis in wheat. It is important to note that while the functional complementation assays in a heterologous expression system provide valuable initial insights, the true physiological relevance and functional implications of these transporters in wheat may be more complex. The expression of *ZIP* transporters in their native cellular and tissue contexts, as well as their regulation under different environmental conditions, can influence their metal transport activities and their contributions to agronomic traits and micronutrient accumulation in wheat (Gong et al., 2022). Similarly, in our results, we could not get a strong phenotype in TILLING lines.

Moreover, the impact of these metal transport activities on agronomic traits and micronutrient levels in wheat plants requires further investigation. Agronomic traits encompass a wide range of characteristics, including plant growth, development, yield, and stress responses, which can be influenced by multiple genetic and environmental

factors. Similarly, the effects of metal transporters on micronutrient levels may vary depending on interactions with other transporters, regulatory pathways, and environmental conditions. In conclusion, our study provides evidence of the metal transport capacities of *TaZIP11* in yeast model. Only *TaZIP11* demonstrates functional complementation and the ability to transport Fe and Zn. These findings contribute to our understanding of the roles of *ZIP* transporters in metal homeostasis and provide a foundation for further investigations into the specific functions and regulatory mechanisms of *TaZIP11*, *TaZIP13*, and *TaZIP14* in wheat. Future studies should focus on unravelling the roles of these transporters and their impact on agronomic traits and micronutrient accumulation in wheat under different environmental conditions.

2.5.3 Similarities and differences between *TaZIP11*, *13* and *14* and known *ZIPs* in wheat and other species

Through analysis of rice *ZIP* genes, 14 *TaZIP* genes discovered in wheat with each a homeolog on the A, B and D genomes. In previous study, only 12 *TaZIP* genes are identified and homeologs not reported (Tiong et al., 2015). Compared to rice, only *TaZIP4* is not identified in wheat. In wheat (*Triticum aestivum*), *TaZIP11*, *TaZIP13*, and *TaZIP14* belong to the *ZIP* (Zinc-regulated Transporter/Iron-Regulated Transporter-like Protein) family of transporters. *TaZIP11*, *TaZIP13*, and *TaZIP14*, like other *ZIP* transporters, participate in the transport of Fe and Zn, *ZIP* transporters in wheat and rice showed tissue-specific expression patterns (Figure 2.5 and 2.6), and our results show the expression patterns of *TaZIP11*, *TaZIP13*, and *TaZIP14* vary, and they are highly expressed in roots, shoots and grains (Figure 2.5-7). Although only *TaZIP11* transports Fe and Zn in yeast, they may have different affinities and selectivity for other metal ions (Guerinot, 2000). *ZIP* transporters can be regulated at the transcriptional or

post-translational level by various factors including metal availability, hormonal signals, and environmental cues (Lin et al., 2009). It is important to note that while *TaZIP11*, *TaZIP13*, and *TaZIP14* are specific to wheat and rice, *ZIP* transporters are found in many plant species including other cereals like maize (*Zea mays*), and barley (*Hordeum vulgare*), as well as in non-cereal species.

Some specific *ZIP* genes have been studied in relation to nutrient uptake and expression patterns in wheat and rice. In wheat, *ZIP1* has been identified as a key gene involved in zinc and iron uptake under zinc and iron deficiency conditions. Its expression increases in response to low zinc and iron availability in the roots (Ma et al., 2019). *ZIP4* is another important gene involved in zinc uptake. In wheat, *ZIP4* expression is upregulated under zinc deficiency, facilitating zinc absorption from the soil. *ZIP5* gene has been implicated in iron uptake in wheat. *ZIP5* expression is upregulated under iron deficiency conditions, suggesting its role in iron acquisition (Evens et al., 2017). Similarly, *OsZIP1* in rice, is known to be involved in zinc uptake. Its expression is induced under low zinc availability, indicating its role in zinc acquisition (Bashir et al., 2012). *OsZIP3* is a rice gene associated with iron uptake. It is upregulated under iron-deficient conditions, suggesting its involvement in iron transport (Sasaki et al., 2015). *OsZIP4* gene is implicated in zinc uptake in rice. *OsZIP4* expression is induced under low zinc conditions, indicating its role in zinc acquisition (Ishimaru et al., 2005). It is important to note that the expression and function of *ZIP* genes can vary depending on the specific experimental conditions, genotypes, and tissues/organs analyzed.

In other cereals like maize, *ZmZIP1*, *ZmZIP3*, and *ZmZIP4* are linked to the uptake of zinc and iron in maize (Li et al., 2013). *HvZIP1* and *HvZIP3* are zinc and iron uptake-

related genes found in barley (Tiong et al., 2015). These genes exhibit differential expression when there is a nutrient shortage, indicating that they are essential for maintaining optimal nutrient levels in cereal crops. Further research and specific studies about wide range of *ZIP* genes in wheat may provide additional insights into the role of different *ZIP* genes in nutrient uptake and accumulation in grain tissues.

Chapter 3: Identifying Novel QTLs Involved in Controlling Grain Iron in Bread Wheat

3.1 Introduction

3.1.1 An Overview of iron metabolism in wheat

Iron (Fe) is a necessary micronutrient for plants, playing a crucial role in various physiological and biochemical processes (Nishito & Kambe, 2018). In wheat, one of the world's most important staple crops, Fe metabolism is a complex and tightly regulated process that influences the plant's growth, development, and overall productivity. Understanding the mechanisms involved in iron uptake, transport, and utilization in wheat is of great significance for plant scientists and breeders seeking to improve crop performance and address Fe deficiency in human populations (Verma & Pandey, 2016). The amount of Fe in the soil is a key factor in determining the Fe nutrition of plants (Yu et al., 2016). But in other soil types, such as alkaline or calcareous soils, where Fe predominately occurs as insoluble ferric hydroxides, the uptake of Fe by plants is frequently hampered (Wallace & Lunt, 1956). Wheat plants have developed sophisticated techniques to improve Fe collection in these conditions. Wheat roots can efficiently take up Fe from the soil because Fe transporters and chelators work together (Zhang et al., 1989) To meet the needs of numerous organs and tissues, Fe must be delivered from the roots to various areas of the plant. The primary pathway for the distribution of Fe in wheat is the xylem, which transports water and nutrients (Sheraz et al., 2021). Specific Fe transport proteins, such as those from the *NRAMP* (natural resistance-associated macrophage protein) and *YS1* (yellow stripe) families, are active during Fe transfer within plants. These proteins aid in the transfer of Fe between various cellular compartments and help the plant allocate Fe properly (Eagling et al., 2014). The vital metabolic activities in wheat require the use of Fe. Numerous enzymes required in key biological processes, including as DNA

replication, respiration, nitrogen metabolism, and chlorophyll synthesis, require Fe as a cofactor (Pahlavan-Rad & Pessaraki, 2009). The effectiveness of these processes, and as a result, the total development and productivity of wheat plants, are directly impacted by the availability of Fe (Sheraz et al., 2021). A major obstacle to the production of wheat and to human nutrition is Fe deficiency. Poor grain quality and lower agricultural yields might result from Fe-deficient soils. Additionally, a lack of Fe in the diet of humans can lead to serious health issues including Fe-deficiency anaemia (Kumar et al., 2022). Therefore, understanding the regulatory mechanisms that control Fe metabolism in wheat is essential for creating efficient methods to increase Fe uptake and utilisation as well as for breeding wheat cultivars with high Fe efficiency that can survive in areas with low levels of Fe.

3.1.2 Limited understanding of the genetic basis of grain iron content

Limited understanding of the genetic basis of grain Fe content has been a challenge for wheat researchers seeking to improve crop productivity and human nutrition. Grain Fe content is controlled by numerous genetic and environmental factors (J. Wang et al., 2022). It has been discovered that there is genetic variability among wheat cultivars and accessions, suggesting the possibility of genetically improving Fe content (Velu et al., 2018). The identification of potential genes linked to Fe build-up has also showed promise using association mapping and a variety of germplasm sets. Transcriptomic research has also shed light on the patterns of gene expression linked to wheat's Fe metabolism (J. Wang et al., 2022). Despite these developments, there are still large gaps in our knowledge of the genetic causes of high Fe grain content in wheat. Unravelling this feature is difficult because to the complexity of Fe metabolism, the participation of numerous genes and regulatory pathways, and the influence of

environmental factors (Beasley, Bonneau, Sánchez-Palacios, et al., 2019). To identify the underlying genetic variables and molecular pathways, comprehensive and integrative techniques that include genomes, transcriptomics, proteomics, and metabolomics are required (Kaur et al., 2023). Emerging technologies, such as high-throughput genotyping and next-generation sequencing, offer unprecedented opportunities for unravelling the genetic basis of complex traits like grain Fe content. Key genetic variations related with Fe build-up may be found applying genome-wide association studies (GWAS) and genomic selection. Further understanding of the functions of potential genes in Fe metabolism can be gained by using functional genomics techniques, such as gene expression research and gene editing methods.

3.1.3 Known QTLs associated with grain iron

Substantial strides forward have been made in the identification and characterization of quantitative trait loci (QTLs) connected to grain Fe content. An overview of the known QTLs for grain Fe content in wheat is given in this part, and it is emphasised how vital it is to find and characterise new QTLs to improve our knowledge of Fe metabolism and assist targeted breeding efforts for higher grain Fe content. In wheat, several known QTLs linked to grain Fe content have been found. The *Gpc-B1* gene on chromosome 6B is an important regulator of the Fe and Zn contents of grains, which is noteworthy (Uauy et al., 2006). Wheat grains accumulate more minerals as a result of the *Gpc-B1* QTL's influence on the gene expressions involved in the transport and storage of Fe and Zn (Xu et al., 2012a). Wheat grain Fe content has also been linked to QTLs on chromosomes 3B, 2A, and 5A in addition to *Gpc-B1*. Through their effects on numerous processes, such as Fe uptake, transport, and allocation within the plant, these QTLs probably act on these processes and affect Fe accumulation (Crespo-

Herrera et al., 2016; Xu et al., 2012a). Another study found 4 QTLs (*QGFe.iari-2A*, *QGFe.iari-5A*, *QGFe.iari-7A* and *QGFe.iari-7B*) for Fe, and these QTLs collectively explained 20.0% of the phenotypic variation for Fe (Krishnappa et al., 2017). Even though there are a number of known QTLs connected to wheat grain Fe content, more new QTLs need to be found and characterised for understanding of the genetic basis of Fe content. The discovery of novel QTLs using cutting-edge genomics methods can improve our comprehension of the genetic influences underpinning Fe metabolism in wheat grains. This information can direct targeted breeding efforts to create wheat varieties that are Fe-biofortified and solve the concerns of Fe deficiency around the world.

3.1.4 Bulk segregant analysis

Pooling individuals with extreme phenotypes is a technique used in bulk segregation analysis (BSA) to conduct linked marker screening or QTL mapping quickly and inexpensively (Li & Xu, 2021). Michelmore et al. (1991) initially introduced BSA, which was used to locate molecular markers connected to DM5/8 (downy mildew resistance loci in lettuce) in F₂ populations. The two extreme behaviors of resistance and susceptibility from one biparental group were used to pool the samples (Figure 3.1). The majority of bulks contain 14–20 distinct plants, and molecular markers such as simple sequence repeats, random amplified polymorphic DNA, amplified regions that are sequence-characterized, and amplified fragment length polymorphism was used to identify the banding polymorphisms in each mixed pool (Michelmore et al., 1991). When compared to genotyping each individual plant, the mixed pool technique can greatly minimise the labour, the cost of reagents and consumables, and improve the effectiveness of linked marker screening. As a result, it can play a significant role in the

gene-mapping of favourite traits based on segregated populations. Scientists have done BSA for many phenotypes in several species using DH and RILs populations to examine the linkage relationship between genetic markers and target genes (Cubillos et al., 2017; S. Kim et al., 2015; Kurlovs et al., 2019; Martinez et al., 2020). The features necessary for BSA have gradually changed from qualitative to quantitative traits commanded by key genes, like disease resistance genes (Aoun et al., 2017; Shoba et al., 2012). BSA mapping for complicated quantitative features has also been tried by several researchers (Sun et al., 2010; Zhang & Panthee, 2020). For instance, Li et al., (2020) used BSA to identify 30 QTLs, with phenotypic variance explained up to 47.99% for decreasing grain protein, grain hardness, and starch pasting characteristics in different environments. *NAM* genes next to *QGPC.cib-4A* probably have effects on grain protein. In a recent study, BSA-seq technique was applied to identify the major genes *PsPS1* that controlled pod softness in pea (*Pisum sativum*) (Zhang et al., 2022).

Identifying QTLs has historically been a challenging and laborious process due to genetic complexity, phenotypic variations, high-dimensional data, limited resources, and technology. However, advancements in genomics technologies, statistical methods, and computational tools have significantly accelerated the pace of QTL discovery in recent years. Prior to the use of next-generation sequencing (NGS), the primary method for creating genetic maps was QTL mapping based on segregating populations. Fruit trees, forest trees, crops, aquatic organisms, flowers, and insects have had their reference genomes revealed over time (Marks et al., 2021), laying a solid grounds for NGS-based BSA as the price of NGS continues to decrease and third generation sequencing, and Hi-C are widely used (Ghurye et al., 2019; Kim et al.,

2019). In this chapter, we phenotype the grain Fe content using Perls staining and identify QTLs associated for grain Fe content using BSA.

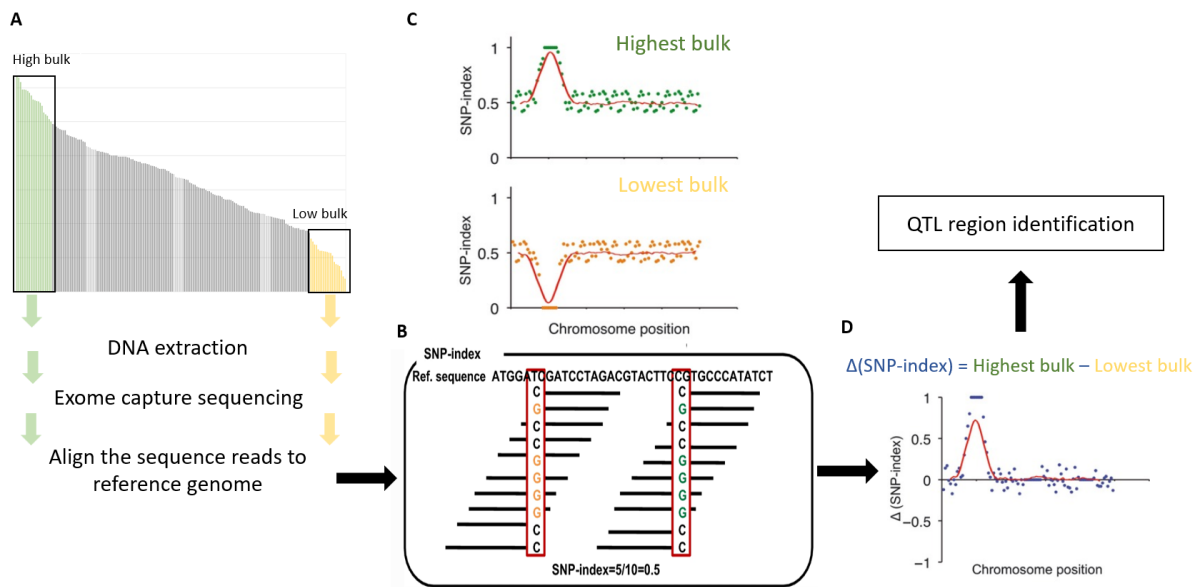


Figure 3.1: A basic scheme of BSA as applied to wheat grain Fe content. Two extreme phenotypes high Fe content (grain) and low Fe content selected and bulk DNAs to make 'High' and 'Low' bulks, respectively. These DNA bulks used to exome capture sequencing and aligned to the reference sequence (A). Then calculated the SNP (single nucleotide polymorphism) index (B). Examples of SNP-index plot (C). The QTLs can be detected as peak of the SNP index plot (D). Each point corresponds to the SNP, and the x-axis links to the chromosomal location. Lines are mean values of SNP index / $\Delta(\text{SNP-index})$ illustrated by sliding window analysis. $\Delta(\text{SNP-index})$ is the subtraction of the highest bulk and lowest bulk. This figure was modified from Takagi et al., (2013)

3.2 Aim

- Explore the potential of EMS (Ethyl methanesulfonate) lines for variation in wheat grain iron content
- Develop a script to analyse the Perls images in a high-throughput and unbiased manner
- Identify the QTLs associated for grain Fe contents in bread wheat using BSA

3.3 Material and methods

3.3.1 Plant growth and population development

3.3.1.1 Screening of EMS population

Initially, 100 EMS Cadenza lines (C_SSD2_7001-7100) were selected randomly to explore wheat grain Fe content. EMS Cadenza population have been generated through a mutagenesis technique known as EMS mutagenesis (Krasileva et al., 2017). EMS is a chemical compound that induces random mutations in the DNA of organisms. EMS treatment can lead to point mutations by alkylating guanine residues in DNA, resulting in base-pair substitutions. These mutations can cause changes in gene function, potentially leading to altered phenotypes in plants. These mutations can affect various traits of the wheat plants, including grain nutrition. These are single seed descent lines F₆ generation (Rakszegi et al., 2010). Then, to enhance the number of seeds, these 100 EMS lines with WT Cadenza were cultivated in growth chambers using speed breeding. 15% horticultural grit and 85% fine peat were used to plant seeds in P96 trays. Individual plants were transferred into 1 L circular pots when they had two to three leaves. The growth chamber was designed to operate at a temperature of 22°C for 22 hours of light and 17°C for 2 hours of darkness, with a 70% humidity setting (Watson et al., 2018). After harvesting, these lines used to phenotype for Fe contents.

3.3.1.2 Initial Perls staining and Visual scoring

After harvesting, six mature grains were chosen at random and dissected with a stainless-steel blade. They were then stained for 45 minutes with a staining solution (2% [w/v] potassium hexacyanoferrate [II] and 2% [v/v] hydrochloric acid), followed by a deionized water wash (Connorton, Jones, et al., 2017). Grain samples were stained

with Perls and then placed under a tiny digital microscope (DigiHero, WT20181120) to capture images for comparison with all 100 lines (Figure 3.2). These images then scored zero to 7 by three individuals (Anham Zafar, Katie Hawkins and Muhammad Ali). Image without Fe content gave a score zero and image with the highest Fe gave score 10.

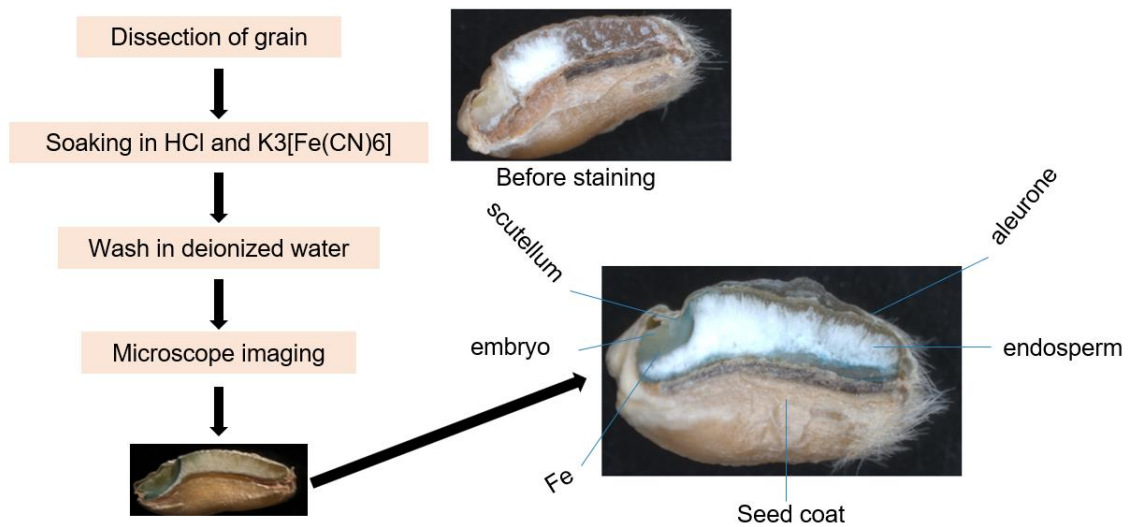


Figure 3.2: A schematic representation of Perls staining. The blue colour indicates the presence of Fe.

3.3.1.3 Generating mapping population

We selected the three lines with the higher Fe content (7054, 7060 and 7077) based on the visual score. These lines were used to develop mapping population. These lines were crossed the Cadenza to minimize the mutation and develop a BC₁F₂ population. Then this segregated population were used to final phenotype the grain Fe content.

3.3.2 Phenotyping

3.3.2.1 Agronomic traits

After developing mapping population, 200 seeds from each BC₁F₂ were grown into P24 trays with 15% horticultural grit. Individual plants were transplanted into 1 L round pots at the two to three leaf stage in the glasshouse (School of Biosciences, University of Birmingham), where there was a Cadenza WT control and a 16:8 hour light:dark cycle at a temperature of 22°C. Before harvesting, we measured plant height and total number of tillers for each plant. We used the Marvin seed analyser to calculate the number of seeds, total weight and thousand grain weight (TGW).

3.3.2.2 ICP-OES analysis

Randomly 3 g of wheat were chosen, dried at 60°C for three hours, coarsely ground in a coffee grinder, and then ground into flour in a pestle and mortar. Three biological and three technical replicates of each sample are used. Samples of flour (0.2 g each) were dried for an entire night at 55°C before being digested for an entire hour at 95°C in ultrapure nitric acid (55 percent by volume) and hydrogen peroxide (6 percent by volume). 2 mL of nitric acid and 0.5 mL of hydrogen peroxide were employed for digestion. ICP-OES (Vista-PRO CCD Simultaneous ICP-OES; Agilent) was used to analyse the samples after diluting them 1:10 in ultrapure water and calibrating it with standards of Fe and Zn. The reference material, soft winter wheat flour (RM 8438; U.S. National Institute of Standards and Technology), was examined concurrently with all experimental samples.

3.3.2.3 Perls staining

Grains from the BC₁F₂ population were stained with Perls using the methods in 3.3.1.2 and imaged using a Zeiss Axio Zoom V16 stereo microscope. Each line has randomly six replicates.

3.3.2.4 Computational scoring

The wheat grain Fe content was quantified by a customized processing pipeline (<https://github.com/SergioGabrielLopez/Colour-Quantification-for-Iron-Content-Estimation>) written in Python, a high-level programming language available under the GNU public license (Anaconda Software Distribution. Computer software. Vers. 3.8.10. Anaconda. 20126. Web. <https://anaconda.com>). The following Python libraries were used: NumPy (Travis, 2006), Pandas (McKinney, 2010), Matplotlib (Hunter, 2007), and Scikit-image (Van Der Walt et al., 2014). In the processing pipeline, each image is first converted to the HSV (Hue, Saturation, Value) format and then a region of interest (ROI) is selected that consists of pixels with H values both above 0.2 and below 0.8, S values above 0.1, and V values above 0.2. To obtain an estimation of Fe content that is independent of grain size, the S values of all the pixels in the ROI are summed up and the result of this summation is divided by the area of the seed. The area of the seed used for this calculation is obtained by thresholding the original image using Otsu's method (Otsu & N., 1979). Additionally, a map of Fe content is generated by displaying the S values within the ROI, superimposed on an outline of the seed that is obtained by means of the Sobel operator (Danielsson & Seger, 1990).

3.3.3 Genetic analysis

3.3.3.1 DNA extraction

Segregated lines (BC₁F₂) were transplanted to the glasshouse after being sowed into individual cells of 96-well seed trays filled with peat and sand. A 96-well collection tray (Qiagen, Germany, 19560) was filled with 5 cm of leaf tissue when plants reached the three-leaf stage, and the material was then stored at 80°C until it was needed. The DNA Qiagen Kit Protocol was followed while extracting DNA using a DNeasy Plant Kit

from Qiagen. DS-11 spectrophotometer (Denovix, DE, USA), Qubit-4 fluorometer (dsDNA BR test, Thermo Fisher Scientific Q32850), and running a DNA sample on an agarose gel (0.8%) to identify high molecular weight DNA were used to assess the quality and amount of the DNA. Six bulks assembled through pooling DNAs from plants which were scored as containing high iron and low iron using Perls staining from three populations (BC₁F₂ for 7054, 7060 7077). Equal amounts of DNA from each plant were pooled into one bulk to reduce bias. Sample were sent to the Arbor Biosciences (<https://arborbiosci.com>) for exome capture sequencing.

3.3.3.2 Sequence alignment

Library preparation and sequencing of each bulk were carried out at the Arbor Biosciences (<https://arborbiosci.com>) using myBaits (v1.53) kit (719384.v5). For BSA analysis, raw reads were aligned to *Triticum aestivum* cv. Chinese Spring RefSeq v1.0 (Appels et al., 2018) using 'BWA-MEM' (version 0.7.15-r1140) with Curio Alignment Processing (version 2.0.0) (H. Li, 2013). Variant calling was performed using 'Curio Variant Calling' (version 2.2.2) with Curio Variant Processing (version 2.0.1). Output files were analysed via 'bcftools' generating multi sample variant call format (.vcf) files.

3.3.3.3 Bulk segregant analysis

A simple analysis workflow was created by Mansfeld & Grumet, 2018. They introduced QTLseqr package in R to import SNP data, filter out SNPs that may complicate analysis, run BSAs, plot results, and export the data. A vignette that includes a step-by-step manual available at <https://github.com/bmansfeld/QTLseqr/blob/master/vignettes/QTLseqrpdf>. This QTLseqr programme was used to import a data frame with each row representing an SNP and each column representing a descriptive field. Each SNP's total reference allele frequency, bulk SNP-index, and delta SNP-index were

calculated. To help reduce noise and improve findings, the "filterSNPs()" function offered parameters for filtering SNPs based on genotype quality score, total read depth, per bulk read depth, and reference allele frequency. We applied filter options with 90% genotype quality score, reference allele frequency between 0.2 to 0.8, total sample depth ≥ 100 (i.e reads in both high plus low bulk), and per sample read depth ≥ 40 (i.e. reads in either high or low bulk). SNPs with poor confidence due to insufficient coverage or SNPs that may be in repeated regions and have exaggerated read depth were removed by filtering by read depth. The total number of SNPs filtered, the entire number of SNPs filtered, the remaining number, and the initial number of SNPs were all reported. The "runQTLseqAnalysis()" method performed QTL-seq analysis after counting the number of SNPs that fall inside the specified window size (10 Mb). "runGprimeAnalysis()" was used to undertake the initial analysis stages for the G prime value after computing the G statistic for each SNP. After counting the SNPs within the predetermined window size (10 Mb), it computed the tricube-smoothed G prime and delta SNP-index values for each SNP. The main charting function "plotGprimeDist()" was then used to visualise the data, which also aided with data control. In order to verify the accuracy of the analysis, the G prime value distribution was shown using the "plotGprimeDist()" function. Plotting the delta SNP-index, G prime numbers, $-\log_{10}(\text{p-value})$, and the number of SNPs per window were done using the "plotQTLStats()" function.

3.4 Results

3.4.1 Initial screening presents three times higher grain iron

To explore the potential of EMS Cadenza lines for wheat grain Fe content, we initially selected 100 lines randomly from the population. These lines were grown in a speed

breeding chamber in uniform conditions to get the grains at the University of Birmingham, UK in 2020. These grains were used for Perls staining and scored for Fe content (Figure 3.3). Randomly, we selected 6 grains for each line and these replicates had a wide range of variability. Figure 3.4 illustrated wheat grains longitudinal and traverse dissection and light green colour in each grain showed the presence of Fe content. We identified a wide range of Fe content in EMS lines, as shown in Figure 3.5, using WT Cadenza as a control. Most of the lines contained higher Fe content compared to WT. The visual score was giving using a scale 0-10. For example, an image with no Fe content gave a score zero, average Fe content gave 5 and maximum Fe content had a score of 7 (Figure 3.3). The visual score was the average of three individual scorers to reduce subjectivity (Anham Zafar, Katie Hawkins and Muhammad Ali). From these distributions, we identified the three best lines (green) with three times higher Fe compared to WT. These lines are 7077, 7060 and 7054 left to right (Figure 3.5). Line 7077 also has Fe accumulations in endosperm (Figure 3.3A). We selected these three best lines to measure Fe and Zn content using ICP-OES to validate our selection for next step.



Figure 3.3: Perls staining of EMS lines and WT. Line 7077 had the highest Fe content with score 7 (A), 7076 had no Fe content with score zero(B) and Cadenza WT demonstrated a medium level of Fe content with score 2 (C). Bars, 5 µm.

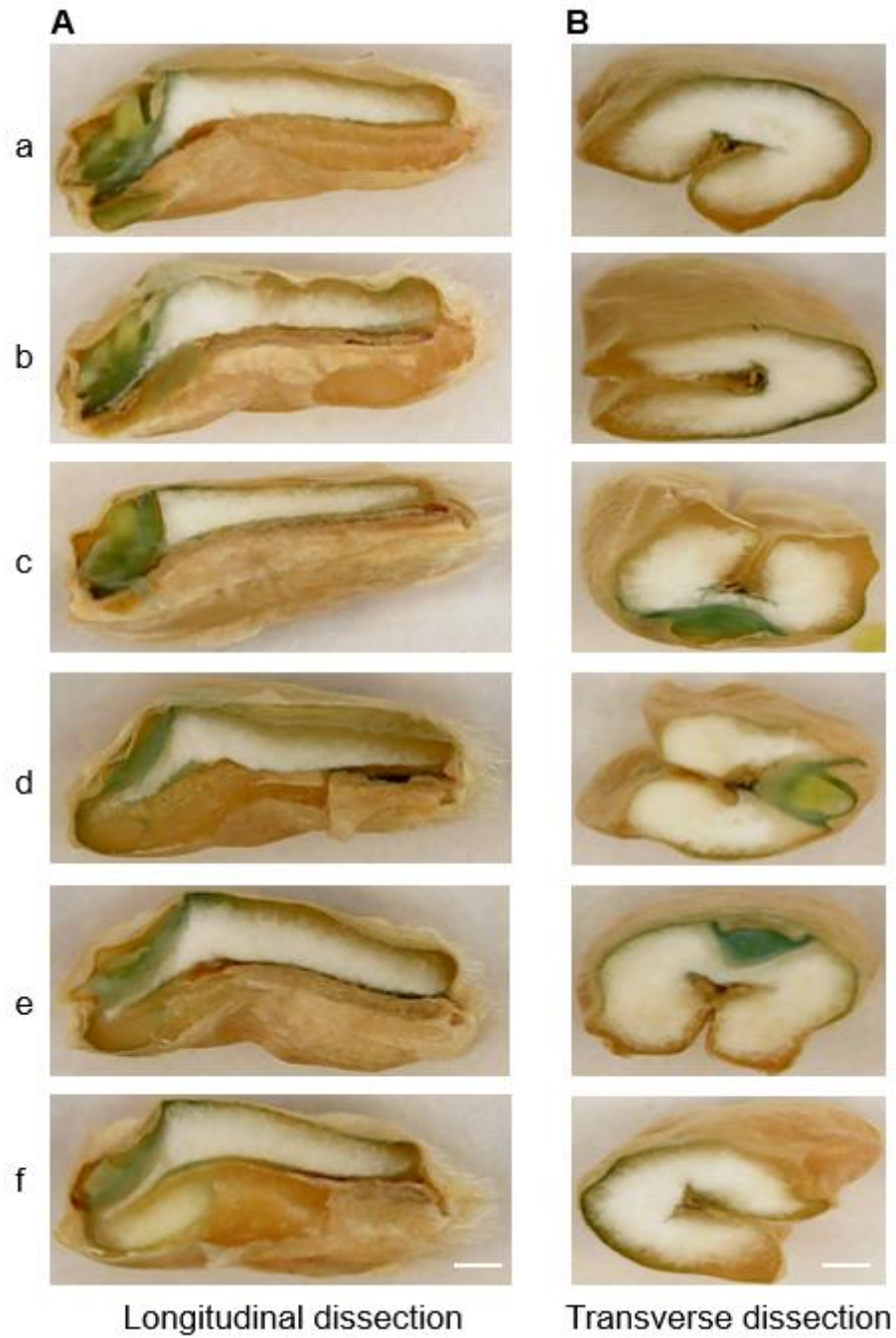


Figure 3.4: Dissection of wheat grains for Perls staining. EMS lines were dissected longitudinally (A) and transversally (B). Randomly six grains (a-f) were selected for Perls staining for each line. Bars, 5 μ m.

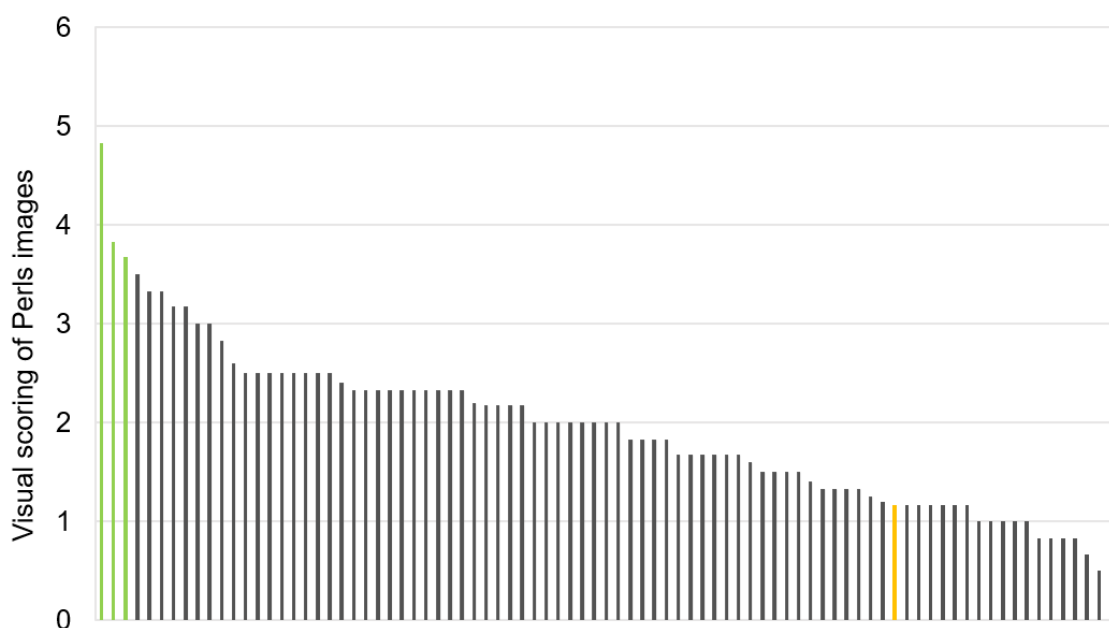


Figure 3.5: Visual scoring of longitudinal dissected of 100 EMS lines. The graph is arranged in the descending order. The yellow bar shows the WT and left side green bars show high Fe lines. Randomly six grains selected for staining for each EMS lines.

3.4.2 Parental lines have higher iron and zinc contents compared to WT

Perls staining gives the rough estimate of Fe content. It also shows the distribution of Fe in the grain tissues. Therefore, we used ICP-OES to measure the accurate Fe and Zn contents in the best EMS lines based on Perls staining. Figure 3.6 shows the Fe and Zn contents in wholemeal and white flour (mg/kg). Line 7077 has significantly ($p < 0.05$, one-way ANOVA with post-hoc Tukey HSD) two times higher Fe and Zn contents compared to WT both in wholemeal and white flour. Similarly, parent lines 7060 and 7054 also have significantly ($p < 0.05$, one-way ANOVA with post-hoc Tukey HSD) higher Fe and Zn compared to WT. These ICP-OES results validate the Perls' results and make these lines best to generate mapping populations to try to identify the underlying genetics for grain Fe contents.

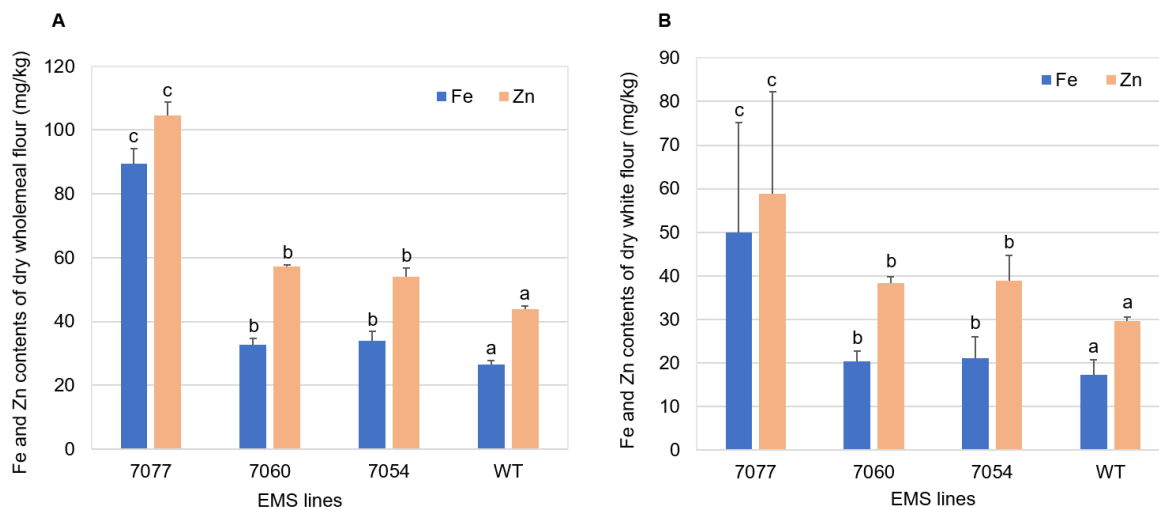


Figure 3.6: Fe and Zn contents of wholemeal (A) and white meal (B) dry flour of EMS parental lines. Error bars denote standard error based on three biological replicates. Lower case letters indicate statistically significant differences ($p < 0.05$) with post-hoc Tukey HSD after one-way ANOVA.

3.4.3 Computation vs personal scoring of Perls images

Computation based scoring offers several advantages for evaluating Perls images. One key benefit is objectivity. By relying on predefined algorithms and metrics, computation-based scoring ensures that evaluations are free from personal biases or subjective interpretations. On the other hand, personal scoring has its limitations. One major concern is subjectivity and bias. As personal scoring involves individual judgment and interpretation, evaluations can be influenced by biases, preferences, or personal interpretations. This can result in inconsistent assessments when different individuals are involved. Figure 3.7 illustrated a comparison of visual score among three different individuals who scored 50 lines of 7077. These results clearly showed the inconsistency in the scoring of Perls images. It also takes a lot of time to score thousands of images. Therefore, we developed a Python (Spyder) based script to analyse the Perls images.

For mapping population, we used stereo microscope (Zeiss Axio Zoom V16) to get a uniform specification for each image and compared it with previous images (DigiHero microscope) to confirm the accuracy of Perl's staining (Figure 3.8). By running the script, each image is first converted to the HSV (Hue, Saturation, Value) format (Figure 3.9) and then a region of interest (ROI) is selected that consists of pixels with H values both above 0.2 and below 0.8, S values above 0.1, and V values above 0.2. Additionally, a map of iron content is generated by displaying the values within the ROI (Figure 3.9C). Then, in red background, the blue colour quantified that represents the Fe contents in each grain. Before using this script, we scored first 50 lines by three individuals and compared those scores with generated by computer (Spyder). After several attempts, we got a final script that has strong correlation ($R^2 = 0.63$) with the personal scores (Figures 3.9 and 3.10).

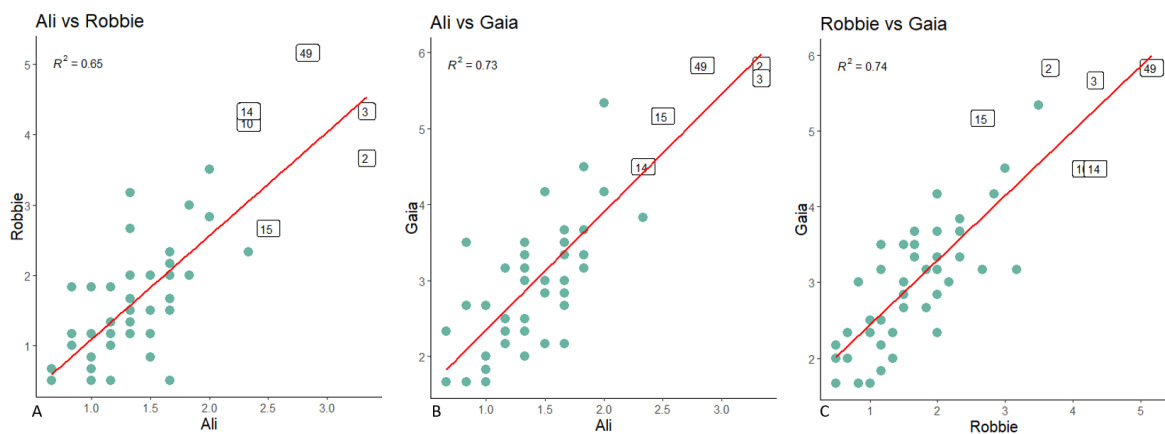


Figure 3.7: Visual score comparison of 50 lines of BC₁F₂ for 7077. The number in the box illustrate the line that had the highest Fe content in each graph. A, B and C showed the correlation between Ali and Robbie, Ali and Gaia, Robbie and Gaia respectively. Randomly six grains selected for staining for each EMS lines.

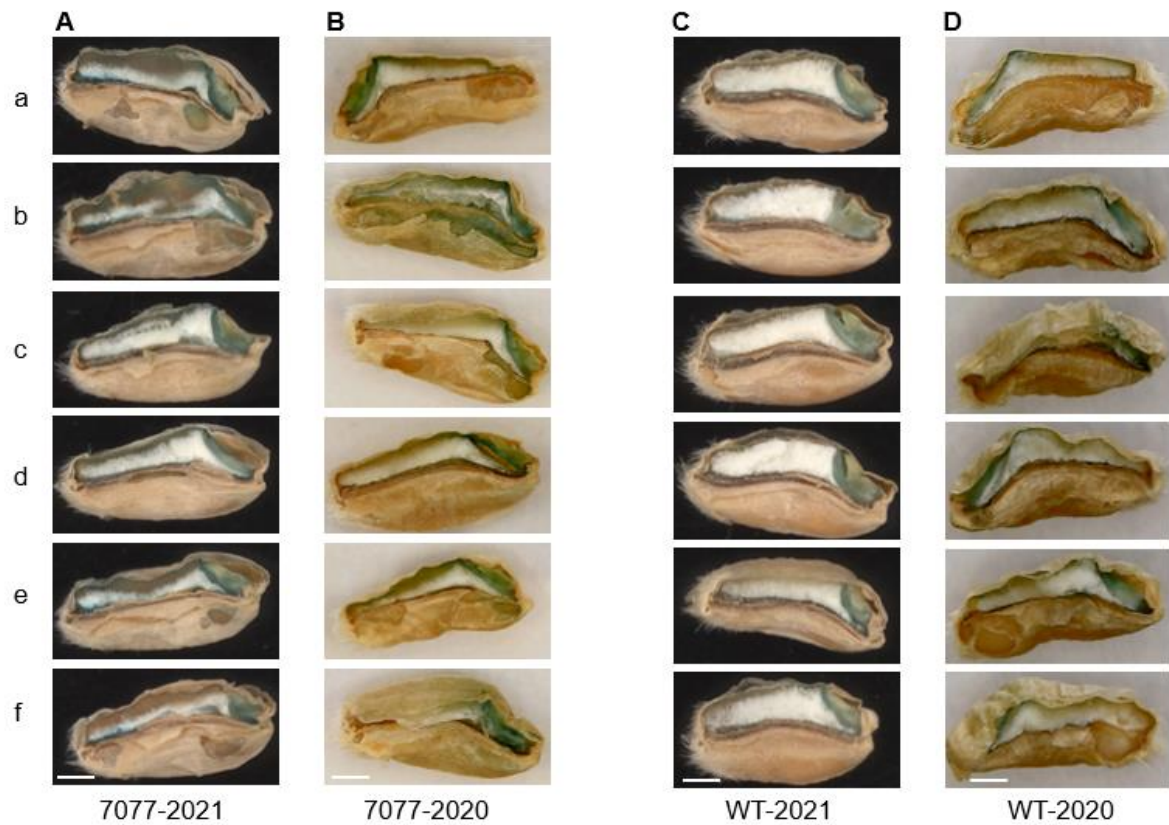


Figure 3.8: Representation of Perl's iron staining of EMS line 7077 parent and WT. A is showing the iron contents of parent in 2021 and B is for 2020. C and D are wild type (Cadenza) for 2021 and 2020. We used stereo microscope (Zeiss Axio Zoom V16) for A and C and DigiHero microscope for B and D. Bars, 5 μ m.

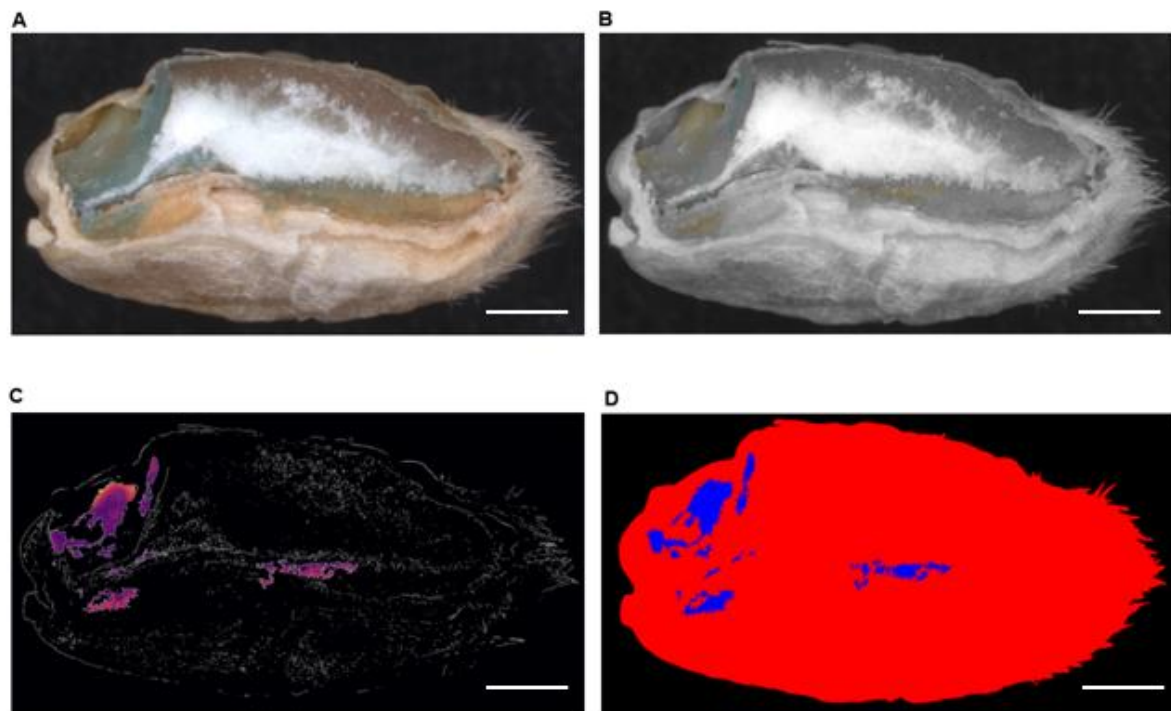


Figure 3.9: Spyder image analysis. Image (A) is the original image after staining. Image (B) is generated in the grayscale and (C) shows the map of Fe content. In (D), the blue area is quantified and represents the Fe content and red area shows whole grain. Bars, 5 μ m.

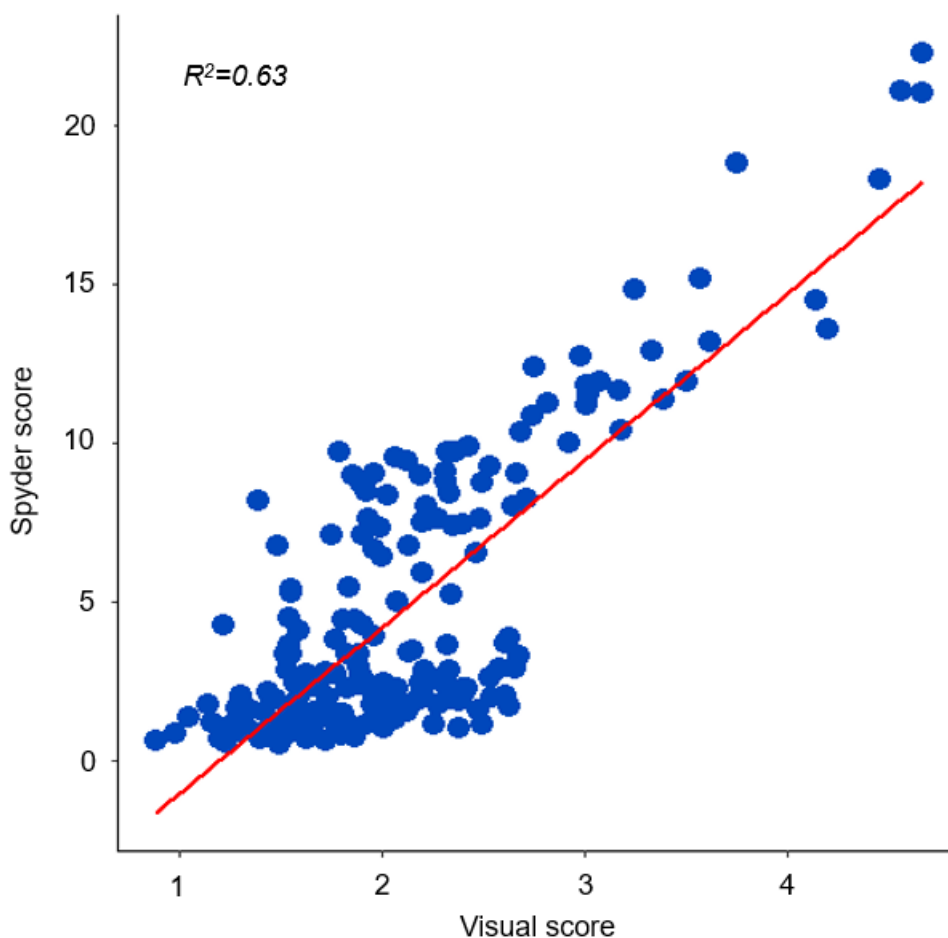


Figure 3.10: Perls image scoring correlation of F₂ population (200 lines) made with parent 7077. Spyder is the computational score of Perls images, and visual score is the average score of three individuals (Robbie Koh Chi Bin, Gaia Galiberti and Muhammad Ali).

3.4.4 Generation of mapping population and selection of extreme bulks by computational scoring

To develop a mapping population, we crossed the best EMS lines (7077, 7060 and 7054) with Cadenza WT. After selfing, we got roughly 200 seeds for each line. We grew these 200 seeds for each population in a greenhouse including Cadenza WT as a control. We observed plant height, number of tillers, number of grains, total weight and thousand grain weight (Figure 3.11). A correlation between agronomic traits and Fe contents showed in table 3.1-3.3. There was no strong correlation between agronomic

traits and grain Fe contents. We applied Perls staining to measure Fe content for these 200 lines for each population. For scoring, we used computational method and quantified Fe content for each line (Figure 3.12, 3.13 and 3.14) for all three populations. We got a wide range of Fe content in whole population.

After computational scoring, this data we used to make two extreme bulks (Figure 3.15). We selected 20 lines for each bulk. In figure 3.12, the left side green bars represent the high bulk (high Fe content) and right yellow side bars represent low bulk (low Fe content). Similarly, figures 3.13 and 3.14 represent the Fe content distributions in population 7060 and 7054 respectively. These extreme bulks are used to identify the QTLs associated for Fe content.

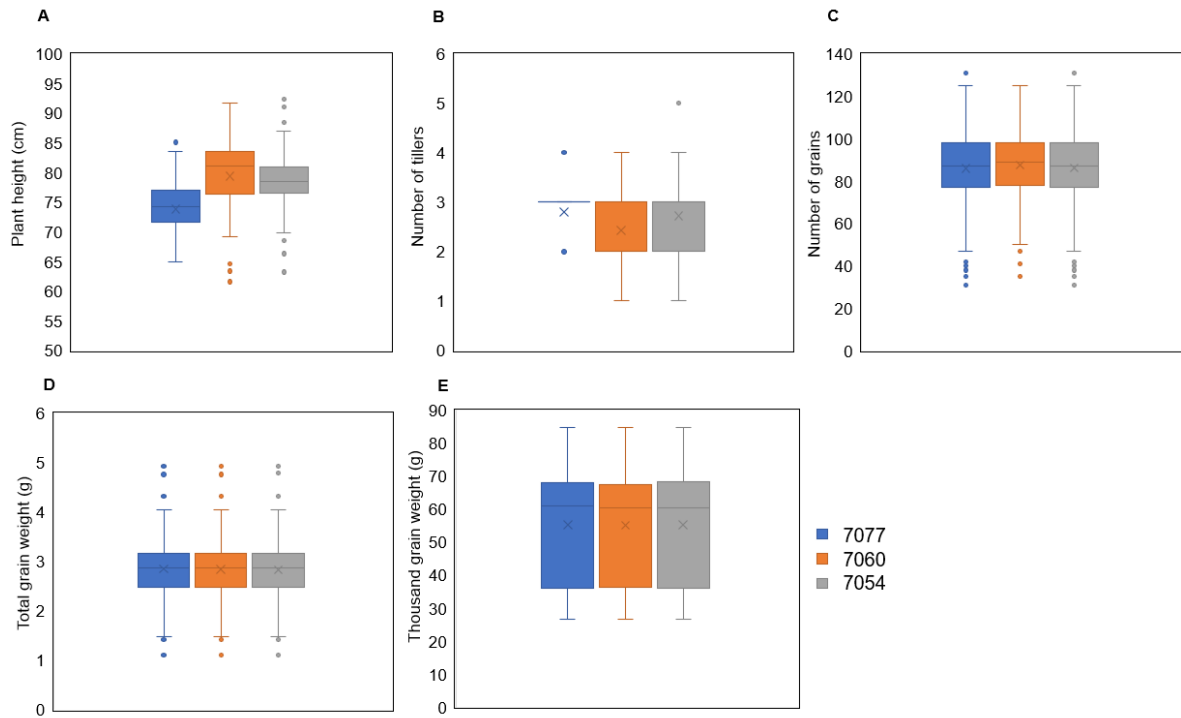


Figure 3.11: Agronomic traits of all three populations. (A) Plant height (cm), (B) Number of tillers per plant, (C) Number of grains, (D) Total weight (g) and (E) Thousand grain weight (g).

Table 3.1: Pearson's correlation coefficients between Fe content and agronomic traits of 7077. Fe content is quantified by computational scoring. PH=plant height, NT=number of tillers. NG=number of grains, TW=total weight TGW=thousand grain weight

Traits	Fe	PH	NT	NG	TW	TGW
Fe	1					
PH	0.180	1				
NT	-0.103	-0.196	1			
NG	-0.277	-0.162	0.468	1		
TW	-0.173	-0.078	0.508	0.852	1	
TGW (g)	0.095	0.141	0.202	0.120	0.268	1

Table 3.2: Pearson's correlation coefficients between Fe content and agronomic traits of 7060. Fe content is quantified by computational scoring. PH=plant height, NT=number of tillers. NG=number of grains, TW=total weight TGW=thousand grain weight

Traits	Fe	PH	NT	NG	TW	TGW
Fe	1					
PH	-0.030	1				
NT	-0.039	0.054	1			
NG	0.023	0.115	-0.065	1		
TW	0.067	-0.002	-0.024	0.768	1	
TGW	0.027	-0.010	-0.087	0.130	0.265	1

Table 3.3: Pearson's correlation coefficients between Fe content and agronomic traits of 7054. Fe content is quantified by computational scoring. PH=plant height, NT=number of tillers. NG=number of grains, TW=total weight TGW=thousand grain weight

Traits	Fe	PH	NT	NG	TW	TGW
Fe	1					
PH	-0.140	1				
NT	0.075	0.205	1			
NG	-0.007	0.024	0.065	1		
TW	0.027	-0.016	0.091	0.848	1	
TGW	0.081	-0.141	-0.060	0.128	0.256	1

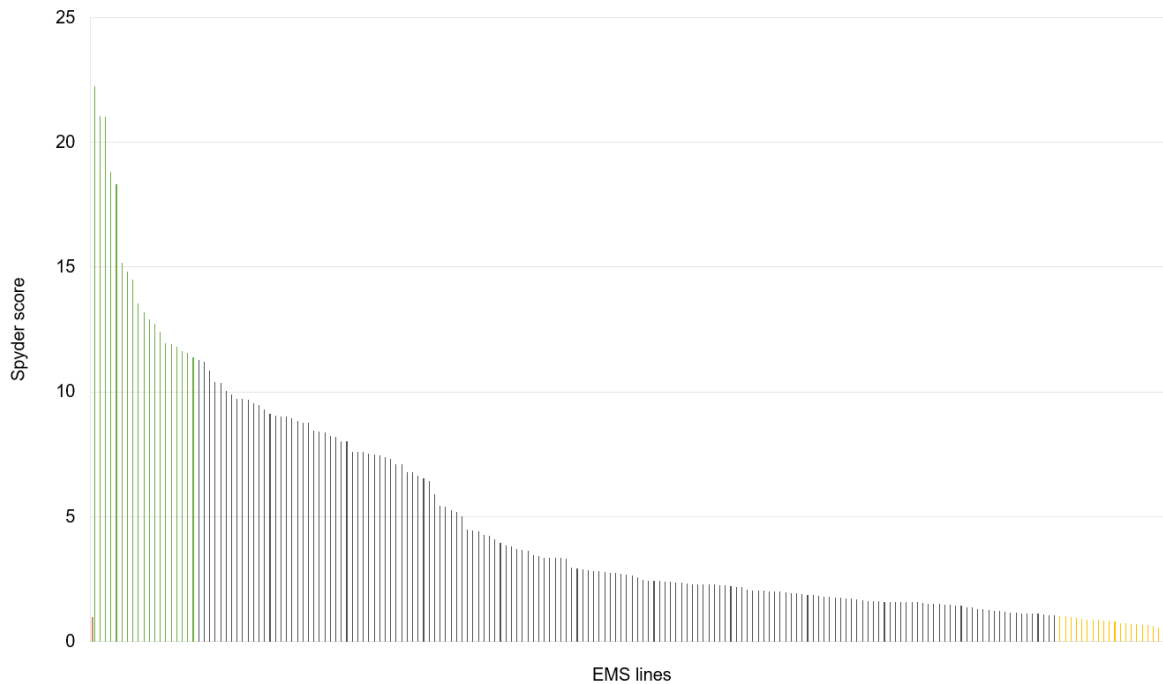


Figure 3.12: This graph shows the computational (Spyder) score for whole F_2 population (200 lines) made with parent 7077. The right-side bars represent the low Fe lines and left side bars with high Fe lines. The yellow and green bars show the lines selected for BSA (bulk segregant analysis). Randomly six grains selected for staining for each F_2 line.

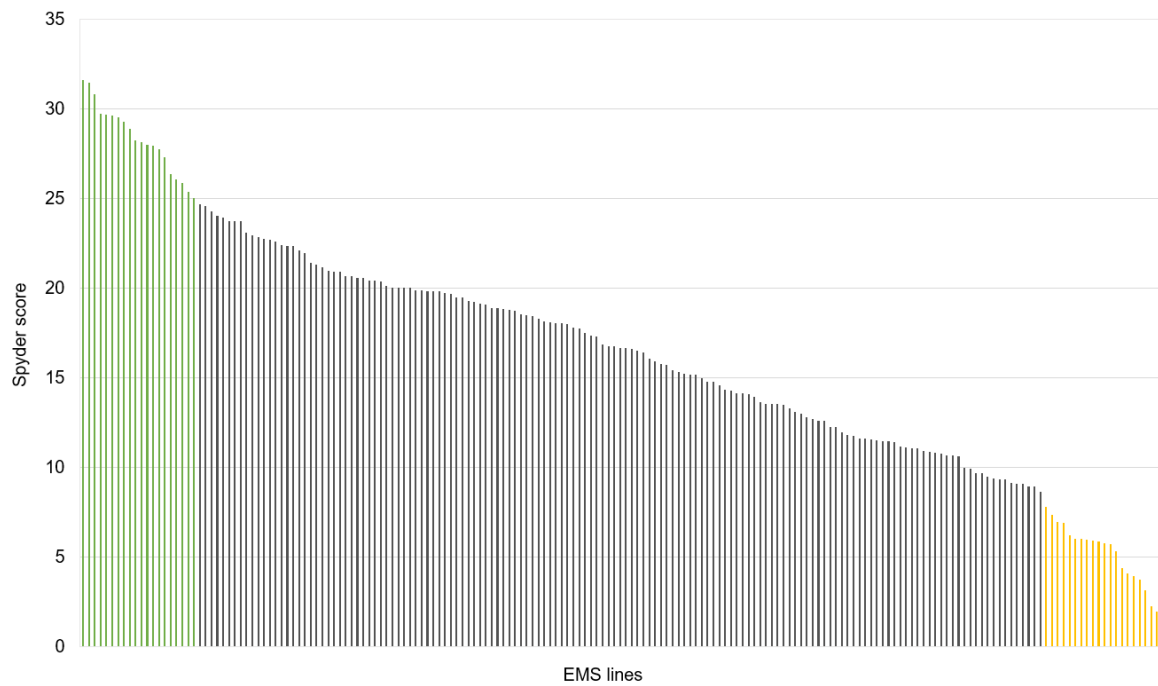


Figure 3.13: This graph shows the computational (Spyder) score for whole F₂ population (200 lines) made with parent 7060. The right-side bars represent the low Fe lines and left side bars with high Fe lines. The yellow and green bars show the lines selected for BSA (bulk segregant analysis). Randomly six grains selected for staining for each F₂ line.

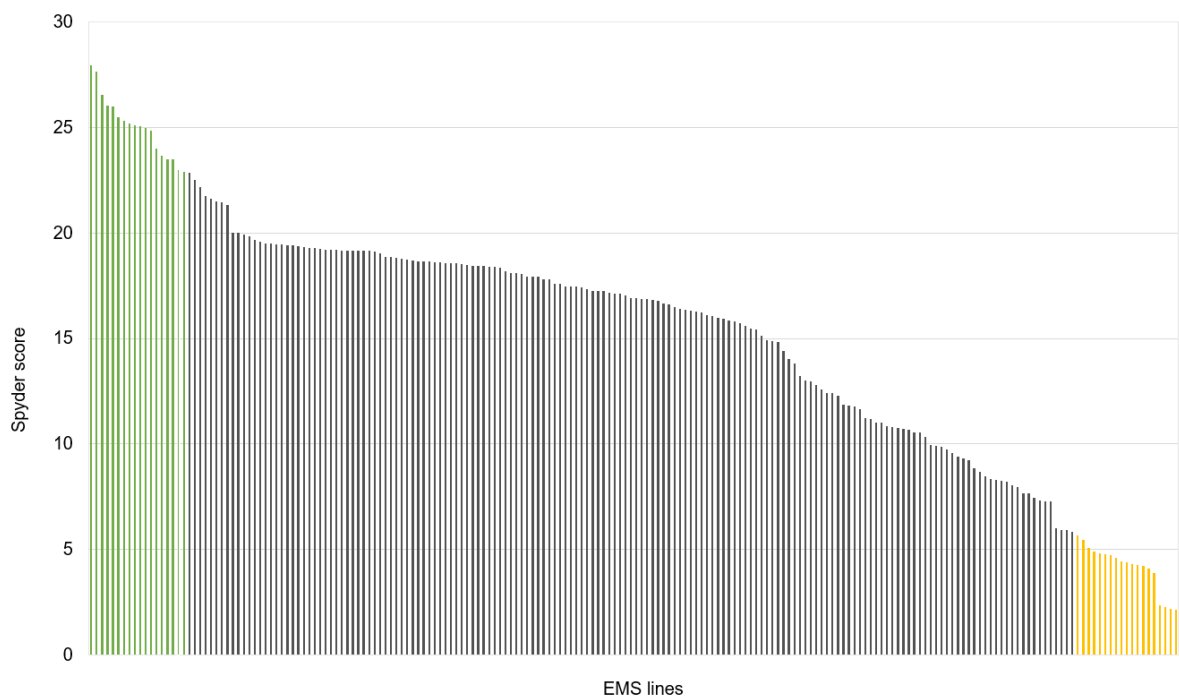


Figure 3.14: This graph shows the computational (Spyder) score for whole F₂ population (200 lines) made with parent 7054. The right-side bars represent the low Fe lines and left side bars with high Fe lines. The yellow and green bars show the lines selected for BSA (bulk segregant analysis). Randomly six grains selected for staining for each F₂ line.

A



B



Figure 3.15: Perls staining images of bulks for BSA 7077. Randomly five lines selected from high Fe bulk (A) and five from low Fe bulk (B). Bars, 5 μ m.

3.4.5 QTLs identified by Bulk segregant analysis

We applied BSA tool to identify the QTLs linked for Fe content. For this, we followed a method known QTLseqr described in Mansfeld & Grumet, 2018. Plant breeders and researchers can undertake NGS-BSA using QTL-seq or G' analysis methods quickly and easily with the QTLseqr software.

3.4.5.1 Filtering SNPs using QTLseqr

BSA is a useful method for quickly finding markers in the genomic region related with a phenotype of interest. Any sort of codominant marker, including SNP markers, can be used with BSA (Giovannoni et al., 1991; Michelmore et al., 1991). This has made it possible to modify this method for use with reads from next-generation sequencing (NGS). The price of NGS has recently dropped, which has further fuelled the growth of this techniques. We looked the SNP data generated by exome-capture on the high bulk and low bulk for each population before applying SNP filtering options (Figure 3.16). We plotted SNP-index per bulk (Figure 3.16C and D) We found peaks on right end and SNPs were approximately normally distributed near 0.5 in an F₂ population of 7077. Filtering options provided by QTLseqr helped to decrease noise and enhance results. As a result, we tried to filter out SNPs with poor confidence due to limited coverage and SNPs that might be in repetitive regions. The basic basis for filtering is read depth for each SNP. Applying filter options with reference allele frequency between 0.2 to 0.8, total sample depth ≥ 100 (i.e reads in both high plus low bulk), and per sample read depth ≥ 40 (i.e. reads in either high or low bulk), total 935,075 SNPs were removed from 998,201.

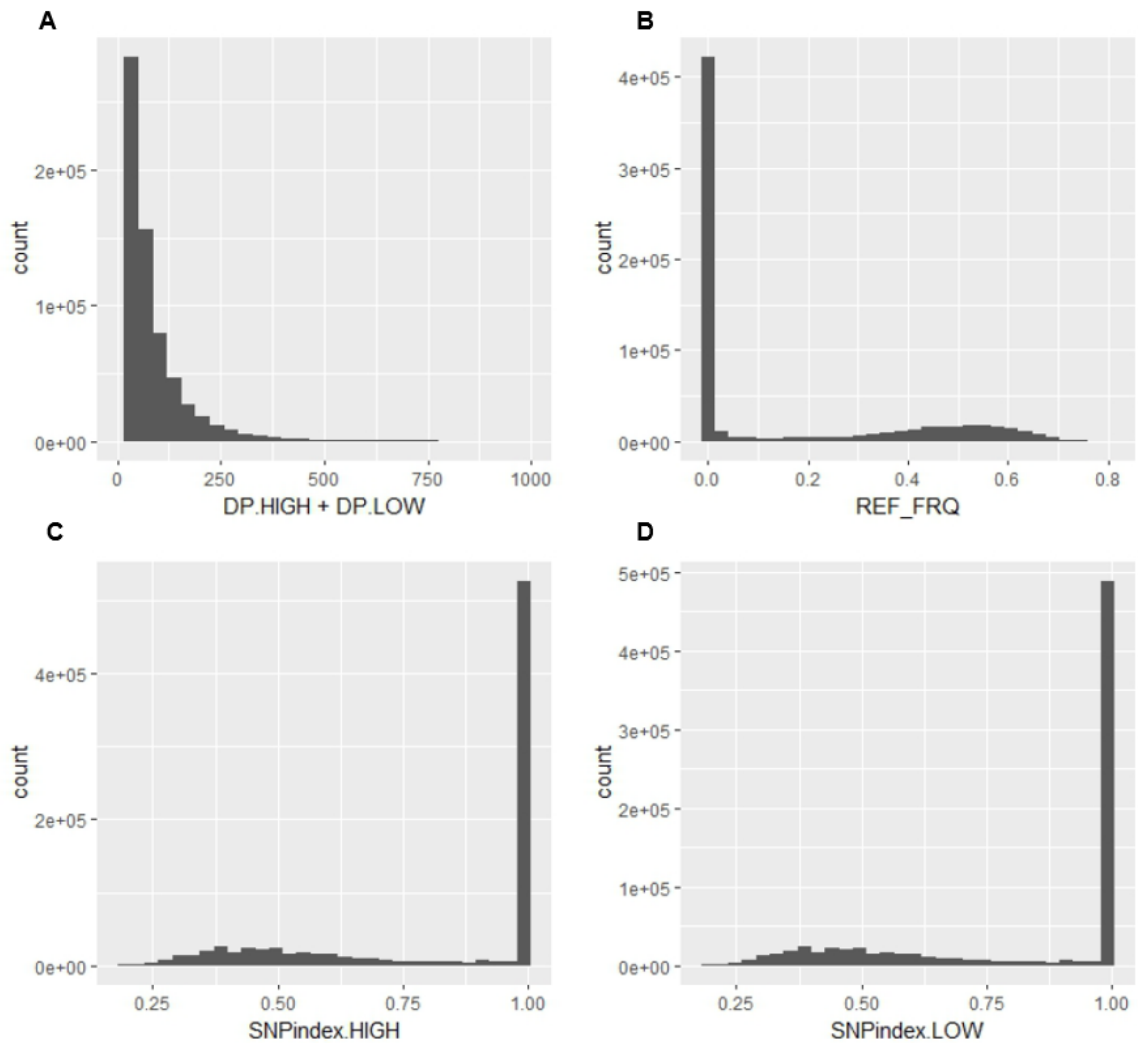


Figure 3.16: This figure shows the data of population 7077 before filtering. Total read depth of both high and low bulks (A), Total reference allele frequency (B), SNP-index of high bulk (C), and SNP-index of low bulk. SNP-index = alternate allele / total reference allele.

After filtering, 902,685 SNPs were removed that were between Cadenza and the reference (Chinese Spring) (Figure 3.16B). This was because of reference allele depth was zero. In filtering, we selected the reference allele frequency 0.1 instead of 0.2 and get more SNPs (Table 3.1) and change the total read depth 400 to 800 as we can see in the histogram the total read depth in this population goes to 800 (Figure 3.17A). We got 95,516 SNPs out of 998,201 and it seems 90% SNPs were removed which might

be due to reference allele frequency We tested different filter options to look the SNPs (Table 3.1)

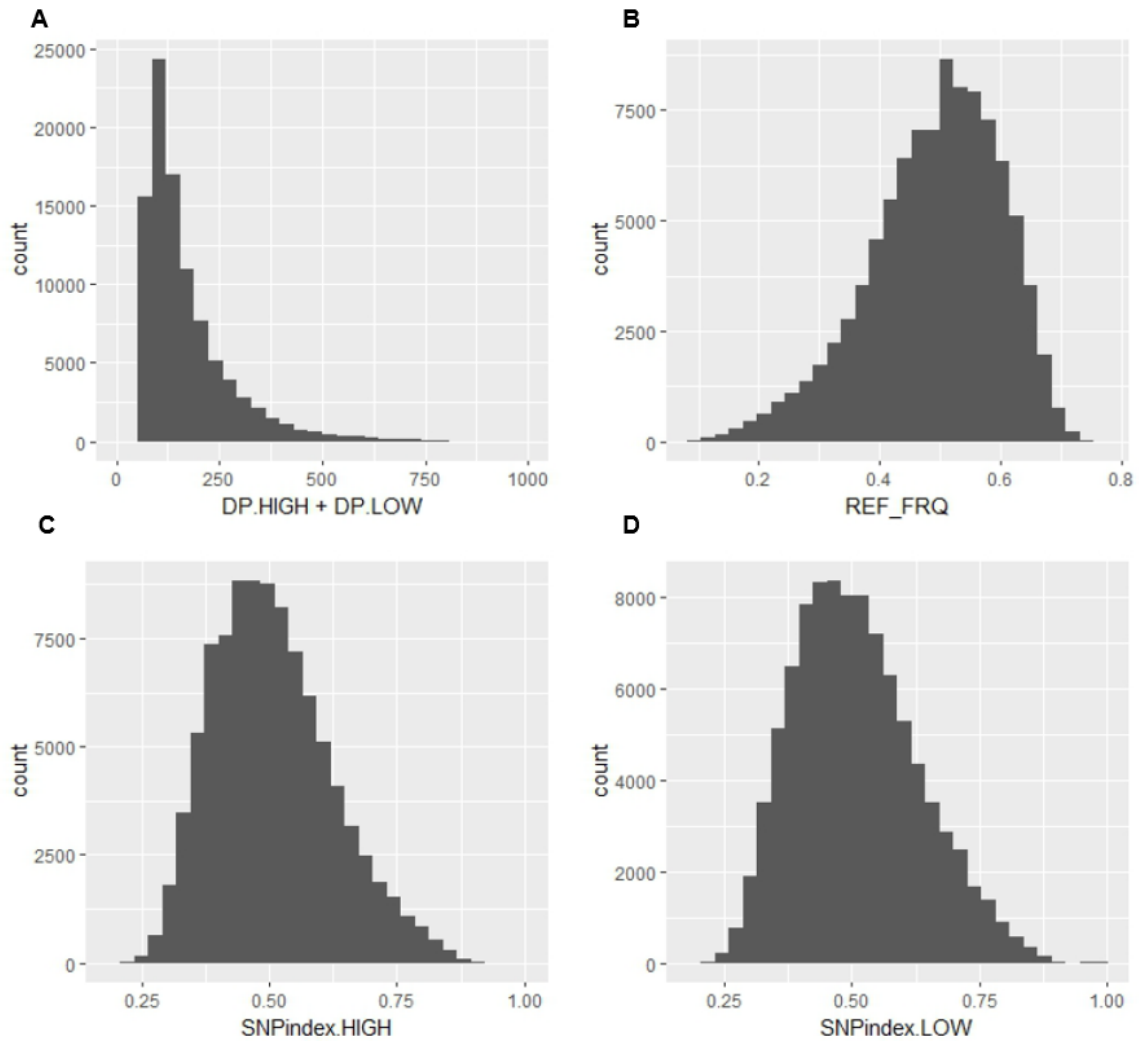


Figure 3.17: This figure shows the data of population 7077 after filtering. Total read depth of both high and low bulks (A), Total reference allele frequency (B), SNP-index of high bulk (C), and SNP-index of low bulk.

Table 3.4: SNPs filter options for 7077. Filt=filter, REE=Reference Allele Frequency, min=minimum, max=maximum

Filter	REF-Frq	minTotalDepth	maxTotalDepth	minSampleDepth	Total nSNPs	Filtered	Remaining
Filt1 (Mansfeld & Grumet, 2018)	0.20	100	400	40	998,201	937,075	61,126
Filt2 (change REF-frq, min and max depth)	0.1	60	800	30	998,201	902,685	95,516
Filt3 (changed min sample depth)	0.1	60	800	20	998,201	892,579	105,622
Filt4 (changed min sample depth)	0.1	60	800	10	998,201	892,238	105,963
Filt5 (changed min total depth)	0.1	30	800	10	998,201	869,411	128,790
Filt6 (changed min total depth)	0.1	20	800	10	998,201	868,338	129,863
Filt7 (Changed min sample depth)	0.1	20	800	5	998,201	868,338	129,863
Filt8 (Changed min sample depth)	0.1	10	800	5	998,201	868,338	129,863

3.4.5.2 BSA analysis using QTLseqr

BSA offers a cost-effective and efficient alternative by utilizing NGS technologies. The approach involves sequencing DNA from individuals with extreme trait values, such as individuals at the opposite ends of a phenotypic distribution. By comparing the genomic sequences of these individuals, BSA can identify genetic variants that are associated with the observed phenotypic differences.

After selecting the threshold level, we applied QTLanalysis function to include the SNPs in the 10 Mb window size. We used a 0.01 threshold level to run the Gprimeanalysis function to plot the G' value. To verify if the null distribution of G' values is close to log normally distributed is crucial since p-values are inferred from the null distribution of G' values. To achieve this, we used the plotGprimeDist function, which displays the log-normal null distribution along with the G' histograms of both the raw and filtered G' sets. (Figure 3.18). In our case, "deltaSNP" with 0.01 threshold revealed a better G' null distribution (Figure 3.18B). It shows that the G' distribution is close to log-normal, therefore, we selected this filter option to plot some genome-wide figures and looked the distribution of SNPs (Figure 3.19). We also measured and plotted the deltaSNP-index. Figure 3.20 shows histogram of the tricube-smoothed $\Delta(\text{SNP-index})$ of all chromosomes in the window size 10 Mb and corresponding two sided confidence intervals (CI) 95% (red), and 99% (green). There are some regions (Chr 1A, 2A, 2B, 3B, 4B, 6A, and 6D) that have $\Delta(\text{SNP-index})$, that pass the CI thresholds and could be putative QTLs. G' is an alternative approach to verify statistical significance of QTLs from NGS. It is a robust method that is less sensitive to sequencing errors and mapping biases than $\Delta(\text{SNP-index})$. For G' analysis, the directionality of the SNP-index is equally crucial. The (SNP-index) should be greater than 0 if the allele causing the trait

comes from a high bulk. Nevertheless, if the $\Delta(\text{SNP-index})$ less than 0 then the contributing is the one with the low bulk. Additionally, we also plotted the G prime values to look if these regions are significant (Figure 3.21). It shows like there are QTL identified on Chr1A, 2A, 2B, 3A, 3B, 3D, 4A, 4B, 5B, 6A, 6D, and 7B. We also used the plotQTLStats function to calculate the $-\log_{10}(\text{p-value})$. Although this number is a straight derivation of G', it may be easier to understand in some regions. The p-value also supports the selected QTLs based on G' value (Figure 3.22).

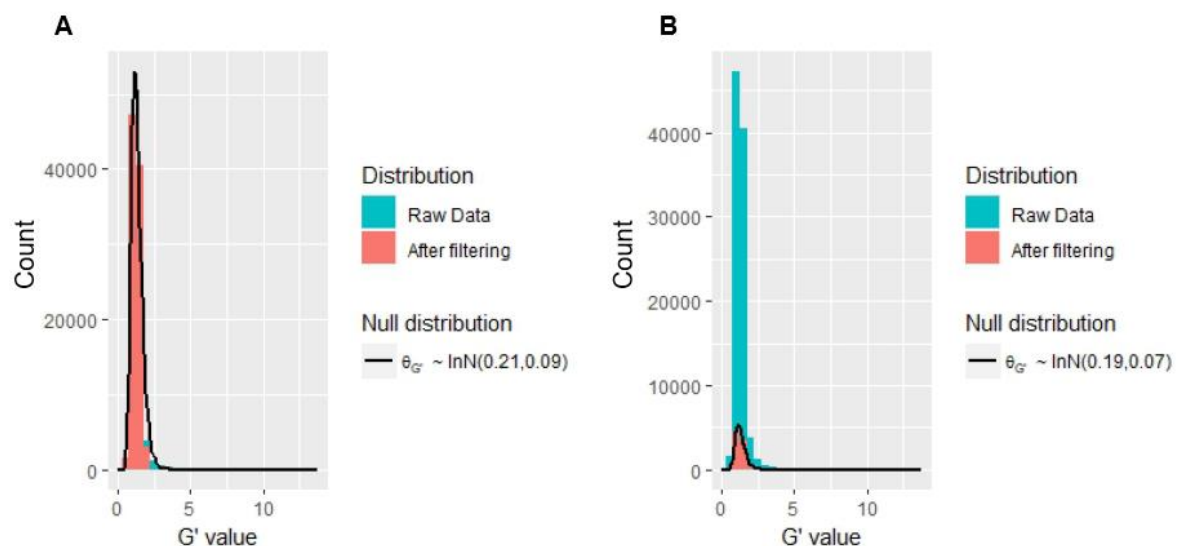


Figure 3.18: These histograms show the G' value distribution with a threshold of 0.01 for P7077 using method “Hamplé” (A) and deltaSNP (B). G' - A tricube-smoothed G statistic is predicted by constant local regression within each chromosome using the tricubeStat function.

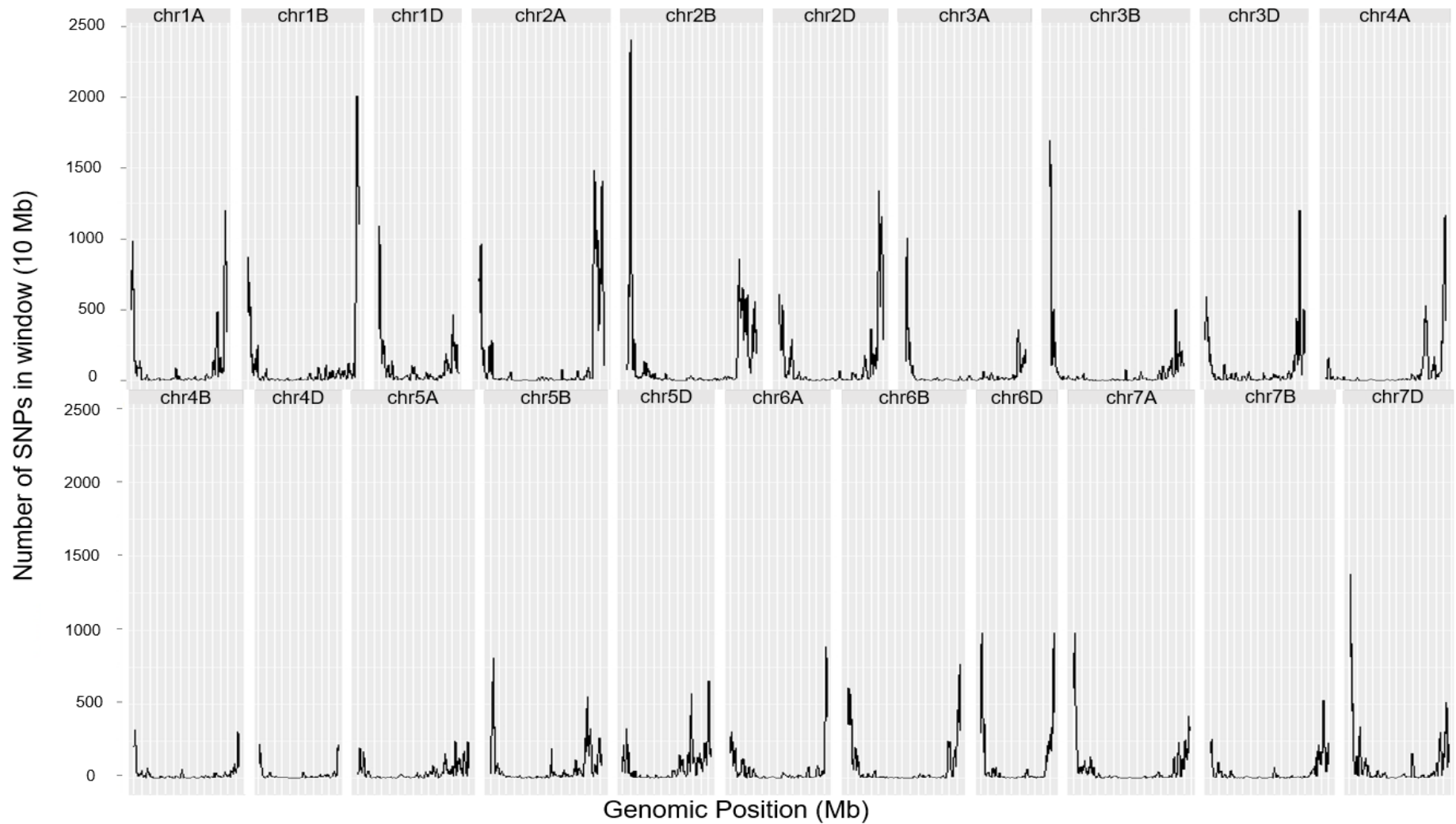


Figure 3.19: Genome-wide distribution of number of SNPs of 7060 in a window size 10Mb.

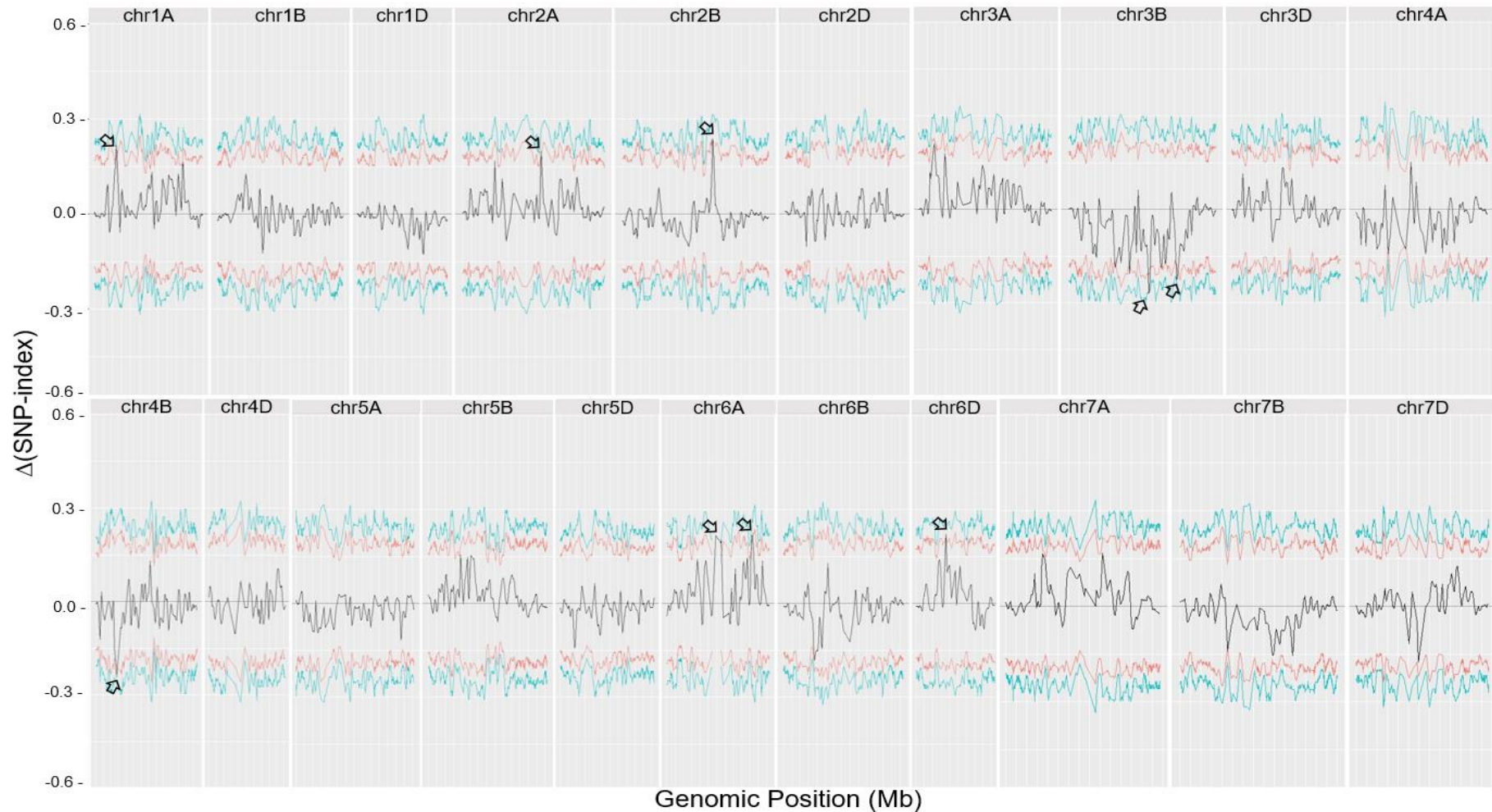


Figure 3.20: The tricube-smoothed $\Delta(\text{SNP-index})$ of 7060. $\Delta(\text{SNP-index})$ of all chromosomes in the window size 10 Mb and corresponding two sided confidence intervals (CI): 95% (red), and 99% (green). The arrows illustrated the significant region that passed the confidence intervals.

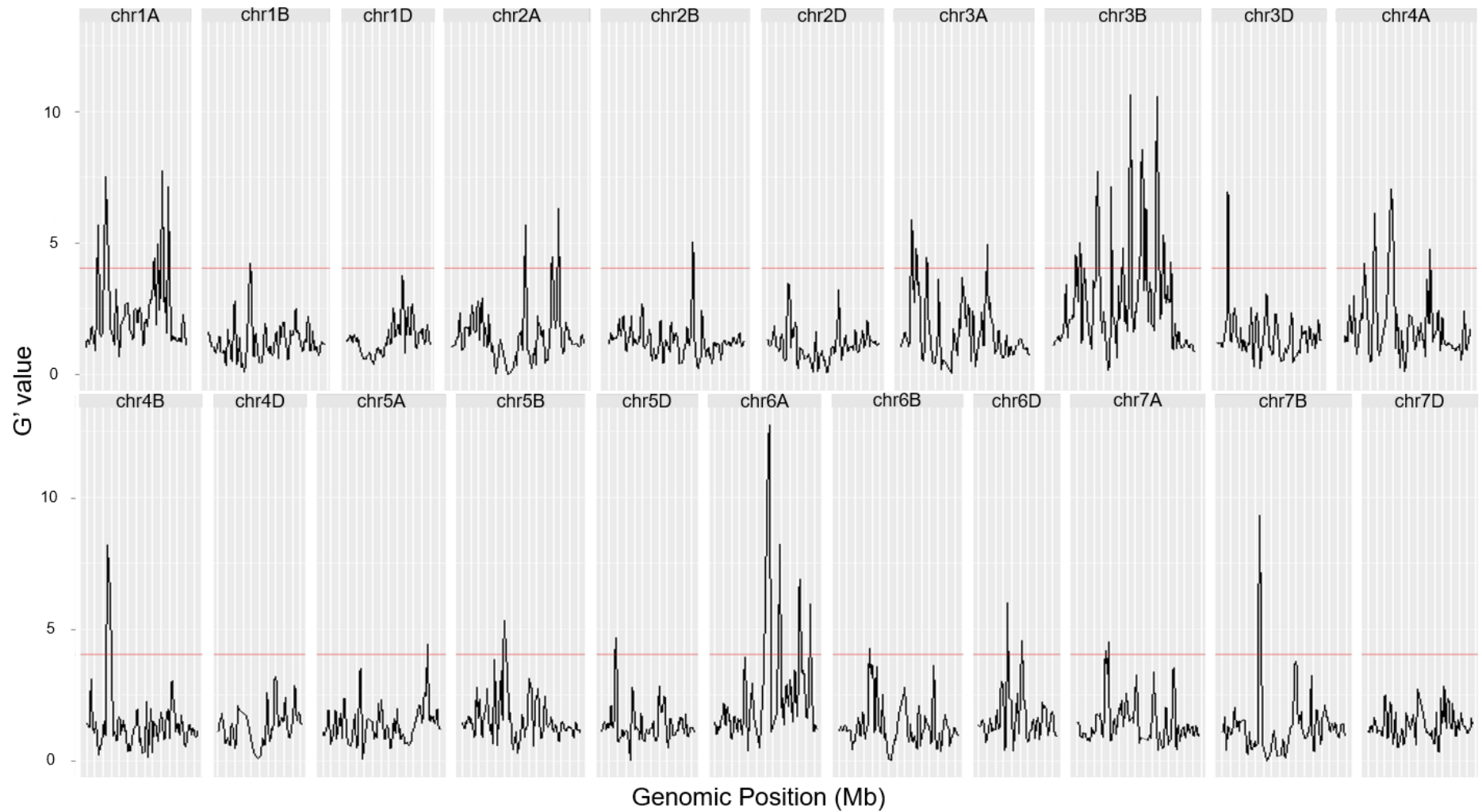


Figure 3.21: G' values distribution of 7060 of all chromosomes in the window size 10 Mb with the FDR (q) of 0.01 (red).

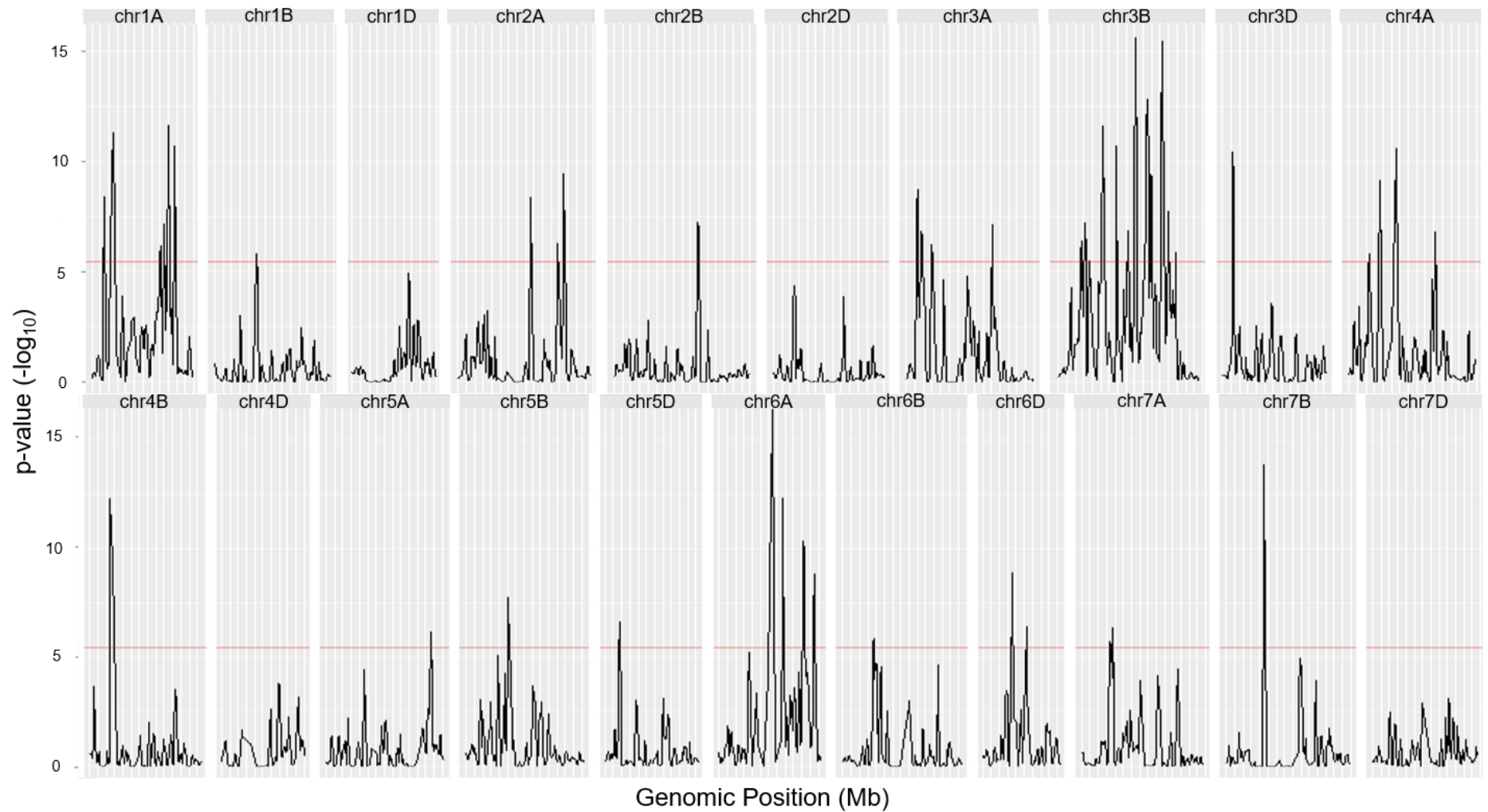


Figure 3.22: p -value ($-\log_{10}$) distribution of 7060 of all chromosomes in the window size 10 Mb with the FDR (q) of 0.01 (red).

3.4.5.3 Putative QTLs identified on Chr3B in population 7060

We followed the above mentioned (section 3.4.5.1-2) steps for all three populations (7077, 7060, and 7054). Unfortunately, population 7077 and 7054 could not pass confidence interval 95 and 99. Only population 7060 has a significant region on chr1A, chr2A, chr2D, chr3B, chr4B, chr5D, chr6A, and chr7D (Figure 3.23) and passed the confidence interval 95. Interesting, chr3B also passed 99 confidence interval and has a strong peak. This region has a $\Delta(\text{SNP-index})$ 0.35 and contributed from high Fe bulk. Chr3B is a 5.2 Mb region with 13 SNPs. This region has 381 genes and 5 of them are heme binding that is a complex compound composed of Fe bound to a porphyrin ring. Based on our results, we can consider Chr3B as a putative QTL. Due to shortage of time, we could not carry this project forward to validate Chr3B.

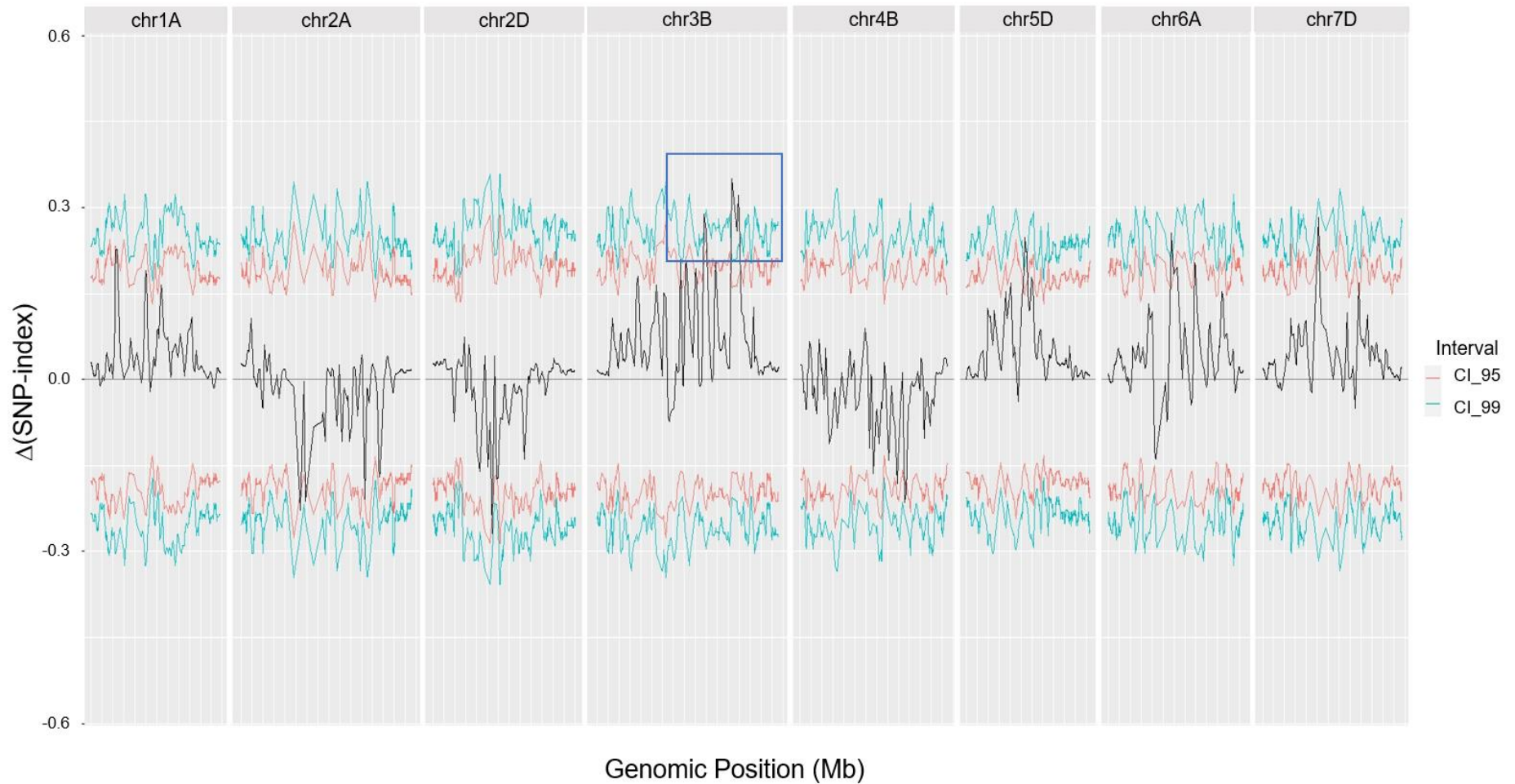


Figure 3.23: The tricube-smoothed $\Delta(\text{SNP-index})$ of 7060. $\Delta(\text{SNP-index})$ of chr1A, 2A, 2D, 3B, 4B, 5D, 6A, and 7D of population 7060 in the window size 10 Mb and corresponding two sided confidence intervals (CI): 95% (red), and 99% (green). Chr3B pass the confidence interval thresholds and shows the contribution from the high bulk.

3.5 Discussions

3.5.1 EMS population shows variations in the grain iron content

This study investigated the potential of EMS population for Fe content and reported two times higher Fe contents compared to Cadenza WT. These findings revealed a previously unexplored EMS population for improving Fe content in wheat, which holds promise for addressing micronutrient deficiencies. Variations in the wheat grain Fe content within an EMS population are of considerable interest in the context of addressing dietary deficiencies and improving food security. In this study, we observed substantial variations in the grain Fe contents among different lines within the EMS population (Figure 3.5, 3.12, 3.13, and 3.14), highlighting the genetic factors influencing Fe accumulation in wheat grains. Some lines had three folds compared to the WT. The observed variations in grain Fe content are largely caused by genetic diversity. Within the EMS population, different wheat lines may have unique genetic characteristics that affect the uptake, transport, and storage of iron in grains. Our results suggest that the EMS population may be used to select and breed wheat lines with greater grain Fe content (Amiri et al., 2020). To promote marker-assisted breeding for high-Fe wheat varieties, future research should concentrate on finding specific genes and genetic markers linked to iron accumulation in wheat grains (Jones et al., 2008).

A successful plant breeding programme depends on genetic variability in the breeding materials since it serves as the basis for selection. Wheat cultivars and wild relatives possess diverse genetic backgrounds, resulting in differences in several traits, including Fe accumulation in grains. For breeding programmes, wild relatives of wheat like wild emmer (*Triticum turgidum* ssp. *dicoccoides*) and *Aegilops* species have

proved an important genetic resource. In comparison to cultivated wheat, they frequently display greater genetic variety, including changes in grain Fe concentration (Peleg et al., 2009; Uauy et al., 2006). Moreover, the Fe content of the grain varies naturally among different wheat cultivars. Significant variations in Fe levels amongst wheat cultivars have been seen in several investigations (Caldelas et al., 2022; Korzeniowska & Stanislawska-Glubiak, 2022). Tiwari et al., (2009) found 17.8–69.7 mg/kg Fe in recombinant inbred lines (RILs) mapping population. As well, Fe contents were reported from 28.5 to 46 mg/kg in doubled haploid (DH) population. The wild family of wheat (*Aegilops tauschii*) explored for this objective, where the Fe contents were ranged from 30.33 to 69.14 mg/kg (Arora et al., 2017). In another study, Kumar et al., (2018) reported grain Fe contents ranged 24.50–44.30 mg/kg using 246 spring wheat genotypes. Interestingly, we found grain Fe contents ranged 32.71–89.48 mg/kg that is higher compared to previously reported. These changes are most likely brought about by variations in the genetic elements controlling the absorption, transport, and storage of Fe within the grains. However, it is crucial to remember that natural variations in Fe content could not always support efforts to increase desired traits. Even though some wheat cultivars and wild relatives may have high grain Fe content, they may also have undesirable agronomic features, lower yield potential, or other drawbacks that need to be overcome by careful breeding techniques (Distelfeld et al., 2007). Some studies show that large grains often result in reduced Fe contents and has a potential dilution effect. Recently a study reported increased grain yield in modern wheat cultivars and associated with decreased Fe and Zn contents (Jiang et al., 2022).

In summary, our results shows that an EMS population of wheat contains sizable variability in grain Fe content. This variation could be due to the genetic variance in EMS population. A comprehensive strategy encompassing genetic improvement, the development of agronomic practises, and biofortification techniques should be explored to improve grain Fe content. The results of this study support ongoing initiatives to address Fe deficiency and enhance the nutritional value of wheat grains.

3.5.2 Advantages of Perls staining vs ICP-OES

The accurate determination of Fe content in wheat grains is crucial for evaluating nutritional quality and leading breeding programs aimed at improving Fe bioavailability. Numerous analytical approaches are available for this purpose, including Perl's staining and inductively coupled plasma optical emission spectroscopy (ICP-OES). In our study, we applied Perls staining to phenotype the EMS lines for grain Fe content and localize the Fe content in thousand images (Figure 3.2). Comparing Perl's staining method to ICP-OES to determine the Fe content in wheat grains reveals considerable cost advantages. Perl's Prussian blue, a straightforward and reasonably priced staining chemical, is used in the staining process (Carleton, 1980). ICP-OES, on the other hand, demands advanced equipment and specialised knowledge, making its implementation significantly more expensive. Perl's staining is an appealing alternative due to its affordability, especially for research initiatives with tight budgets or investigations involving many samples.

One of the unique advantages of Perl's staining is its ability to provide information on the localization of iron within the wheat grain. The Prussian blue stain from Perl forms a blue complex when it reacts only with ferric iron (Fe^{3+}) (Iezzoni, 2018). The distribution of Fe in various anatomical locations, such as the aleurone layer,

endosperm, and embryo, can be seen by viewing the stained grains under a microscope. Understanding the bioavailability of Fe in the grain and identifying potential genetic improvement targets can both benefit from this information. In contrast, ICP-OES, gives a broad measurement of the sample's total Fe concentration without differentiating between how it is distributed throughout the various grain tissues. ICP-OES can accurately and sensitively measure total Fe concentrations (R. Ma et al., 2004), however it is unable to provide information on the location of Fe inside the grain. Combining Perl's staining and ICP-OES allows us to better understand the dynamics of Fe in wheat grains by providing quantitative data on total iron concentration (from ICP-OES) and qualitative information on Fe localisation (from Perl's staining).

3.5.3 Computational scoring handles large datasets and standardise for complex traits like iron

In this study, we employed computational scoring methods to handle large datasets generated by Perl's staining and standardize the assessment of complex traits such as Fe levels. Due to the availability of high-throughput genomic and phenotypic data as well as the demand for effective and dependable analysis techniques, the use of computational methodologies has grown in importance in agricultural research. We aimed to overcome the difficulties involved in analysing Fe levels in wheat grains and create a standardised framework for determining Fe levels by using computational scoring approaches.

The capability of employing computational scoring approach to process enormous datasets quickly is one of their main benefits. The development of genotyping and phenotyping technology has given agricultural researchers access to a wealth of

information from plant research. When working with huge datasets, manual scoring systems are frequently time-consuming and prone to human mistake. On the other hand, computational approaches can process large datasets in a fraction of the time, enabling quicker analysis and hypothesis testing (Manavalan, 2020; Singh et al., 2019). Additionally, the scalability of computational scoring techniques enables researchers to work with ever-larger datasets, enabling more thorough analyses of complicated features like wheat grain Fe content (Peng et al., 2022). Computational scoring techniques also have the benefit of impartiality and reproducibility. The reproducibility of research can be hampered by this subjectivity's potential to add bias and variability into the findings. The use of predetermined procedures and criteria in computational scoring methods, however, ensures objective evaluations (Meena et al., 2022). In the initial screening of EMS lines for grain Fe content, we used a manual (visual) scoring approach. However, in mapping population, it was not possible to score thousands of images manually. Therefore, we used a computation script to analysis the Perls images and quantify the Fe content in wheat grains.

3.5.4 Comparison of identified QTLs with previous studies

We focused on the identification of QTLs associated with wheat grain Fe content specifically on chromosome 3B. A genome-wide association study (GWAS) was carried out by Velu et al., (2018) to find QTLs linked to wheat grain iron and zinc contents. 29 QTLs for grain Fe were found in the study. Twelve of these QTLs were shown to be associated with both grain iron and zinc. The study also compared the discovered QTLs with earlier research and discovered that several of the QTLs were compatible with earlier research. But in this investigation, no QTLs for grain Fe concentration on chromosome 3B were found, whereas that was the most significant

locus we discovered in the EMS population 7060. Another study by Xu et al., (2012b) identified QTLs associated with grain iron and zinc concentrations in a RIL population developed from a cross between two cultivars of Chinese wheat. The study identified 12 QTLs for grain iron and 16 QTLs for grain zinc. Among these QTLs, three QTLs were identified for both grain iron and zinc. The study also compared the identified QTLs with previous studies and found that several QTLs identified in this study were consistent with earlier studies. However, no QTLs were identified on chromosome 3B for grain Fe content in this study as well. We identified novel QTLs on chromosome 3B that have not been previously reported. These novel QTLs highlight the possibility of discovering new genetic variables controlling Fe accumulation and offer more proof of the genetic complexity underlying grain Fe levels in wheat. The discovery of these novel QTLs expands our understanding of the genetic architecture on chromosome 3B and emphasizes its role in determining grain Fe content. These findings provide valuable insights for breeders and geneticists aiming to enhance the dietary quality of wheat grains. Further research is needed to fully characterize the identified QTLs and unravel their functional implications.

Chapter 4: General Discussion

4.1 Summary of the thesis

In this thesis, we focused on the investigation of genes affecting Fe and Zn in wheat grains through the implementation of forward and reverse genetic approaches. Micronutrients play a crucial role in human nutrition, and wheat, being a staple food for a significant portion of the global population, holds immense importance in addressing micronutrient deficiencies worldwide. This research aimed to elucidate the genetic factors and underlying mechanisms responsible for the accumulation of essential micronutrients in wheat grains, thereby providing valuable insights for crop improvement and human health.

In the first part of the thesis, we identified and characterized candidate genes associated with micronutrient accumulation in the *ZIP* gene family. We identified 14 *TaZIP* genes in wheat and selected three highly expressed candidate genes for functional characterization. We tested the role of *TaZIP11*, *TaZIP13*, and *TaZIP14* in plant growth and their effect on wheat grain micronutrients by generating homozygous null mutants. Only the one cross from *TaZIP13* has the ability to alter Fe and Zn and other crosses could not affect the micronutrients. This could be due to burden of mutations in TILLING population and need further investigation to understand the role of these genes.

Secondly, we used a forward genetics approach to gain a deeper understanding of the genes and molecular pathways influencing micronutrient content in wheat grains. For this study, we screened EMS population using Perls staining for the phenotyping of Fe contents in wheat grains. Perls staining presented a wide range of Fe contents and localization in grain tissues. By selecting the high Fe lines based on staining and ICP-OES, we generated three mapping populations. We used bulk segregant analysis

(BSA) to map genetic loci associated with high Fe contents. However, we only found significant loci in one of the three populations. These significant loci were located on Chromosome 3B.

The findings from both forward and reverse genetics approaches collectively contribute to the understanding of the genetic basis of micronutrient accumulation in wheat grains. This study can serve as a foundation for developing targeted strategies to enhance the bioavailability and nutritional value of wheat, ultimately aiming to combat widespread micronutrient deficiencies.

4.2 Nutrition as a complex trait and its demand to increase in wheat grain

Nutrition in wheat grains is a complex trait induced by multiple genetic and environmental factors. Understanding the genetic basis and molecular mechanisms underlying nutritional traits is essential for their improvement (Alomari et al., 2021). Traditional breeding, QTL mapping, genomic selection, and genome editing are valuable approaches that have been employed to enhance the nutritional content of wheat grains. Continued research and the integration of these genetic and genomic approaches are crucial for developing wheat varieties with improved nutritional profiles (Pu et al., 2014; Shi et al., 2013). These advancements will contribute to addressing global food security and human health challenges associated with malnutrition and nutrient deficiencies.

Due to the varied nutritional demands of plants at various growth stages and across different tissues, as well as the fluctuation observed in the growth media, plants have evolved sophisticated homeostatic systems to deal with variations in nutrient requirements (Pinto & Ferreira, 2015). This thesis characterised the members of the

ZIP genes in wheat and identified putative QTLs associated for Fe contents. Our research findings about QTLs associated with Fe contents suggest that genetic and genomic approaches have the potential to improve Fe levels in wheat grain by identifying the genes and molecular mechanisms involved in Fe uptake, transport, and storage in wheat grains. This is a significant contribution to the research because, in the past, wheat has trailed behind other species in the identification and characterization of Fe and Zn transporters. This is the most likely because of the complex hexaploid wheat genome and the inherent problems of wheat transformation to explore aspects of gene function.

4.3 Unveiling the *TaZIP* family for Fe and Zn content

The *ZIP* family of genes plays a significant role in regulating the uptake, transport, and accumulation of microelements such as Fe, Zn, Mn, and Cu in plants. Using yeast complementation, three of the identified *TaZIP* genes were characterised and only *TaZIP11* showed the ability of Fe and Zn transportation. In TILLING population, one of the crosses from *TaZIP13* has the higher Fe and Zn content compared to WT. The differences in results between yeast experiments and TILLING can arise due to several reasons, despite the expectation that a phenotype observed in TILLING might lead to differences in transport in yeast. In yeast, a protein with similar transport capabilities might be compensating for the loss of function caused by the TILLING-induced mutation. One of the other reasons could be phenotypic effects that observed in TILLING by multiple pathways and factors, whereas the yeast transport system might be more simplified or specialized, leading to different responses. Further research and experimentation are needed to fully understand and elucidate the relationship between phenotypes observed in TILLING and transport mechanisms in yeast. In Arabidopsis,

the *ZIP* family of micronutrient transporters has been extensively studied to improve our understanding of plant micronutrients such as Zn, Fe, Mn, and Cu homeostasis. Membrane transporters from the *ZIP* genes have been demonstrated to transport a variety of cations, including Zn, Fe, Cu, and Cd, using heterologous yeast expression studies (Grotz et al., 1998; S. Li et al., 2013; Y. F. Lin et al., 2009; Pedas et al., 2009; Tiong et al., 2015). The *ZIP* genes in *Arabidopsis* have received the greatest attention. Fe and Zn is the most frequent substrate transported by the 18 members of the *Arabidopsis ZIP* family, with at least nine of them (*AtIRT1*, 2, 3, *AtZIP1*, 2, 3, 7, 11 and 12) demonstrating Zn transport ability (Korshunova et al., 1999; Lin et al., 2009; Vert et al., 2001). At least half of the *Arabidopsis ZIP* genes had been shown to transport Zn but based on our results and Evens et al., (2017) results, six *ZIP* genes out of 14 had the ability to transport Zn in wheat. Both *AtZIP1* and *AtZIP2* complemented the mutants for Zn and Mn uptake, indicating that they may both transport Zn and Mn. Both genes expression is restricted to the root stele, while *AtZIP1* expression was also discovered in the veins of the leaves. Additionally, it was discovered that *AtZIP2* is confined to the plasma membrane while *AtZIP1* is a vacuolar transporter. *Arabidopsis AtZIP1* and *AtZIP2* T-DNA knockout lines have been used in functional experiments, and the results indicate that both transporters are important for Mn translocation from the root to the shoot. In root stellar cells, *AtZIP1* may remobilize Mn from the vacuole to the cytoplasm and help with radial transport to the xylem. This extensive upregulation shows how crucial this family is to the Fe and Zn transport pathways.

Previously *ZIP* family has been recognized and studied in major crops including rice, maize, soybean, barley, and bean. According to Bashir et al., (2012) the *OsZIP1* and *OsZIP3* are engaged in Zn uptake from soil, the *OsZIP4*, *OsZIP5*, and *OsZIP8* are

included in root to shoot translocation, and the *OsZIP4* and *OsZIP8* help grains accumulate Zn. Under Zn-deficient conditions, it is discovered that the *ZIP* genes are expressed throughout the entire rice plant, including the roots, shoots, nodes, leaves, culms, spikelets, and grain. Rice Zn absorption, transport, and dispersion are all actively facilitated by *OsZIPs*. Similarly, our results show *OsZIP1*, *OsZIP3*, *OsZIP11*, *OsZIP13*, and *OsZIP14* highly expressed in root tissues (Chapter 2). *OsZIP1*, *OsZIP3*, and *OsZIP4* are all substantially expressed in rice root tissue when Zn is low (W. Chen et al., 2008). Under Zn-deficient circumstances, the *OsZIP1* is expressed only in the rice root. *OsZIP1* plays a specialised role in absorbing Zn from the soil solution. Under both Zn-deficient and Zn-sufficient circumstances, the *OsZIP3* gene is elevated in rice root and shoot tissue (Ramesh et al., 2003). It demonstrated that the *OsZIP* genes are essential for rice Zn transport and absorption in both Zn-sufficient and Zn-deficient circumstances. Additionally, the research related to *ZIP* family done on barley is also important for understanding wheat (Pedas et al., 2009; Tiong et al., 2014, 2015). Thirteen *HvZIPs* were found in barley, and their expression patterns in several tissues under Zn deficiency conditions were analysed. Six *HvZIP* genes were shown to be significantly elevated in this study's Zn-deficient condition, including *HvZIP3*, *HvZIP5*, *HvZIP7*, *HvZIP8*, *HvZIP10*, and *HvZIP13*. The plasma membrane of the cell contains each of these six *HvZIP* transporter proteins (Tiong et al., 2015). When Zn is lacking in wheat, the *HvZIP* genes are extremely important for Zn uptake.

The bioinformatic analysis of rice and wheat identified 15 *ZIP* genes in rice and 14 *ZIP* genes in wheat (Chapter 2). In a previous study, 13 *ZIP* genes were identified in wheat and analysed using phylogenetic analysis, which revealed two separate clades, one of which contained three *TaZIPs* (*TaZIP12*, *TaZIP14* and *TaZIP16*), and the other of which

contained the remaining ten (Evens et al., 2017). A wheat TILLING population was used to characterise three (*TaZIP11*, *TaZIP13*, and *TaZIP14*) of the discovered *TaZIPs*. Unfortunately, we could not find a significant role of these *ZIP* genes in the transportation of Fe and Zn in wheat grains except the *TaZIP13* that had different results in both crosses. This might be due to genetic or environmental factors. In a recent study, expression pattern analysis indicated that a majority of *TaZIP* genes exhibited high expression in roots, and nine genes displayed significant expression during the grain-filling stage (Li et al., 2021). When subjected to solutions of ZnSO₄ and FeCl₃, the *TaZIP* genes exhibited varied expression patterns. Furthermore, six *ZIP* genes demonstrated responses to Fe and Zn deficiency. Like our results, *TaZIP11*, *TaZIP13* and *TaZIP14* were highly expressed in root, leaf, and stem. Overexpression of *TaZIP13-B* gene showed that the transgenic plants exhibited enhanced tolerance to stresses related to Fe and Zn. Additionally, these transgenic plants were able to accumulate higher levels of elements in their seeds compared to the wild-type *Arabidopsis* (Li et al., 2021). Similarly, in our study, *TaZIP13-1* had the higher Fe and Zn contents compared to control (WT) in wheat TILLING population.

4.4 Perls staining and image analysis help to localize the grain Fe content

Perls staining also known as Perl's Prussian blue staining is a histochemical technique used to detect the presence of Fe in tissue samples, such as grains. This method is based on the reaction between potassium ferrocyanide and ferric ions (Fe³⁺), which produces the blue complex known as Prussian blue. Fe deposits in a variety of clinical diseases, including hemochromatosis and hemosiderosis, are frequently detected using Perl's staining (Brumbarova & Ivanov, 2014). The outcomes of Perls staining can vary depending on the Fe compounds used. We used this method to quantify and

localize the Fe content in wheat grain tissues. The staining images were used for image analyse and the results showed a wide range of Fe content. One hundred EMS lines were screened, and three high Fe lines selected to generate mapping population (Chapter 3). In addition, ICP-OES applied to quantify the Fe contents in wheat flour in parental lines. The mapping population was used to locate QTLs by bulk segregant analysis (BSA).

In addition to Perl's staining, other methods can be used to quantify and localize Fe content in grains or other samples such as Atomic Absorption Spectroscopy (AAS), Scanning electron microscopy (SEM), X-ray Fluorescence (XRF), Nanoscale secondary ion mass spectrometry (Nano-SIMS), and Inductively Coupled Plasma Optical Emission Spectrometry (ICP-OES). These techniques are used to quantify the Fe contents in samples in different studies. For example, a study used ICP-OES to measure the Fe concentration in Arabidopsis roots and leaves under different Fe treatments (Roschztardt et al., 2010). Another study used AAS to measure the Fe concentration in xylem sap of Arabidopsis plants under iron-deficient conditions (Sheraz et al., 2021). Another study examined the tissue-specific distribution of Fe and the elemental make-up of immature wheat grains using XRF (Bicchieri et al., 2002). According to the study, Fe was primarily concentrated in the grain's embryo and endosperm. SEM and XRF can offer more thorough information regarding Fe localization in plant tissues than other methods like AAS and ICP-OES. For instance, high-resolution images of the distribution of Fe in plant tissues can be obtained using SEM, whereas elemental composition data can be obtained using XRF. Overall, the study of Fe localization in plant tissues can be aided using SEM and XRF, which can also offer complementary data on the distribution and concentration of Fe in various

plant tissues. The choice of technique depends on the specific requirements of the study, such as the number of samples to be analysed, the sensitivity required, and the available resources. In future, we can use these various methods to phenotype the Fe contents in wheat grains and can improve for image analysis.

Computational approaches can be used to analyse the images obtained from these techniques and extract quantitative information about Fe localization in plant tissues. For instance, Fe staining in plant tissues that has been detected using Perls staining (Brumbarova & Ivanov, 2014). Additionally, samples obtained from Nano-SIMS can have their elemental composition examined using computational methods (Sheraz et al., 2021). These methods can help us understand Fe homeostasis and create biofortification strategies by revealing important details regarding the distribution and concentration of Fe in various plant tissues. In this thesis, we used Perls staining technique to quantify the Fe contents in EMS population. This technique is much cheaper than other methods and offers the localization of Fe contents in grain tissues. For image analysis, we developed a Python based script was developed to analyse the Perls images. This computational script not only saved the time but also provided the images with different colour backgrounds to understand the localization of Fe contents in wheat grain tissues.

4.5 Bulk segregant analysis offers cost-effective and rapid QTLs detection

In this thesis (Chapter 3), we used a pipeline known QTLseqr generated in R designed for the plant breeder and geneticist to perform BSA (bulk segregant analysis) (Mansfeld & Grumet, 2018). This method provided delta SNP value, G prime, $\log_{10}(\text{p-value})$ and was used to plot the graphs for locating the significant QTL regions. We applied this pipeline for all three populations (7077, 7060, and 7054). Population 7077 and 7054

did not pass the confidence interval 95 and 99. Effect of Fe content may be small and achieving statistical significance is difficult to detect such small effects. Only population 7060 has a significant region on chr1A, chr2A, chr2D, chr3B, chr4B, chr5D, chr6A, and chr7D and passed the confidence interval 95. We observed chr3B also passed 99 confidence interval and has a strong peak. This region has a $\Delta(\text{SNP-index})$ 0.35 and contributed from high Fe bulk. This region can be considered for further investigation to understand their role in the grain Fe contents.

BSA is an instant approach for identifying QTLs. It incorporates a screening of DNA pools developed from an F_2 population that originated from a cross between two diverse parents. Two pooled DNA samples are comparing for a selected phenotype (Michelmore et al., 1991). In a recent study, a prominent QTL, QTgw.cib-6A from the high TGW (thousand grain weight) parent was identified, having a positive impact on TGW without negative effects on other grain-related traits. This QTL was further confirmed using BSA (Liu et al., 2022). To our knowledge, the identification of QTLs for Fe contents in wheat grain using BSA is reported for the first time in our study. Tiwari et al., (2016) identified QTLs using the composite interval mapping approach. They found two QTLs for Zn contents, located on chromosomes 1B and 2B. The 2B QTL also coincided with a QTL for Fe contents. These QTLs explained significant portions of the observed variation, with the 1B QTL accounting for up to 23.1% and the 2B QTL explaining up to 35.9% of the phenotypic variation in Zn concentrations. The Fe QTL on chromosome 2B explained up to 22.2% of Fe variation and was co-located with the Zn QTL (Tiwari et al., 2016). In another study, meta-QTL (MQTL) analysis approach was used to find the QTLs for wheat grain Fe and Zn contents. The analysis incorporated data from seven independent populations to construct a consensus map

with 558 DNA markers, spanning 1028 cM of the wheat genome. Notably, seven MQTLs were identified on six chromosomes (1B, 2B, 4A, 5A, 7A and 7B), displaying narrower confidence intervals compared to original QTLs. Among these, three crucial MQTLs covering multiple initial QTLs emerged as pivotal hotspots governing grain Fe and Zn traits across diverse genetic backgrounds (Shariatipour et al., 2021). In our study, we found a putative QTL on a chr3B from high Fe bulk. This is novel variation in the EMS population that is not found in natural variation, which has been the focus of most previous studies. This region has 381 genes and 5 of them are heme binding. Due to shortage of time, we could not carry this project forward to validate Chr3B. Our results suggest that the EMS population may be used to select and breed wheat lines with higher grain Fe content. To promote marker-assisted breeding for high-Fe wheat varieties, future research should concentrate on finding specific genes and genetic markers linked to Fe accumulation in wheat grains.

4.6 Future Directions and Recommendations

The genetic characterization of Fe and Zn in wheat grains has been reported in this thesis. The characterization of *TaZIP* genes showed that *TaZIP11* has the capacity to transfer Fe and Zn in yeast complementation and the null mutants of *TaZIP13* showed higher Fe and Zn levels in the *TaZIP13-1* cross. In EMS population, we established a sophisticated approach to quantify and localize the grain Fe contents. We also identified that chromosome 3B could be a promising QTL to increase the Fe content in wheat grains. Overall, the findings of this study offer a solid basis for further characterising the Fe and Zn levels in wheat grains.

4.6.1 *TaZIP* lines

Given the results so far, there may be multiple opportunities to test *TaZIP* lines with increased Fe and Zn contents or improved tolerance to micronutrients deficient soils. Performance under both replete and depleted Fe and Zn circumstances should also be evaluated, as well as *TaZIP* gene expression assessments. Furthermore, it is essential to investigate the constitutive and endosperm-targeted overexpression of found and described *TaZIPs*. It is important to study the function of a particular gene and targeting endosperm to enhance the nutritional content of grains by expressing genes that produce specific nutrients. If we find that *TaZIP* genes can increase Fe or Zn we could breed them into elite cultivars, or genetic transformation approaches could be used to incorporate this genetic potential into current high-yielding varieties.

4.6.2 EMS populations

A successful plant breeding programme depends on genetic variety in the breeding materials since it serves as the basis for selection. Cadenza EMS population contains the potential to increase grain Fe in grain tissues. Amiri et al., (2020) suggests that the EMS population may be used to select and breed wheat lines with higher grain Fe contents. In our study, we found a wide range of Fe contents in EMS population. For the purpose of functional investigation of the trait, the EMS-induced mutation offers genetic variations (Rawat et al., 2019). Like other breeding techniques, EMS population has drawbacks, such as a high mutation load and few beneficial mutations (Ke et al., 2019). Additionally, it is still challenging to identify, clone, and characterise mutations in polyploid genomes. Although the most recent gene editing technology, such as the CRISPR/Cas9 system, which is quicker, more precise, and extensively employed in plant research, is challenging for because we do not know which genes

to target. This is also fascinating because EMS population is a non-GMO application, therefore this is exempt from governing laws for genetic modification.

4.6.3 Wheat improvement plans

Wheat biofortification has enormous potential for addressing widespread micronutrient shortages, notably those in Fe and Zn. Future directions and suggestions for improvement in this field can be enumerated. First and foremost, high yielding biofortified wheat varieties should be developed with a focus on qualities like adaptation and disease resistance. Marker-assisted selection (MAS) and genomic selection are two contemporary molecular techniques that breeding programmes should use in tandem to quickly identify and introduce the genes that increase the Fe and Zn content of wheat grains (Arruda et al., 2016). These methods can speed up the process of variety development by enabling more accurate and effective selection of desired features. Additionally, agronomic treatments including better soil management techniques, nitrogen management, and irrigation methods should be combined with biofortification activities (Abid et al., 2020). For instance, improving the soil's pH, organic matter content, and accessibility to other vital micronutrients like manganese and copper might improve the Fe and Zn bioavailability and uptake by wheat plants. Additionally, it is essential to comprehend how nutrients interact in the body and in the soil to direct breeding efforts and inform dietary recommendations.

To increase Fe and Zn bioavailability and absorption in the human digestive system, research should investigate how they interact, either positively or negatively, with other nutrients such phytates, fibre, and certain vitamins. With this knowledge, wheat cultivars with better nutrient profiles can be developed, and biofortified wheat can benefit from tactics that maximise its nutritious value. To maximise the impact,

biofortified wheat cultivars must be distributed to communities and areas where Fe and Zn deficiency is most common. This requires comprehensive mapping of micronutrient deficiency prevalence, as well as an assessment of dietary patterns and cultural practices that may influence the acceptance and adoption of biofortified wheat (Govindan et al., 2022). The consumption of biofortified wheat should be encouraged through a variety of channels, such as educational institutions, healthcare facilities, and neighbourhood initiatives. The development of markets for biofortified wheat products, such as fortified flour and bread, depends on cooperation with food processors, millers, and retailers. The establishment of monitoring and evaluation methods to judge the success of biofortification initiatives is crucial for ongoing development and well-informed decision-making (Garcia-Casal et al., 2017 and Garcia-Casal et al., 2017). Regular monitoring can give input on target population nutritional status changes, nutrient levels in harvested grains, and adoption rates of biofortified cultivars. Assessment studies can determine how biofortification affects lowering Fe and Zn deficiency and enhancing general health outcomes. By embracing these future directions and recommendations, wheat biofortification can significantly contribute to mitigating Fe and Zn deficiencies and enhancing the nutritional status of vulnerable populations.

With an additional 3-5 years to dedicate to this research, we would have the opportunity to delve deeper into the details of *ZIP* transporters and expand the scope of these experiments. Our primary focus would be on *TaZIP13*, and the contradictory results observed in different crosses regarding its role in Fe and Zn transport. To address this, we would design a series of experiments aimed at uncovering the underlying factors contributing to the observed discrepancies. One possible avenue would be to

investigate the genetic variations in the two crosses that might be responsible for the divergent phenotypes. For this we can consider CRISPR-Cas9 approach to avoid background mutations. Additionally, we would analyse the expression profiles of other Fe-related genes in these crosses to identify potential regulatory networks at play. To further elucidate the role of *TaZIP13*, we would indeed consider growing plants with varying levels of Fe and Zn in controlled environments. This would allow us to systematically study how different nutrient ratios influence *TaZIP13* expression and function. Moreover, field experiments would be an essential next step, as they provide a more realistic setting for understanding how *TaZIP13* operates in field conditions. By conducting field trials, we could assess the impact of *TaZIP13* mutations on plant growth, yield, and nutrient accumulation under natural variations in Fe and Zn availability.

Turning our attention to the EMS populations, the subsequent steps would involve thoroughly validation of the identified 3B QTL and the associated genes. To achieve this, we would refine the location of the QTL on the chromosome through fine mapping techniques, such as using more markers, or advanced genotyping technologies and identify potential candidate genes. This genetic characterisation would provide a clearer understanding of the functional consequences of the identified QTL and help establish causal relationships between specific genetic variants and Fe variations. Additionally, conducting expression profiling and biochemical assays would allow us to dissect the underlying molecular mechanisms connecting the candidate genes with the observed traits. These insights would not only validate the role of the 3B QTL but also offer a deeper understanding of the broader genetic networks governing nutrient uptake and homeostasis. Germplasm sources play a crucial role in accessing genetic

diversity. We will look for varieties or lines that carry the desired loci. This may involve accessing gene banks, breeding programs, or collaborating with other researchers. Once we have identified the loci and germplasm sources, we can devise a strategy for pyramiding. This might involve traditional breeding methods or more advanced techniques like marker-assisted selection or genomic selection.

4.7 Conclusion

In this thesis, we attempted to understand the molecular mechanism of Fe and Zn biofortification in wheat grains. Firstly, we explored the *ZIP* gene family in wheat and functionally characterized the role of *TaZIP11*, *TaZIP13* and *TaZIP14* using TILLING. We found that *TaZIP11* could transport Fe and Zn in a heterologous system but did not observe consistent effects on micronutrients in any wheat mutant lines. Secondly, we investigated the potential of EMS lines to increase wheat grain Fe contents through Perls staining. Perls staining can be an effective screening approach to identify Fe containing wheat lines and we developed a rapid computational method to quantify Fe staining. This allowed us to identify a novel QTL on chromosome 3B for Fe contents. Further investigation is required to ascertain how these *TaZIP* genes and novel QTL contribute to wheat biofortification.

References:

- Abid, M., Batool, T., Siddique, G., Ali, S., Binyamin, R., Shahid, M. J., Rizwan, M., Alsahli, A. A., & Alyemeni, M. N. (2020). Integrated nutrient management enhances soil quality and crop productivity in maize-based cropping system. *Sustainability (Switzerland)*, *12*(23), 1–15. <https://doi.org/10.3390/su122310214>
- Ali, M. W., & Borrill, P. (2020). Applying genomic resources to accelerate wheat biofortification. *Heredity*. <https://doi.org/10.1038/s41437-020-0326-8>
- Allan, R. E. (1989). Agronomic Comparisons Between Rht1 and Rht2 Semidwarf Genes in Winter Wheat. *Crop Science*, *29*(5), <https://doi.org/10.2135/cropsci1989.0011183X002900050001x>
- Alloway, B. J. (2008). *Zn in Soils and Crop Nutrition (Second)*. IZA and IFA Brussels, Belgium and Paris, France. [https://doi.org/10.1016/S0065-2113\(06\)94003-6](https://doi.org/10.1016/S0065-2113(06)94003-6)
- Alomari, D. Z., Alqudah, A. M., Pillen, K., von Wirén, N., & Röder, M. S. (2021). Toward identification of a putative candidate gene for nutrient mineral accumulation in wheat grains for human nutrition purposes. *Journal of Experimental Botany*, *72*(18), 6305–6318. <https://doi.org/10.1093/jxb/erab297>
- Amiri, R., Bahraminejad, S., Cheghamirza, K., & Arzani, A. (2020). Genetic analysis of iron and zinc concentrations in bread wheat grains. *Journal of Cereal Science*, *95*(June), 103077. <https://doi.org/10.1016/j.jcs.2020.103077>
- Aoun, M., Kolmer, J. A., Rouse, M. N., Chao, S., Bulbula, W. D., Elias, E. M., & Acevedo, M. (2017). Inheritance and bulked segregant analysis of leaf rust and

stem rust resistance in durum wheat genotypes. *Phytopathology*, 107(12), 1496–1506. <https://doi.org/10.1094/PHYTO-12-16-0444-R>

Appels, R., Eversole, K., Feuillet, C., Keller, B., Rogers, J., Stein, N., Pozniak, C. J., Choulet, F., Distelfeld, A., Poland, J., Ronen, G., Barad, O., Baruch, K., Keeble-Gagnère, G., Mascher, M., Ben-Zvi, G., Josselin, A. A., Himmelbach, A., Balfourier, F., ... Wang, L. (2018). Shifting the limits in wheat research and breeding using a fully annotated reference genome. *Science*, 361(6403). <https://doi.org/10.1126/science.aar7191>

Arora, S., Singh, N., Kaur, S., Bains, N. S., Uauy, C., Poland, J., & Chhuneja, P. (2017). Genome-wide association study of grain architecture in wild wheat *Aegilops tauschii*. *Frontiers in Plant Science*, 8, 886.

Arruda, M. P., Lipka, A. E., Brown, P. J., Krill, A. M., Thurber, C., Brown-Guedira, G., Dong, Y., Foresman, B. J., & Kolb, F. L. (2016). Comparing genomic selection and marker-assisted selection for Fusarium head blight resistance in wheat (*Triticum aestivum* L.). *Molecular Breeding*, 36(7), 1–11. <https://doi.org/10.1007/s11032-016-0508-5>

Arzani, A., & Ashraf, M. (2017). Cultivated Ancient Wheats (*Triticum* spp.): A Potential Source of Health-Beneficial Food Products. *Comprehensive Reviews in Food Science and Food Safety*, 16(3), 477–488. <https://doi.org/10.1111/1541-4337.12262>

Aschner, J. L., & Aschner, M. (2005). Nutritional aspects of manganese homeostasis. *Molecular Aspects of Medicine*, 26(4-5 SPEC. ISS.), 353–362. <https://doi.org/10.1016/j.mam.2005.07.003>

- Assunção, A. G. L., Herrero, E., Lin, Y. F., Huettel, B., Talukdar, S., Smaczniak, C., Immink, R. G. H., Van Eldik, M., Fiers, M., Schat, H., & Aarts, M. G. M. (2010). Arabidopsis thaliana transcription factors *bZIP19* and *bZIP23* regulate the adaptation to zinc deficiency. *Proceedings of the National Academy of Sciences of the United States of America*, *107*(22), 10296–10301. <https://doi.org/10.1073/pnas.1004788107>
- Avni, R., Nave, M., Barad, O., Baruch, K., Twardziok, S. O., Gundlach, H., Hale, I., Mascher, M., Spannagl, M., & Wiebe, K. (2017). Wild emmer genome architecture and diversity elucidate wheat evolution and domestication. *Science*, *357*(6346), 93–97.
- Bagci, S. A., Ekiz, H., Yilmaz, A., & Cakmak, I. (2007). *Effects of Zinc Deficiency and Drought on Grain Yield of Field-grown Wheat Cultivars in Central Anatolia*. *206*, 198–206. <https://doi.org/10.1111/j.1439-037X.2007.00256.x>
- Banakar, R., Alvarez Fernandez, A., Díaz-Benito, P., Abadia, J., Capell, T., & Christou, P. (2017). Phytosiderophores determine thresholds for iron and zinc accumulation in biofortified rice endosperm while inhibiting the accumulation of cadmium. *Journal of Experimental Botany*, *68*(17), 4983–4995. <https://doi.org/10.1093/jxb/erx304>
- Bashir, K., Inoue, H., Nagasaka, S., Takahashi, M., Nakanishi, H., Mori, S., & Nishizawa, N. K. (2006). Cloning and characterization of deoxymugineic acid synthase genes from graminaceous plants. *Journal of Biological Chemistry*, *281*(43), 32395–32402. <https://doi.org/10.1074/jbc.M604133200>
- Bashir, K., Ishimaru, Y., & Nishizawa, N. K. (2012). Molecular mechanisms of zinc

- uptake and translocation in rice. *Plant and Soil*, 361(1–2), 189–201.
<https://doi.org/10.1007/s11104-012-1240-5>
- Beal, T., Massiot, E., Arsenault, J. E., Smith, M. R., & Hijmans, R. J. (2017). Global trends in dietary micronutrient supplies and estimated prevalence of inadequate intakes. *PLOS ONE*, 12(4), e0175554.
<https://doi.org/10.1371/journal.pone.0175554>
- Beasley, J. T., Bonneau, J. P., Sánchez-Palacios, J. T., Moreno-Moyano, L. T., Callahan, D. L., Tako, E., Glahn, R. P., Lombi, E., & Johnson, A. A. T. (2019). Metabolic engineering of bread wheat improves grain iron concentration and bioavailability. *Plant Biotechnology Journal*, 17(8), 1514–1526.
<https://doi.org/10.1111/pbi.13074>
- Beasley, J. T., Bonneau, J. P., Sánchez-Palacios, J. T., Moreno-Moyano, L. T., Callahan, D. L., Tako, E., Glahn, R. P., Lombi, E., & Johnson, A. A. T. (2019). Metabolic engineering of bread wheat improves grain iron concentration and bioavailability. *Plant Biotechnology Journal*, 17(8), 1514–1526.
- Bicchieri, M., Ronconi, S., Romano, F. P., Pappalardo, L., Corsi, M., Cristoforetti, G., Legnaioli, S., Palleschi, V., Salvetti, A., & Tognoni, E. (2002). Study of foxing stains on paper by chemical methods, infrared spectroscopy, micro-X-ray fluorescence spectrometry and laser induced breakdown spectroscopy. *Spectrochimica Acta - Part B Atomic Spectroscopy*, 57(7), 1235–1249.
[https://doi.org/10.1016/S0584-8547\(02\)00056-3](https://doi.org/10.1016/S0584-8547(02)00056-3)
- Borg, S., Brinch-Pedersen, H., Tauris, B., & Holm, P. B. (2009). Iron transport, deposition and bioavailability in the wheat and barley grain. *Plant and Soil*, 325(1),

15–24. <https://doi.org/10.1007/s11104-009-0046-6>

- Borg, S., Brinch-Pedersen, H., Tauris, B., Madsen, L. H., Darbani, B., Noeparvar, S., & Holm, P. B. (2012). Wheat ferritins: Improving the iron content of the wheat grain. *Journal of Cereal Science*, *56*(2), 204–213. <https://doi.org/10.1016/J.JCS.2012.03.005>
- Borrill, P., Miller, A. J., Uauy, C., Balk, J., Sanders, D., & Connorton, J. M. (2014). Biofortification of wheat grain with iron and zinc: integrating novel genomic resources and knowledge from model crops. *Frontiers in Plant Science*, *5*(February), 1–8. <https://doi.org/10.3389/fpls.2014.00053>
- Bouis, H. E., & Saltzman, A. (2017). Improving nutrition through biofortification: A review of evidence from HarvestPlus, 2003 through 2016. *Global Food Security*, *12*(January), 49–58. <https://doi.org/10.1016/j.gfs.2017.01.009>
- Brown, K. H., Hambidge, K. M., & Ranum, P. (2010). Zinc fortification of cereal flours: current recommendations and research needs. *Food and Nutrition Bulletin*, *31*(1_suppl1), S62–S74.
- Brumbarova, T., & Ivanov, R. (2014). *Perls Staining for Histochemical Detection of Iron in Plant Samples*.
- Cakmak, I. (2008a). Enrichment of cereal grains with zinc: Agronomic or genetic biofortification? *Plant and Soil*, *302*(1–2), 1–17. <https://doi.org/10.1007/s11104-007-9466-3>
- Cakmak, I. (2008b). Zinc deficiency in wheat in Turkey. *Micronutrient Deficiencies in Global Crop Production*, 181–200. https://doi.org/10.1007/978-1-4020-6860-7_7

- Cakmak, I., & Marschner, H. (1986). Mechanism of phosphorus-induced zinc deficiency in cotton. I. Zinc deficiency-enhanced uptake rate of phosphorus. *Physiologia Plantarum*, 68(3), 483–490.
- Cakmak, I., & Marschner, H. (1988). Increase in membrane permeability and exudation in roots of zinc deficient plants. *Journal of Plant Physiology*, 132(3), 356–361.
- Cakmak, I., Torun, A., Özkan, H., Millet, E., Feldman, M., Fahima, T., Korol, A., Nevo, E., & Braun, H. J. (2004). *Triticum dicoccoides*: An important genetic resource for increasing zinc and iron concentration in modern cultivated wheat. *Soil Science and Plant Nutrition*, 50(7), 1047–1054.
<https://doi.org/10.1080/00380768.2004.10408573>
- Caldelas, C., Rezzouk, F. Z., Aparicio, N., & Araus, J. L. (2023). Cultivar diversity in the mineral content of wheat grain under different nitrogen regimes. In *agriRxiv*. [agriRxiv](https://doi.org/10.31220/agriRxiv.2022.00123). <https://doi.org/10.31220/agriRxiv.2022.00123>
- Callaway, E. (2018). CRISPR plants now subject to tough GM laws in European Union. *Nature*, 560(7716), 16–17.
- Carleton, H. M. (Harry M. (1980). *Carleton's Histological technique* (R. A. B. (Roger A. B. Drury & E. A. Wallington (eds.)). Oxford University Press.
- Caulfield, L. E., de Onis, M., Blössner, M., & Black, R. E. (2004). Undernutrition as an underlying cause of child deaths associated with diarrhea, pneumonia, malaria, and measles. *The American Journal of Clinical Nutrition*, 80(1), 193–198.
<https://doi.org/10.1093/ajcn/80.1.193>
- Cauvain, S. P. (2012). *Breadmaking: improving quality*. Elsevier.

- Chen, L., Huang, L., Min, D., Phillips, A., Wang, S., Madgwick, P. J., Parry, M. A. J., & Hu, Y. G. (2012). Development and characterization of a new TILLING population of common bread wheat (*Triticum aestivum* L. *PLoS ONE*, 7(7). <https://doi.org/10.1371/journal.pone.0041570>
- Chen, W., Yang, X., He, Z., Feng, Y., & Hu, F. (2008). Differential changes in photosynthetic capacity, 77 K chlorophyll fluorescence and chloroplast ultrastructure between Zn-efficient and Zn-inefficient rice genotypes (*Oryza sativa*) under low zinc stress. *Physiologia Plantarum*, 132(1), 89–101.
- Chu, H.-H., Chiecko, J., Punshon, T., Lanzirotti, A., Lahner, B., Salt, D. E., & Walker, E. L. (2010). Successful Reproduction Requires the Function of Arabidopsis YELLOW STRIPE-LIKE1 and YELLOW STRIPE-LIKE3 Metal-Nicotianamine Transporters in Both Vegetative and Reproductive Structures. *Plant Physiology*, 154(1), 197–210. <https://doi.org/10.1104/pp.110.159103>
- Clemens, S., Deinlein, U., Ahmadi, H., Höreth, S., & Uraguchi, S. (2013). Nicotianamine is a major player in plant Zn homeostasis. *BioMetals*, 26(4), 623–632. <https://doi.org/10.1007/s10534-013-9643-1>
- Coleman, J. E. (1998). Zinc enzymes. *Current Opinion in Chemical Biology*, 2(2), 222–234. [https://doi.org/10.1016/S1367-5931\(98\)80064-1](https://doi.org/10.1016/S1367-5931(98)80064-1)
- Collins, J. F., & Klevay, L. M. (2011). Copper. *Advances in Nutrition*, 2(6), 520–522. <https://doi.org/10.3945/an.111.001222>
- Connorton, J. M., & Balk, J. (2019). Iron Biofortification of Staple Crops: Lessons and Challenges in Plant Genetics. *Plant and Cell Physiology*, 60(May), 1447–1456. <https://doi.org/10.1093/pcp/pcz079>

- Connorton, J. M., Balk, J., & Rodríguez-Celma, J. (2017). Iron homeostasis in plants—a brief overview. *Metallomics*, 9(7), 813–823. <https://doi.org/10.1039/c7mt00136c>
- Connorton, J. M., Jones, E. R., Rodríguez-Ramiro, I., Fairweather-Tait, S., Uauy, C., & Balk, J. (2017). Wheat vacuolar iron transporter TaVIT2 transports Fe and Mn and is effective for biofortification. *Plant Physiology*, 174(4), 2434–2444. <https://doi.org/10.1104/pp.17.00672>
- Cook, J. D., Skikne, B. S., Lynch, S. R., & Reusser, M. E. (1986). *Estimates of iron sufficiency in the US population*.
- Crespo-Herrera, L. A., Velu, G., & Singh, R. P. (2016). Quantitative trait loci mapping reveals pleiotropic effect for grain iron and zinc concentrations in wheat. *Annals of Applied Biology*, 169(1), 27–35. <https://doi.org/10.1111/aab.12276>
- Cubillos, F. A., Brice, C., Molinet, J., Tisné, S., Abarca, V., Tapia, S. M., Oporto, C., García, V., Liti, G., & Martínez, C. (2017). Identification of nitrogen consumption genetic variants in yeast through QTL mapping and bulk segregant RNA-Seq analyses. *G3: Genes, Genomes, Genetics*, 7(6), 1693–1705. <https://doi.org/10.1534/g3.117.042127>
- Danielsson, P.-E., & Seger, O. (1990). Generalized and Separable Sobel Operators. *Machine Vision for Three-Dimensional Scenes*, 347–379. <https://doi.org/10.1016/B978-0-12-266722-0.50016-6>
- Davletova, S., Schlauch, K., Coutu, J., & Mittler, R. (2005). The zinc-finger protein *Zat12* plays a central role in reactive oxygen and abiotic stress signaling in *Arabidopsis*. *Plant Physiology*, 139(2), 847–856.

- de Valena, A. W., Bake, A., Brouwer, I. D., & Giller, K. E. (2017). Agronomic biofortification of crops to fight hidden hunger in sub-Saharan Africa. *Global Food Security*, 12, 8–14. <https://doi.org/10.1016/J.GFS.2016.12.001>
- Deinlein, U., Weber, M., Schmidt, H., Rensch, S., Trampczynska, A., Hansen, T. H., Husted, S., Schjoerring, J. K., Talke, I. N., Kramer, U., & Clemens, S. (2012). Elevated nicotianamine levels in *Arabidopsis halleri* roots play a key role in zinc hyperaccumulation. *Plant Cell*, 24(2), 708–723. <https://doi.org/10.1105/tpc.111.095000>
- Distelfeld, A., Cakmak, I., Peleg, Z., Ozturk, L., Yazici, A. M., Budak, H., Saranga, Y., & Fahima, T. (2007). Multiple QTL-effects of wheat *Gpc-B1* locus on grain protein and micronutrient concentrations. *Physiologia Plantarum*, 129(3), 635–643. <https://doi.org/10.1111/j.1399-3054.2006.00841.x>
- Dixon, J. (2007). The economics of wheat: research challenges from field to fork. *Wheat Production in Stressed Environments: Proceedings of the 7th International Wheat Conference, 27 November–2 December 2005, Mar Del Plata, Argentina*, 9–22.
- Dubcovsky, J., & Dvorak, J. (2007). Genome plasticity a key factor in the success of polyploid wheat under domestication. *Science*, 316 (5833), 1862–1866. <https://doi.org/10.1126/science.1143986>
- Durrett, T. P., Gassmann, W., & Rogers, E. E. (2007). The FRD3-mediated efflux of citrate into the root vasculature is necessary for efficient iron translocation. *Plant Physiology*, 144(1), 197–205.
- Eagling, T., Wawer, A. A., Shewry, P. R., Zhao, F.-J., & Fairweather-Tait, S. J. (2014).

- Iron bioavailability in two commercial cultivars of wheat: comparison between wholegrain and white flour and the effects of nicotianamine and 2'-deoxymugineic acid on iron uptake into Caco-2 cells. *Journal of Agricultural and Food Chemistry*, 62(42), 10320–10325. <https://doi.org/10.1021/jf5026295>
- Eng, B. H., Guerinot, M. L., Eide, D., & Saier, M. H. (1998). Sequence analyses and phylogenetic characterization of the *ZIP* family of metal ion transport proteins. *Journal of Membrane Biology*, 166(1), 1–7. <https://doi.org/10.1007/s002329900442>
- Evans, J. R., & Lawson, T. (2020). From green to gold: Agricultural revolution for food security. *Journal of Experimental Botany*, 71(7), 2211–2215. <https://doi.org/10.1093/jxb/eraa110>
- Evens, N. P., Buchner, P., Williams, L. E., & Hawkesford, M. J. (2017). The role of *ZIP* transporters and group F bZIP transcription factors in the Zn-deficiency response of wheat (*Triticum aestivum*). *Plant Journal*, 92(2), 291–304. <https://doi.org/10.1111/tpj.13655>
- Fan, M.-S., Zhao, F.-J., Fairweather-Tait, S. J., Poulton, P. R., Dunham, S. J., & McGrath, S. P. (2008). Evidence of decreasing mineral density in wheat grain over the last 160 years. *Journal of Trace Elements in Medicine and Biology*, 22(4), 315–324. <https://doi.org/10.1016/J.JTEMB.2008.07.002>
- FAO. (2017). FAOSTAT statistics database, Food balance sheets. www.fao.org/faostat/en/#data/FBS
- FAO. (2020). “Food and agriculture data.” Crop Statistics. Available online: <http://www.fao.org/faostat>

- Feuillet, C., Langridge, P., & Waugh, R. (2008). Cereal breeding takes a walk on the wild side. *Trends in Genetics*, 24(1), 24–32. <https://doi.org/10.1016/j.tig.2007.11.001>
- Foley, J. A., Ramankutty, N., Brauman, K. A., Cassidy, E. S., Gerber, J. S., Johnston, M., Mueller, N. D., O'Connell, C., Ray, D. K., West, P. C., Balzer, C., Bennett, E. M., Carpenter, S. R., Hill, J., Monfreda, C., Polasky, S., Rockström, J., Sheehan, J., Siebert, S., ... Zaks, D. P. M. (2011). Solutions for a cultivated planet. *Nature*, 478(7369), 337–342. <https://doi.org/10.1038/nature10452>
- Forrest H Nielsen, C. D. E. (2020). Nutrient Information: Boron. *Advances in Nutrition*, 11(1), 461–462. www.ebscohost.com
- Garcia-Casal, M. N., Peña-Rosas, J. P., Giyose, B., & Groups, C. W. (2017). Staple crops biofortified with increased vitamins and minerals: considerations for a public health strategy. *Annals of the New York Academy of Sciences*, 1390(1), 3–13.
- Garg, M., Sharma, N., Sharma, S., Kapoor, P., Kumar, A., Chunduri, V., & Arora, P. (2018). Biofortified Crops Generated by Breeding, Agronomy, and Transgenic Approaches Are Improving Lives of Millions of People around the World. *Frontiers in Nutrition*, 5(February). <https://doi.org/10.3389/fnut.2018.00012>
- Genc, Y., Verbyla, A. P., Torun, A. A., Cakmak, I., Willsmore, K., Wallwork, H., & McDonald, G. K. (2009). Quantitative trait loci analysis of zinc efficiency and grain zinc concentration in wheat using whole genome average interval mapping. *Plant and Soil*, 314(1), 49–66.
- Ghurye, J., Rhie, A., Walenz, B. P., Schmitt, A., Selvaraj, S., Pop, M., Phillippy, A. M., & Koren, S. (2019). Integrating Hi-C links with assembly graphs for chromosome-

scale assembly. *PLoS Computational Biology*, 15(8), 1–19.
<https://doi.org/10.1371/journal.pcbi.1007273>

Giovannoni, J. J., Wing, R. A., Ganai, M. W., & Tanksley, S. D. (1991). Isolation of molecular markers from specific chromosomal intervals using DNA pools from existing mapping populations. *Nucleic Acids Research*, 19(23), 6553–6568.
<https://doi.org/10.1093/nar/19.23.6553>

Godfray et al. (2010). Food security: The challenge of the present. *Science*, 327(February). <https://doi.org/10.1016/j.geoforum.2018.02.030>

Gong, F., Qi, T., Hu, Y., Jin, Y., Liu, J., Wang, W., He, J., Tu, B., Zhang, T., Jiang, B., Wang, Y., Zhang, L., Zheng, Y., Liu, D., Huang, L., & Wu, B. (2022). Genome-Wide Investigation and Functional Verification of the ZIP Family Transporters in Wild Emmer Wheat. *International Journal of Molecular Sciences*, 23(5).
<https://doi.org/10.3390/ijms23052866>

Gorafi, Y. S. A., Ishii, T., Kim, J.-S., Elbashir, A. A. E., & Tsujimoto, H. (2018). Genetic variation and association mapping of grain iron and zinc contents in synthetic hexaploid wheat germplasm. *Plant Genetic Resources: Characterization and Utilization*, 16(1), 9–17. <https://doi.org/10.1017/S1479262116000265>

Govindan, V., Michaux, K. D., & Pfeiffer, W. H. (2022). Nutritionally enhanced wheat for food and nutrition security. In *Wheat Improvement: Food Security in a Changing Climate* (pp. 195–214). Springer International Publishing Cham.

Graham, R., Senadhira, D., Beebe, S., Iglesias, C., & Monasterio, I. (1999). Breeding for micronutrient density in edible portions of staple food crops: conventional approaches. *Field Crops Research*, 60(1–2), 57–80.

- Grotz, N., Fox, T., Connolly, E., Park, W., Guerinot, M. Lou, & Eide, D. (1998). Identification of a family of zinc transporter genes from Arabidopsis that respond to zinc deficiency. *Proceedings of the National Academy of Sciences*, *95*(12), 7220–7224. <https://doi.org/10.1073/PNAS.95.12.7220>
- Guerinot, M. Lou. (2000). The ZIP family of metal transporters. *Biochimica et Biophysica Acta (BBA) - Biomembranes*, *1465*(1–2), 190–198. [https://doi.org/10.1016/S0005-2736\(00\)00138-3](https://doi.org/10.1016/S0005-2736(00)00138-3)
- Gurdev S. Khush. (2001). Green revolution: the way forward. *Nature Reviews Genetics*, *2*(October).
- Hajiboland, R. (2012). Effect of micronutrient deficiencies on plants stress responses. In *Abiotic stress responses in plants* (pp. 283–329). Springer.
- Hao, Y., Rasheed, A., Jackson, R., Xiao, Y., Zhang, Y., Xia, X., & He, Z. (2020). Advanced genomics and breeding tools to accelerate the development of climate resilient wheat. *Genomic Designing of Climate-Smart Cereal Crops; Springer International Publishing: Cham, Switzerland*, 45–95.
- Harlan, J. R., & Zohary, D. (1966). Distribution of Wild Wheats and Barley - The present distribution of wild forms may provide clues to the regions of early cereal domestication. *Science*, *153*, 1074–1080.
- Hawkesford, M. J., Araus, J. L., Park, R., Calderini, D., Miralles, D., Shen, T., Zhang, J., & Parry, M. A. J. (2013). Prospects of doubling global wheat yields. *Food and Energy Security*, *2*(1), 34–48. <https://doi.org/10.1002/fes3.15>
- Hedden, P. (2003). The genes of the Green Revolution. *Trends in Genetics*, *19*(1), 5–

9. [https://doi.org/10.1016/S0168-9525\(02\)00009-4](https://doi.org/10.1016/S0168-9525(02)00009-4)

- Heffner, E. L., Lorenz, A. J., Jannink, J., & Sorrells, M. E. (2010). Plant breeding with genomic selection: gain per unit time and cost. *Crop Science*, *50*(5), 1681–1690.
- Hooley, R. (1994). Gibberellins: perception, transduction and responses. *Plant Molecular Biology*, *26*(5), 1529–1555. <https://doi.org/10.1007/BF00016489>
- Hu, H., & Sparks, D. (1991). Zinc Deficiency Inhibits Chlorophyll Synthesis and Gas Exchange in Stuart Pecan. *HortScience*, *26*(3), 267–268.
- Hunter, J. D. (2007). Matplotlib: A 2D Graphics Environment. *Computing in Science & Engineering*, *9.03*, 90–95.
- Hurrell, R. F. (1997). Preventing iron deficiency through food fortification. *Nutrition Reviews*, *55*(6), 210–222.
- Iezzoni, J. C. (2018). Diagnostic histochemistry in hepatic pathology. *Seminars in Diagnostic Pathology*, *35*(6), 381–389. <https://doi.org/10.1053/J.SEMDP.2018.10.003>
- Irshad, A., Guo, H., Zhang, S., & Liu, L. (2020). TILLING in cereal crops for allele expansion and mutation detection by using modern sequencing technologies. *Agronomy*, *10*(3). <https://doi.org/10.3390/agronomy10030405>
- Ishimaru, Y., Masuda, H., Bashir, K., Inoue, H., Tsukamoto, T., Takahashi, M., Nakanishi, H., Aoki, N., Hirose, T., Ohsugi, R., & Nishizawa, N. K. (2010). Rice metal-nicotianamine transporter, OsYSL2, is required for the long-distance transport of iron and manganese. *Plant Journal*, *62*(3), 379–390. <https://doi.org/10.1111/j.1365-313X.2010.04158.x>

- Ishimaru, Y., Masuda, H., Suzuki, M., Bashir, K., Takahashi, M., Nakanishi, H., Mori, S., & Nishizawa, N. K. (2007). Overexpression of the *OsZIP4* zinc transporter confers disarrangement of zinc distribution in rice plants. *Journal of Experimental Botany*, *58*(11), 2909–2915. <https://doi.org/10.1093/jxb/erm147>
- Ishimaru, Y., Suzuki, M., Kobayashi, T., Takahashi, M., Nakanishi, H., Mori, S., & Nishizawa, N. K. (2005). *OsZIP4*, a novel zinc-regulated zinc transporter in rice. *Journal of Experimental Botany*, *56*(422), 3207–3214. <https://doi.org/10.1093/jxb/eri317>
- IWGSC. (2014). A chromosome-based draft sequence of the hexaploid bread wheat (*Triticum aestivum*) genome Ancient hybridizations among the ancestral genomes of bread wheat Genome interplay in the grain transcriptome of hexaploid bread wheat Structural and functional pa. *Science (New York, N.Y.)*, *345*(6194), 1251788. <https://doi.org/10.1126/science.1251788>
- IWGSC. (2018). Shifting the limits in wheat research and breeding using a fully annotated reference genome. *Science*, *361*(6403). <https://doi.org/10.1126/science.aar7191>
- Jain, M., Nijhawan, A., Arora, R., Agarwal, P., Ray, S., Sharma, P., Kapoor, S., Tyagi, A. K., & Khurana, J. P. (2007). F-Box proteins in rice. Genome-wide analysis, classification, temporal and spatial gene expression during panicle and seed development, and regulation by light and abiotic stress. *Plant Physiology*, *143*(4), 1467–1483. <https://doi.org/10.1104/pp.106.091900>
- JIANG, L. na, MA, J. li, WANG, X. jie, LIU, G. gang, ZHU, Z. long, QI, C. yang, ZHANG, L. fang, LI, C. xi, WANG, Z. min, & HAO, B. zhen. (2022). Grain zinc and iron

- concentrations of Chinese wheat landraces and cultivars and their responses to foliar micronutrient applications. *Journal of Integrative Agriculture*, 21(2), 532–541. [https://doi.org/10.1016/S2095-3119\(21\)63614-6](https://doi.org/10.1016/S2095-3119(21)63614-6)
- Joann M. McDermid, B. L. (2012). Iron. *Advances in Nutrition*, 3:(1), 532–533. <https://doi.org/10.3945/an.112.002261.Table>
- Jones, H., Leigh, F. J., Mackay, I., Bower, M. A., Smith, L. M. J., Charles, M. P., Jones, G., Jones, M. K., Brown, T. A., & Powell, W. (2008). Population-based resequencing reveals that the flowering time adaptation of cultivated barley originated east of the Fertile Crescent. *Molecular Biology and Evolution*, 25(10), 2211–2219. <https://doi.org/10.1093/molbev/msn167>
- Kaur, G., Meena, V., Kumar, A., Suman, G., Tyagi, D., Joon, R., Balk, J., & Pandey, A. K. (2023). Asymmetric expression of homoeologous genes in wheat roots modulates the early phase of iron-deficiency signalling. *Environmental and Experimental Botany*, 208, 105254. <https://doi.org/10.1016/J.ENVEXPBOT.2023.105254>
- Ke, C., Guan, W., Bu, S., Li, X., Deng, Y., Wei, Z., Wu, W., & Zheng, Y. (2019). Determination of absorption dose in chemical mutagenesis in plants. *PloS One*, 14(1), e0210596.
- Kim, H. S., Jeon, S., Kim, C., Kim, Y. K., Cho, Y. S., Kim, J., Blazyte, A., Manica, A., Lee, S., & Bhak, J. (2019). Chromosome-scale assembly comparison of the Korean Reference Genome KOREF from PromethION and PacBio with Hi-C mapping information. *GigaScience*, 8(12), 1–5. <https://doi.org/10.1093/gigascience/giz125>

- Kim, S. A., Punshon, T., Lanzirotti, A., Li, A., Alonso, J. M., Ecker, J. R., Kaplan, J., & Guerinot, M. Lou. (2006). Localization of iron in Arabidopsis seed requires the vacuolar membrane transporter *VIT1*. *Science*, 314(5803), 1295–1298. <https://doi.org/10.1126/science.1132563>
- Kim, S., Kim, C. W., Park, M., & Choi, D. (2015). Identification of candidate genes associated with fertility restoration of cytoplasmic male-sterility in onion (*Allium cepa* L.) using a combination of bulked segregant analysis and RNA-seq. *Theoretical and Applied Genetics*, 128(11), 2289–2299. <https://doi.org/10.1007/s00122-015-2584-z>
- Korshunova, Y. O., Eide, D., Gregg Clark, W., Lou Guerinot, M., & Pakrasi, H. B. (1999). The *IRT1* protein from Arabidopsis thaliana is a metal transporter with a broad substrate range. *Plant Molecular Biology*, 40, 37–44.
- Korzeniowska, J., & Stanislawski-Glubiak, E. (2022). Differences in the Concentration of Micronutrients in Young Shoots of Numerous Cultivars of Wheat, Maize and Oilseed Rape. *Agronomy*, 12(11). <https://doi.org/10.3390/agronomy12112639>
- Krasileva, K. V., Vasquez-Gross, H. A., Howell, T., Bailey, P., Paraiso, F., Clissold, L., Simmonds, J., Ramirez-Gonzalez, R. H., Wang, X., Borrill, P., Fosker, C., Ayling, S., Phillips, A. L., Uauy, C., & Dubcovsky, J. (2017). Uncovering hidden variation in polyploid wheat. *Proceedings of the National Academy of Sciences of the United States of America*, 114(6), E913–E921. <https://doi.org/10.1073/pnas.1619268114>
- Krishnappa, G., Singh, A. M., Chaudhary, S., Ahlawat, A. K., Singh, S. K., Shukla, R. B., Jaiswal, J. P., Singh, G. P., & Solanki, I. S. (2017). Molecular mapping of the

- grain iron and zinc concentration, protein content and thousand kernel weight in wheat (*Triticum aestivum* L.). *PLoS ONE*, 12(4). <https://doi.org/10.1371/journal.pone.0174972>
- Kumar, A., Kaur, G., Singh, P., Meena, V., Sharma, S., Tiwari, M., Bauer, P., & Pandey, A. K. (2022). Strategies and Bottlenecks in Hexaploid Wheat to Mobilize Soil Iron to Grains. *Frontiers in Plant Science*, 13(April). <https://doi.org/10.3389/fpls.2022.863849>
- Kumar, J., Saripalli, G., Gahlaut, V., Goel, N., Meher, P. K., Mishra, K. K., Mishra, P. C., Sehgal, D., Vikram, P., Sansaloni, C., Singh, S., Sharma, P. K., & Gupta, P. K. (2018). Genetics of Fe, Zn, β -carotene, GPC and yield traits in bread wheat (*Triticum aestivum* L.) using multi-locus and multi-traits GWAS. *Euphytica*, 214(11), 1–17. <https://doi.org/10.1007/s10681-018-2284-2>
- Kumssa, D. B., Joy, E. J. M., Ander, E. L., Watts, M. J., Young, S. D., Walker, S., & Broadley, M. R. (2015). Dietary calcium and zinc deficiency risks are decreasing but remain prevalent. *Scientific Reports*, 5, 1–11. <https://doi.org/10.1038/srep10974>
- Kurlovs, A. H., Snoeck, S., Kosterlitz, O., Van Leeuwen, T., & Clark, R. M. (2019). Trait mapping in diverse arthropods by bulked segregant analysis. *Current Opinion in Insect Science*, 36(Figure 1), 57–65. <https://doi.org/10.1016/j.cois.2019.08.004>
- Kyriacou, B., Moore, K. L., Paterson, D., de Jonge, M. D., Howard, D. L., Stangoulis, J., Tester, M., Lombi, E., & Johnson, A. A. T. (2014). Localization of iron in rice grain using synchrotron X-ray fluorescence microscopy and high resolution secondary ion mass spectrometry. *Journal of Cereal Science*, 59(2), 173–180.

<https://doi.org/10.1016/J.JCS.2013.12.006>

- Lee, S. C., Kim, Y. Y., Lee, Y. S., & An, G. H. (2007). Rice P1B-Type heavy-metal ATPase, *OsHMA9*, is a metal efflux protein. *Plant Physiol*, *145*. <https://doi.org/10.1104/pp.107.102236>
- Lee, S., Jeong, H. J., Kim, S. A., Lee, J., Guerinot, M. Lou, & An, G. (2010). *OsZIP5* is a plasma membrane zinc transporter in rice. *Plant Molecular Biology*, *73*(4), 507–517. <https://doi.org/10.1007/s11103-010-9637-0>
- Lee, S., Kim, S. A., Lee, J., Guerinot, M. Lou, & An, G. (2010). Zinc deficiency-inducible *OsZIP8* encodes a plasma membrane-localized zinc transporter in rice. *Molecules and Cells*, *29*(6), 551–558. <https://doi.org/10.1007/s10059-010-0069-0>
- Lee, S., Lee, J., Ricachenevsky, F. K., Punshon, T., Tappero, R., Salt, D. E., & Guerinot, M. Lou. (2021). Redundant roles of four *ZIP* family members in zinc homeostasis and seed development in *Arabidopsis thaliana*. *Plant Journal*, *108*(4), 1162–1173. <https://doi.org/10.1111/tpj.15506>
- Li, H. (2013). Aligning sequence reads, clone sequences and assembly contigs with BWA-MEM. *00*(00), 1–3. <http://arxiv.org/abs/1303.3997>
- Li, J., Li, H., Chen, J., Yan, L., & Xia, L. (2020). Toward precision genome editing in crop plants. *Molecular Plant*, *13*(6), 811–813.
- Li, Q., Pan, Z., Gao, Y., Li, T., Liang, J., Zhang, Z., Zhang, H., Deng, G., Long, H., & Yu, M. (2020). Quantitative Trait Locus (QTLs) Mapping for Quality Traits of Wheat Based on High Density Genetic Map Combined With Bulk Segregant Analysis RNA-seq (BSR-Seq) Indicates That the Basic 7S Globulin Gene Is Related to

- Falling Number. *Frontiers in Plant Science*, 11(December), 1–21.
<https://doi.org/10.3389/fpls.2020.600788>
- Li, S., Liu, Z., Guo, L., Li, H., Nie, X., Chai, S., & Zheng, W. (2019). *Genome-wide identification of ZIP gene family members in wheat*. Research Square.
<https://doi.org/10.21203/rs.2.19334/v1>
- Li, S., Liu, Z., Guo, L., Li, H., Nie, X., Chai, S., & Zheng, W. (2021). Genome-Wide Identification of Wheat ZIP Gene Family and Functional Characterization of the TaZIP13-B in Plants. *Frontiers in Plant Science*, 12(November).
<https://doi.org/10.3389/fpls.2021.748146>
- Li, S., Zhou, X., Huang, Y., Zhu, L., Zhang, S., Zhao, Y., Guo, J., Chen, J., & Chen, R. (2013). Identification and characterization of the zinc-regulated transporters, iron-regulated transporter-like protein (ZIP) gene family in maize. *BMC Plant Biology*, 13(1). <https://doi.org/10.1186/1471-2229-13-114>
- Li, Z., & Xu, Y. (2021). Bulk segregation analysis in the NGS era: a review of its teenage years. *Plant Journal*, 109(6), 1355–1374. <https://doi.org/10.1111/tpj.15646>
- Lin, Q., Zong, Y., Xue, C., Wang, S., Jin, S., Zhu, Z., Wang, Y., Anzalone, A. V, Raguram, A., & Doman, J. L. (2020). Prime genome editing in rice and wheat. *Nature Biotechnology*, 38(5), 582–585.
- Lin, Y. F., Liang, H. M., Yang, S. Y., Boch, A., Clemens, S., Chen, C. C., Wu, J. F., Huang, J. L., & Yeh, K. C. (2009). Arabidopsis *IRT3* is a zinc-regulated and plasma membrane localized zinc/iron transporter. *New Phytologist*, 182(2), 392–404.
<https://doi.org/10.1111/j.1469-8137.2009.02766.x>

- Liping Huang, V. J. D. and E. H. (2015). Nutrient Information: Zinc. *Advances in Nutrition*, 1934, 224–226. <https://doi.org/10.3945/an.114.006874>.
- Liu, X., Xu, Z., Feng, B., Zhou, Q., Ji, G., Guo, S., Liao, S., Lin, D., Fan, X., & Wang, T. (2022). Quantitative trait loci identification and breeding value estimation of grain weight-related traits based on a new wheat 50K single nucleotide polymorphism array-derived genetic map. *Frontiers in Plant Science*, 13(August), 1–17. <https://doi.org/10.3389/fpls.2022.967432>
- Loveday, S. M., Huang, V. T., Reid, D. S., & Winger, R. J. (2012). Water Dynamics in Fresh and Frozen Yeasted Dough. *Critical Reviews in Food Science and Nutrition*, 52(5), 390–409. <https://doi.org/10.1080/10408398.2010.500265>
- Ma, R., McLeod, C. W., Tomlinson, K., & Poole, R. K. (2004). Speciation of protein-bound trace elements by gel electrophoresis and atomic spectrometry. *Electrophoresis*, 25(15), 2469–2477. <https://doi.org/10.1002/elps.200405999>
- Ma, X., Liu, H., Cao, H., Qi, R., Yang, K., Zhao, R., Lv, W., & Zhang, Y. (2019). Genome-wide analysis of zinc- and iron-regulated transporter-like protein family members in apple and functional validation of *ZIP10*. *BioMetals*, 32(4), 657–669. <https://doi.org/10.1007/s10534-019-00203-6>
- Manavalan, R. (2020). Automatic identification of diseases in grains crops through computational approaches: A review. *Computers and Electronics in Agriculture*, 178, 105802. <https://doi.org/10.1016/J.COMPAG.2020.105802>
- Mansfeld, B. N., & Grumet, R. (2018). QTLseqr: An R Package for Bulk Segregant Analysis with Next-Generation Sequencing. *The Plant Genome*, 11(2), 180006. <https://doi.org/10.3835/plantgenome2018.01.0006>

- Marks, R. A., Hotaling, S., Frandsen, P. B., & VanBuren, R. (2021). Representation and participation across 20 years of plant genome sequencing. *Nature Plants*, 7(12), 1571–1578. <https://doi.org/10.1038/s41477-021-01031-8>
- Marschner, H. (1995). Mineral nutrition of higher plants 2nd edition. *Academic Press*.
- Martens, D. C., & Westermann, D. T. (1991). Fertilizer applications for correcting micronutrient deficiencies. *Micronutrients in Agriculture*, 4, 549–592.
- Martinez, S. A., Shorinola, O., Conselman, S., See, D., Skinner, D. Z., Uauy, C., & Steber, C. M. (2020). Exome sequencing of bulked segregants identified a novel *TaMKK3-A* allele linked to the wheat ERA8 ABA-hypersensitive germination phenotype. *Theoretical and Applied Genetics*, 133(3), 719–736. <https://doi.org/10.1007/s00122-019-03503-0>
- McKinney, W. (2010). Data Structures for Statistical Computing in Python. *Proceedings of the 9th Python in Science Conference*, 1(Scipy), 56–61. <https://doi.org/10.25080/majora-92bf1922-00a>
- McLean, E., Cogswell, M., Egli, I., Wojdyla, D., & de Benoist, B. (2009). Worldwide prevalence of anaemia, WHO Vitamin and Mineral Nutrition Information System, 1993–2005. *Public Health Nutrition*, 12(04), 444. <https://doi.org/10.1017/S1368980008002401>
- Meena, R., Joshi, S., & Raghuwanshi, S. (2022). Detection of Varieties of Diseases in Rice Plants using Deep Learning Techniques. *2022 4th International Conference on Inventive Research in Computing Applications (ICIRCA)*, 664–674. <https://doi.org/10.1109/ICIRCA54612.2022.9985745>

- Mendoza-Cózatl, D. G., Xie, Q., Akmakjian, G. Z., Jobe, T. O., Patel, A., Stacey, M. G., Song, L., Demoin, D. W., Jurisson, S. S., Stacey, G., & Schroeder, J. I. (2014). OPT3 Is a Component of the Iron-Signaling Network between Leaves and Roots and Misregulation of *OPT3* Leads to an Over-Accumulation of Cadmium in Seeds. *Molecular Plant*, 7(9), 1455–1469. <https://doi.org/10.1093/MP/SSU067>
- Meziani, S., Jasniewski, J., Gaiani, C., Ioannou, I., Muller, J. M., Ghoul, M., & Desobry, S. (2011). Effects of freezing treatments on viscoelastic and structural behavior of frozen sweet dough. *Journal of Food Engineering*, 107(3–4), 358–365. <https://doi.org/10.1016/j.jfoodeng.2011.07.003>
- Michelmore, R. W., Paran, I., & Kesseli, R. V. (1991). Identification of markers linked to disease-resistance genes by bulked segregant analysis: A rapid method to detect markers in specific genomic regions by using segregating populations. *Proceedings of the National Academy of Sciences of the United States of America*, 88(21), 9828–9832. <https://doi.org/10.1073/pnas.88.21.9828>
- Mladěnka, P., Macáková, K., Zatloukalová, L., Řeháková, Z., Singh, B. K., Prasad, A. K., Parmar, V. S., Jahodář, L., Hrdina, R., & Saso, L. (2010). In vitro interactions of coumarins with iron. *Biochimie*, 92(9), 1108–1114. <https://doi.org/10.1016/J.BIOCHI.2010.03.025>
- Moore, K. L., Zhao, F.-J., Gritsch, C. S., Tosi, P., Hawkesford, M. J., McGrath, S. P., Shewry, P. R., & Grovenor, C. R. M. (2012a). Localisation of iron in wheat grain using high resolution secondary ion mass spectrometry. *Journal of Cereal Science*, 55(2), 183–187.
- Moore, K. L., Zhao, F. J., Gritsch, C. S., Tosi, P., Hawkesford, M. J., McGrath, S. P.,

- Shewry, P. R., & Grovenor, C. R. M. (2012b). Localisation of iron in wheat grain using high resolution secondary ion mass spectrometry. *Journal of Cereal Science*, 55(2), 183–187. <https://doi.org/10.1016/J.JCS.2011.11.005>
- Morrissey, J., Baxter, I. R., Lee, J., Li, L., Lahner, B., Grotz, N., Kaplan, J., Salt, D. E., & Guerinot, M. Lou. (2009). The ferroportin metal efflux proteins function in iron and cobalt homeostasis in Arabidopsis. *The Plant Cell*, 21(10), 3326–3338.
- Morrissey, J., & Guerinot, M. Lou. (2009). Iron uptake and transport in plants: The good, the bad, and the ionome. *Chemical Reviews*, 109(10), 4553–4567. <https://doi.org/10.1021/cr900112r>
- Nevo, Y., & Nelson, N. (2006). The NRAMP family of metal-ion transporters. *Biochimica et Biophysica Acta (BBA) - Molecular Cell Research*, 1763(7), 609–620. <https://doi.org/10.1016/J.BBAMCR.2006.05.007>
- Nielsen, F. H., & Meacham, S. L. (2011). Growing Evidence for Human Health Benefits of Boron. *Journal of Evidence-Based Complementary & Alternative Medicine*, 16(3), 169–180. <https://doi.org/10.1177/2156587211407638>
- Nishito, Y., & Kambe, T. (2018). Absorption mechanisms of iron, copper, and zinc: An overview. *Journal of Nutritional Science and Vitaminology*, 64(1), 1–7. <https://doi.org/10.3177/jnsv.64.1>
- O'BRIEN, S. Y. Z. and T. P. (1970). A special type of tracheary element associated with “xylem discontinuity” in the floral axis of wheat. *Australian Journal of Biological Sciences*, 23, 783–791.
- Ohki, K. (1976). Effect of zinc nutrition on photosynthesis and carbonic anhydrase

activity in cotton. *Physiologia Plantarum*, 38(4), 300–304.

- Otsu, & N. (1979). A threshold selection method from gray-level histograms. *IEEE Trans. on Systems, Man and Cybernetics*, 9(1), 62–66.
https://cw.fel.cvut.cz/b201/_media/courses/a6m33bio/otsu.pdf
- Oury, F.-X., Leenhardt, F., Remesy, C., Chanliaud, E., Duperrier, B., Balfourier, F., & Charmet, G. (2006). Genetic variability and stability of grain magnesium, zinc and iron concentrations in bread wheat. *European Journal of Agronomy*, 25(2), 177–185.
- Pahlavan-Rad, M. R., & Pessarakli, M. (2009). Response of Wheat Plants to Zinc, Iron, and Manganese Applications and Uptake and Concentration of Zinc, Iron, and Manganese in Wheat Grains. *Communications in Soil Science and Plant Analysis*, 40(7–8), 1322–1332. <https://doi.org/10.1080/00103620902761262>
- Pallotta, M. A., Warner, P., Fox, R. L., Kuchel, H., Jefferies, S. J., & Langridge, P. (2003). Marker assisted wheat breeding in the southern region of Australia. *Proceedings of the Tenth International Wheat Genetics Symposium*, 789–791.
- Palmer, C. A., & Gilbert, J. A. (2012). Position of the Academy of Nutrition and Dietetics: The Impact of Fluoride on Health. *Journal of the Academy of Nutrition and Dietetics*, 112(9), 1443–1453. <https://doi.org/10.1016/j.jand.2012.07.012>
- Parr, R. M., & Fjeld, C. R. (1994). Human health and nutrition: how isotopes are helping to overcome “hidden hunger.” *IAEA Bulletin*, 4, 18–27.
- Pasquale Strazzullo, C. L. (2014). Sodium. *Advances in Nutrition*, 5, 188–190.
<https://doi.org/10.3945/an.113.005215.amount>

- Pedas, P., Schjoerring, J. K., & Husted, S. (2009). Identification and characterization of zinc-starvation-induced ZIP transporters from barley roots. *Plant Physiology and Biochemistry*, 47(5), 377–383. <https://doi.org/10.1016/J.PLAPHY.2009.01.006>
- Peleg, Z., Cakmak, I., Ozturk, L., Yazici, A., Jun, Y., Budak, H., Korol, A. B., Fahima, T., & Saranga, Y. (2009). Quantitative trait loci conferring grain mineral nutrient concentrations in durum wheat × wild emmer wheat RIL population. *Theoretical and Applied Genetics*, 119(2), 353–369. <https://doi.org/10.1007/s00122-009-1044-z>
- Peng, J. H., Sun, D., & Nevo, E. (2011). Domestication evolution, genetics and genomics in wheat. *Molecular Breeding*, 28(3), 281–301. <https://doi.org/10.1007/s11032-011-9608-4>
- Peng, L., Wang, F., Wang, Z., Tan, J., Huang, L., Tian, X., Liu, G., & Zhou, L. (2022). Cell-cell communication inference and analysis in the tumour microenvironments from single-cell transcriptomics: data resources and computational strategies. *Briefings in Bioinformatics*, 23(4). <https://doi.org/10.1093/bib/bbac234>
- Petersen, G., Seberg, O., Yde, M., & Berthelsen, K. (2006). Phylogenetic relationships of Triticum and Aegilops and evidence for the origin of the A, B, and D genomes of common wheat (*Triticum aestivum*). *Molecular Phylogenetics and Evolution*, 39(1), 70–82. <https://doi.org/10.1016/j.ympev.2006.01.023>
- Petolino, J. F., Srivastava, V., & Daniell, H. (2016). Editing Plant Genomes: a new era of crop improvement. *Plant Biotechnology Journal*, 14(2), 435–436.
- Phimolsiripol, Y., Siripatrawan, U., Tulyathan, V., & Cleland, D. J. (2008). Effects of

- freezing and temperature fluctuations during frozen storage on frozen dough and bread quality. *Journal of Food Engineering*, 84(1), 48–56.
<https://doi.org/10.1016/j.jfoodeng.2007.04.016>
- Pinto, E., & Ferreira, I. M. P. L. V. O. (2015). Cation transporters/channels in plants: Tools for nutrient biofortification. *Journal of Plant Physiology*, 179, 64–82.
<https://doi.org/10.1016/J.JPLPH.2015.02.010>
- Pu, Z. E., Yu, M., He, Q. Y., Chen, G. Y., Wang, J. R., Liu, Y. X., Jiang, Q. T., Li, W., Dai, S. F., Wei, Y. M., & Zheng, Y. L. (2014). Quantitative Trait Loci Associated with Micronutrient Concentrations in Two Recombinant Inbred Wheat Lines. *Journal of Integrative Agriculture*, 13(11), 2322–2329.
[https://doi.org/10.1016/S2095-3119\(13\)60640-1](https://doi.org/10.1016/S2095-3119(13)60640-1)
- Quarshie, S. D. G., Xiao, X., & Zhang, L. (2021). Enhanced Phytoremediation of Soil Heavy Metal Pollution and Commercial Utilization of Harvested Plant Biomass: a Review. *Water, Air, and Soil Pollution*, 232(11). <https://doi.org/10.1007/s11270-021-05430-7>
- Raboy, V. (2001). Seeds for a better future: 'low phytate' grains help to overcome malnutrition and reduce pollution. *Trends in Plant Science*, 6(10), 458–462.
[https://doi.org/10.1016/S1360-1385\(01\)02104-5](https://doi.org/10.1016/S1360-1385(01)02104-5)
- Rakszegi, M., Kisgyörgy, B. N., Tearall, K., Shewry, P. R., Láng, L., Phillips, A., & Bedő, Z. (2010). Diversity of agronomic and morphological traits in a mutant population of bread wheat studied in the Healthgrain program. *Euphytica*, 174(3), 409–421.
<https://doi.org/10.1007/s10681-010-0149-4>
- Ramesh, S. A., Shin, R., Eide, D. J., & Schachtman, D. P. (2003). Differential Metal

- Selectivity and Gene Expression of Two Zinc Transporters from Rice. *Plant Physiology*, 133(1), 126 LP – 134. <https://doi.org/10.1104/pp.103.026815>
- Ramírez-González, R. H., Borrill, P., Lang, D., Harrington, S. A., Brinton, J., Venturini, L., Davey, M., Jacobs, J., Van Ex, F., Pasha, A., Khedikar, Y., Robinson, S. J., Cory, A. T., Florio, T., Concia, L., Juery, C., Schoonbeek, H., Steuernagel, B., Xiang, D., ... Uauy, C. (2018). The transcriptional landscape of polyploid wheat. *Science*, 361(6403). <https://doi.org/10.1126/science.aar6089>
- Ramirez-Gonzalez, R. H., Uauy, C., & Caccamo, M. (2015). PolyMarker: A fast polyploid primer design pipeline. *Bioinformatics*, 31(12), 2038–2039. <https://doi.org/10.1093/bioinformatics/btv069>
- Randall, P. J., & Bouma, D. (1973). Zinc deficiency, carbonic anhydrase, and photosynthesis in leaves of spinach. *Plant Physiology*, 52(3), 229–232.
- Ravet, K., Touraine, B., Kim, S. A., Cellier, F., Thomine, S., Guerinot, M. Lou, Briat, J.-F., & Gaymard, F. (2009). Post-Translational Regulation of *AtFER2* Ferritin in Response to Intracellular Iron Trafficking during Fruit Development in Arabidopsis. *Molecular Plant*, 2(5), 1095–1106. <https://doi.org/10.1093/MP/SSP041>
- Rawat, N., Joshi, A., Pumphrey, M., Singh, L., Mahlandt, A., Chhabra, B., Wilson, D., Gill, B., Poland, J., & Tiwari, V. (2019). A TILLING resource for hard red winter wheat variety Jagger. *Crop Science*, 59(4), 1666–1671.
- Rawat, N., Sehgal, S. K., Joshi, A., Rothe, N., Wilson, D. L., McGraw, N., Vadlani, P. V., Li, W., & Gill, B. S. (2012). A diploid wheat TILLING resource for wheat functional genomics. *BMC Plant Biology*, 12. <https://doi.org/10.1186/1471-2229-12-205>

- Rayman, M. P. (2000). The importance of selenium to human health: review. *The Lancet*, 356(7), 233–241.
- Rellán-Álvarez, R., Giner-Martínez-Sierra, J., Orduna, J., Orera, I., Rodríguez-Castrilln, J. Á., García-Alonso, J. I., Abadía, J., & Álvarez-Fernández, A. (2010). Identification of a Tri-Iron(III), Tri-Citrate Complex in the Xylem Sap of Iron-Deficient Tomato Resupplied with Iron: New Insights into Plant Iron Long-Distance Transport. *Plant and Cell Physiology*, 51(1), 91–102. <https://doi.org/10.1093/pcp/pcp170>
- Roschztardt, H., Conéjero, G., Curie, C., & Mari, S. (2010). Straightforward histochemical staining of Fe by the adaptation of an old-school technique: identification of the endodermal vacuole as the site of Fe storage in Arabidopsis embryos. *Plant Signaling & Behavior*, 5(1), 56–57. <https://doi.org/10.4161/psb.5.1.10159>
- Rout, G. R., & Sahoo, S. (2015). Role of Iron in Plant Growth and Metabolism. *Reviews in Agricultural Science*, 3(0), 1–24. <https://doi.org/10.7831/ras.3.1>
- Sadeghzadeh, B., & Rengel, Z. (2011). Zinc in soils and crop nutrition. *The Molecular and Physiological Basis of Nutrient Use Efficiency in Crops*, 335–375.
- Sasaki, A., Yamaji, N., Mitani-Ueno, N., Kashino, M., & Ma, J. F. (2015). A node-localized transporter *OsZIP3* is responsible for the preferential distribution of Zn to developing tissues in rice. In *Plant Journal* (Vol. 84, Issue 2, pp. 374–384). <https://doi.org/10.1111/tpj.13005>
- Segond, D., Dellagi, A., Lanquar, V., Rigault, M., Patrit, O., Thomine, S., & Expert, D. (2009). *NRAMP* genes function in Arabidopsis thaliana resistance to Erwinia

- chrysanthemi infection. *Plant Journal*, *58*(2), 195–207.
<https://doi.org/10.1111/j.1365-313X.2008.03775.x>
- Senoura, T., Sakashita, E., Kobayashi, T., Takahashi, M., Aung, M. S., Masuda, H., Nakanishi, H., & Nishizawa, N. K. (2017). The iron-chelate transporter *OsYSL9* plays a role in iron distribution in developing rice grains. *Plant Molecular Biology*, *95*(4), 375–387.
- Sestili, F., Garcia-Molina, M. D., Gambacorta, G., Beleggia, R., Botticella, E., De Vita, P., Savatin, D. V., Masci, S., & Lafiandra, D. (2019). Provitamin A Biofortification of Durum Wheat through a TILLING Approach. *International Journal of Molecular Sciences*, *20*(22). <https://doi.org/10.3390/ijms20225703>
- Shahzad, Z., Rouached, H., & Rakha, A. (2014). Combating Mineral Malnutrition through Iron and Zinc Biofortification of Cereals. *Comprehensive Reviews in Food Science and Food Safety*, *13*(3), 329–346. <https://doi.org/10.1111/1541-4337.12063>
- Shariatipour, N., Heidari, B., & Richards, C. M. (2021). Meta-analysis of QTLome for grain zinc and iron contents in wheat (*Triticum aestivum* L.). *Euphytica*, *217*(5), 1–14. <https://doi.org/10.1007/s10681-021-02818-8>
- Sharma, P. N., Chatterjee, C., Agarwala, S. C., & Sharma, C. P. (1990). Zinc deficiency and pollen fertility in maize (*Zea mays*). In *Plant Nutrition—Physiology and Applications: Proceedings of the Eleventh International Plant Nutrition Colloquium, 30 July–4 August 1989, Wageningen, The Netherlands* (pp. 261–265). Springer Netherlands.
- Sheraz, S., Wan, Y., Venter, E., Verma, S. K., Xiong, Q., Waites, J., Connorton, J. M.,

- Shewry, P. R., Moore, K. L., & Balk, J. (2021). Subcellular dynamics studies of iron reveal how tissue-specific distribution patterns are established in developing wheat grains. *New Phytologist*, 231(4), 1644–1657. <https://doi.org/10.1111/nph.17440>
- Shewry, P. R. (2009). Wheat. *Journal of Experimental Botany*, 60(6), 1537–1553. <https://doi.org/10.1093/jxb/erp058>
- Shewry, P. R., Pellny, T. K., & Lovegrove, A. (2016). Is modern wheat bad for health? *Nature Plants*, 2(7), 1–3.
- SHI, R., TONG, Y., JING, R., ZHANG, F., & ZOU, C. (2013). Characterization of Quantitative Trait Loci for Grain Minerals in Hexaploid Wheat (*Triticum aestivum* L.). *Journal of Integrative Agriculture*, 12(9), 1512–1521. [https://doi.org/10.1016/S2095-3119\(13\)60559-6](https://doi.org/10.1016/S2095-3119(13)60559-6)
- Shoba, D., Manivannan, N., Vindhiyavarman, P., & Nigam, S. N. (2012). SSR markers associated for late leaf spot disease resistance by bulked segregant analysis in groundnut (*Arachis hypogaea* L.). *Euphytica*, 188(2), 265–272. <https://doi.org/10.1007/s10681-012-0718-9>
- Shuman, L. M. (1998). Micronutrient fertilizers. *Journal of Crop Production*, 1(2), 165–195.
- Sinclair, S. A., Senger, T., Talke, I. N., Cobbett, C. S., Haydon, M. J., & Krämer, U. (2018). Systemic upregulation of *MTP2* and *HMA2* mediated Zn partitioning to the shoot supplements local Zn deficiency responses. *The Plant Cell*, 30(10), 2463–2479.

- Singh, H., Singh Rawat, C., & Verma, D. (2019). Image Processing Techniques for Analysing Food Grains. *2019 3rd International Conference on Computing Methodologies and Communication (ICCMC)*, 1–4. <https://doi.org/10.1109/ICCMC.2019.8819760>
- Sun, Y., Wang, J., Crouch, J. H., & Xu, Y. (2010). Efficiency of selective genotyping for genetic analysis of complex traits and potential applications in crop improvement. *Molecular Breeding*, *26*(3), 493–511. <https://doi.org/10.1007/s11032-010-9390-8>
- Tabbita, F., Pearce, S., & Barneix, A. J. (2017). Breeding for increased grain protein and micronutrient content in wheat: ten years of the *GPC-B1* gene. *Journal of Cereal Science*, *73*, 183–191.
- Takagi, H., Abe, A., Yoshida, K., Kosugi, S., Natsume, S., Mitsuoka, C., Uemura, A., Utsushi, H., Tamiru, M., Takuno, S., Innan, H., Cano, L. M., Kamoun, S., & Terauchi, R. (2013). QTL-seq: Rapid mapping of quantitative trait loci in rice by whole genome resequencing of DNA from two bulked populations. *Plant Journal*, *74*(1), 174–183. <https://doi.org/10.1111/tpj.12105>
- Thomine, S., Lelièvre, F., Debarbieux, E., Schroeder, J. I., & Barbier-Brygoo, H. (2003). *AtNRAMP3*, a multispecific vacuolar metal transporter involved in plant responses to iron deficiency. *Plant Journal*, *34*(5), 685–695. <https://doi.org/10.1046/j.1365-313X.2003.01760.x>
- Timmer, C. P. (2003). Biotechnology and food systems in developing countries. *The Journal of Nutrition*, *133*(11), 3319–3322.
- Tiong, J., Mcdonald, G., Genc, Y., Shirley, N., Langridge, P., & Huang, C. Y. (2015). Increased expression of six *ZIP* family genes by zinc (Zn) deficiency is associated

- with enhanced uptake and root-to-shoot translocation of Zn in barley (*Hordeum vulgare*). *New Phytologist*, 207(4), 1097–1109. <https://doi.org/10.1111/nph.13413>
- Tiong, J., Mcdonald, G. K., Genc, Y., Pedas, P., Hayes, J. E., Toubia, J., Langridge, P., & Huang, C. Y. (2014). *HvZIP7* mediates zinc accumulation in barley (*Hordeum vulgare*) at moderately high zinc supply. *New Phytologist*, 201(1), 131–143. <https://doi.org/10.1111/nph.12468>
- Tiwari, C., Wallwork, H., Arun, B., Mishra, V. K., Velu, G., Stangoulis, J., Kumar, U., & Joshi, A. K. (2016). Molecular mapping of quantitative trait loci for zinc, iron and protein content in the grains of hexaploid wheat. *Euphytica*, 207(3), 563–570. <https://doi.org/10.1007/s10681-015-1544-7>
- Tiwari, V. K., Rawat, N., Chhuneja, P., Neelam, K., Aggarwal, R., Randhawa, G. S., Dhaliwal, H. S., Keller, B., & Singh, K. (2009). Mapping of quantitative trait loci for grain iron and zinc concentration in diploid a genome wheat. *Journal of Heredity*, 100(6), 771–776. <https://doi.org/10.1093/jhered/esp030>
- Tontisirin, K., Nantel, G., & Bhattacharjee, L. (2002). Food-based strategies to meet the challenges of micronutrient malnutrition in the developing world. *Proceedings of the Nutrition Society*, 61(2), 243–250. <https://doi.org/10.1079/PNS2002155>
- Travis, O. (2006). Guide to NumPy. *Trelgol Publishing USA*, 378.
- Trumbo, M. Z. and P. R. (2013). Nutrient Information : Iodine. *Advances in Nutrition*, 262–264. <https://doi.org/10.3945/an.113.003665>.Table
- Uauy, C., Borrill, P., & Adamski, N. (2015). Genomics as the key to unlocking the polyploid potential of wheat. *New Phytologist*, 1008–1022.

- Uauy, C., Distelfeld, A., Fahima, T., Blechl, A., & Dubcovsky, J. (2006). A NAC gene regulating senescence improves grain protein, zinc, and iron content in wheat. *Science*, *314*(5803), 1298–1301.
- Van Der Walt, S., Schönberger, J. L., Nunez-Iglesias, J., Boulogne, F., Warner, J. D., Yager, N., Gouillart, E., & Yu, T. (2014). Scikit-image: Image processing in python. *PeerJ*, *2014*(1), 1–18. <https://doi.org/10.7717/peerj.453>
- Velu, G., Crossa, J., Singh, R. P., Hao, Y., Dreisigacker, S., Perez-Rodriguez, P., Joshi, A. K., Chatrath, R., Gupta, V., Balasubramaniam, A., Tiwari, C., Mishra, V. K., Sohu, V. S., & Mavi, G. S. (2016). Genomic prediction for grain zinc and iron concentrations in spring wheat. *Theoretical and Applied Genetics*, *129*(8), 1595–1605. <https://doi.org/10.1007/s00122-016-2726-y>
- Velu, G., Singh, R. P., Crespo-Herrera, L., Juliana, P., Dreisigacker, S., Valluru, R., Stangoulis, J., Sohu, V. S., Mavi, G. S., Mishra, V. K., Balasubramaniam, A., Chatrath, R., Gupta, V., Singh, G. P., & Joshi, A. K. (2018). Genetic dissection of grain zinc concentration in spring wheat for mainstreaming biofortification in CIMMYT wheat breeding. *Scientific Reports*, *8*(1), 1–10. <https://doi.org/10.1038/s41598-018-31951-z>
- Venske, E., Dos Santos, R. S., Busanello, C., Gustafson, P., & Costa de Oliveira, A. (2019). Bread wheat: a role model for plant domestication and breeding. *Hereditas*, *156*, 16. <https://doi.org/10.1186/s41065-019-0093-9>
- Verma, L., & Pandey, N. K. (2016). Effect of iron stress on oxidative metabolism in wheat plants (*Triticum aestivum* (L)). *IRON STRESS IN WHEAT*.
- Vert, G., Briat, J. F., & Curie, C. (2001). Arabidopsis *IRT2* gene encodes a root-

- periphery iron transporter. *Plant Journal*, 26(2), 181–189.
<https://doi.org/10.1046/j.1365-313X.2001.01018.x>
- Wallace, A., & Lunt, O. R. (1956). Reactions of some iron, zinc, and manganese chelates in various soils. *Soil Science Society of America Journal*, 20(4), 479–482.
- Wang, J., Shi, X., Zhou, Z., Qin, M., Wang, Y., Li, W., Yang, P., Wu, Z., & Lei, Z. (2022). Genetic dissection of grain iron concentration in hexaploid wheat (*Triticum aestivum* L.) using a genome-wide association analysis method. *PeerJ*, 10, e13625. <https://doi.org/10.7717/peerj.13625>
- Wang, L., Czedik-Eysenberg, A., Mertz, R. A., Si, Y., Tohge, T., Nunes-Nesi, A., Arrivault, S., Dedow, L. K., Bryant, D. W., Zhou, W., Xu, J., Weissmann, S., Studer, A., Li, P., Zhang, C., LaRue, T., Shao, Y., Ding, Z., Sun, Q., ... Brutnell, T. P. (2014). Comparative analyses of C4 and C3 photosynthesis in developing leaves of maize and rice. *Nature Biotechnology*, 32(11), 1158–1164.
<https://doi.org/10.1038/nbt.3019>
- Wang, P., Chen, H., Mohanad, B., Xu, L., Ning, Y., Xu, J., Wu, F., Yang, N., Jin, Z., & Xu, X. (2014). Effect of frozen storage on physico-chemistry of wheat gluten proteins: Studies on gluten-, glutenin- and gliadin-rich fractions. *Food Hydrocolloids*, 39, 187–194. <https://doi.org/10.1016/j.foodhyd.2014.01.009>
- Wang, P., Xu, L., Nikoo, M., Ocen, D., Wu, F., Yang, N., Jin, Z., & Xu, X. (2014). Effect of frozen storage on the conformational, thermal and microscopic properties of gluten: Comparative studies on gluten-, glutenin- and gliadin-rich fractions. *Food Hydrocolloids*, 35, 238–246. <https://doi.org/10.1016/j.foodhyd.2013.05.015>
- Waters, B. M., Chu, H.-H., DiDonato, R. J., Roberts, L. A., Easley, R. B., Lahner, B.,

- Salt, D. E., & Walker, E. L. (2006). Mutations in Arabidopsis yellow stripe-like1 and yellow stripe-like3 reveal their roles in metal ion homeostasis and loading of metal ions in seeds. *Plant Physiology*, 141(4), 1446–1458. <https://doi.org/10.1104/pp.106.082586>
- Watson, A., Ghosh, S., Williams, M. J., Cuddy, W. S., Simmonds, J., Rey, M. D., Asyraf Md Hatta, M., Hinchliffe, A., Steed, A., Reynolds, D., Adamski, N. M., Breakspear, A., Korolev, A., Rayner, T., Dixon, L. E., Riaz, A., Martin, W., Ryan, M., Edwards, D., ... Hickey, L. T. (2018). Speed breeding is a powerful tool to accelerate crop research and breeding. *Nature Plants*, 4(1), 23–29. <https://doi.org/10.1038/s41477-017-0083-8>
- Welch, R. M., & Shuman, L. (1995). Micronutrient Nutrition of Plants. *Critical Reviews in Plant Sciences*, 14(1), 49–82. <https://doi.org/10.1080/07352689509701922>
- Wenzel, A. A., & Mehlhorn, H. (1995). Zinc deficiency enhances ozone toxicity in bush beans (*Phaseolus vulgaris* L. cv. Saxa). *Journal of Experimental Botany*, 46(7), 867–872.
- Wessells, K. R., & Brown, K. H. (2012). Estimating the Global Prevalence of Zinc Deficiency: Results Based on Zinc Availability in National Food Supplies and the Prevalence of Stunting. *PLOS ONE*, 7(11), 1–11. <https://doi.org/10.1371/journal.pone.0050568>
- White, P. J., & Broadley, M. R. (2005). Biofortifying crops with essential mineral elements. *Trends in Plant Science*, 10(12), 586–593. <https://doi.org/10.1016/j.tplants.2005.10.001>
- WHO. (2012). *Guideline: Sodium intake for adults and children*. World Health

Organization.

- WHO. (2018). *The state of food security and nutrition in the world 2018: building climate resilience for food security and nutrition*.
<http://www.fao.org/3/i9553en/i9553en.pdf>
- Winter, D., Vinegar, B., Nahal, H., Ammar, R., Wilson, G. V., & Provart, N. J. (2007). An “electronic fluorescent pictograph” Browser for exploring and analyzing large-scale biological data sets. *PLoS ONE*, 2(8), 1–12.
<https://doi.org/10.1371/journal.pone.0000718>
- Wu, J., Zhao, F. J., Ghandilyan, A., Logoteta, B., Guzman, M. O., Schat, H., Wang, X., & Aarts, M. G. M. (2009). Identification and functional analysis of two ZIP metal transporters of the hyperaccumulator *Thlaspi caerulescens*. *Plant and Soil*, 325(1), 79–95. <https://doi.org/10.1007/s11104-009-0151-6>
- Xu, Y., An, D., Liu, D., Zhang, A., Xu, H., & Li, B. (2012a). Molecular mapping of QTLs for grain zinc, iron and protein concentration of wheat across two environments. *Field Crops Research*, 138, 57–62. <https://doi.org/10.1016/J.FCR.2012.09.017>
- Xu, Y., An, D., Liu, D., Zhang, A., Xu, H., & Li, B. (2012b). Molecular mapping of QTLs for grain zinc, iron and protein concentration of wheat across two environments. *Field Crops Research*, 138, 57–62. <https://doi.org/10.1016/J.FCR.2012.09.017>
- Xu, Y., Li, P., Zou, C., Lu, Y., Xie, C., Zhang, X., Prasanna, B. M., & Olsen, M. S. (2017). Enhancing genetic gain in the era of molecular breeding. *Journal of Experimental Botany*, 68(11), 2641–2666.
- Yamaji, N., Xia, J., Mitani-Ueno, N., Yokosho, K., & Feng Ma, J. (2013). Preferential

delivery of zinc to developing tissues in rice is mediated by P-type heavy metal ATPase *OshMA2*. *Plant Physiology*, 162(2), 927–939.

Yilmaz, A., Ekiz, H., Gültekin, I., Torun, B., Barut, H., Karanlik, S., & Cakmak, I. (1998). Effect of seed zinc content on grain yield and zinc concentration of wheat grown in zinc-deficient calcareous soils. *Journal of Plant Nutrition*, 21(10), 2257–2264.

Yoneyama, T., Ishikawa, S., & Fujimaki, S. (2015). Route and Regulation of Zinc, Cadmium, and Iron Transport in Rice Plants (*Oryza sativa* L.) during Vegetative Growth and Grain Filling: Metal Transporters, Metal Speciation, Grain Cd Reduction and Zn and Fe Biofortification. In *International Journal of Molecular Sciences* (Vol. 16, Issue 8). <https://doi.org/10.3390/ijms160819111>

Yu, H. Y., Liu, C., Zhu, J., Li, F., Deng, D. M., Wang, Q., & Liu, C. (2016). Cadmium availability in rice paddy fields from a mining area: The effects of soil properties highlighting iron fractions and pH value. *Environmental Pollution*, 209, 38–45. <https://doi.org/10.1016/j.envpol.2015.11.021>

Zhai, Z., Gayomba, S. R., Jung, H., Vimalakumari, N. K., Piñeros, M., Craft, E., Rutzke, M. A., Danku, J., Lahner, B., Punshon, T., Guerinot, M. Lou, Salt, D. E., Kochian, L. V., & Vatamaniuk, O. K. (2014). *OPT3* Is a Phloem-Specific Iron Transporter That Is Essential for Systemic Iron Signaling and Redistribution of Iron and Cadmium in *Arabidopsis*. *The Plant Cell*, 26(5), 2249–2264. <https://doi.org/10.1105/tpc.114.123737>

Zhang, C., Gao, L., Sun, J., Jia, J., & Ren, Z. (2014). Haplotype variation of Green Revolution gene *Rht-D1* during wheat domestication and improvement. *Journal of Integrative Plant Biology*, 56(8), 774–780. <https://doi.org/10.1111/jipb.12197>

- Zhang, F., Römheld, V., & Marschner, H. (1989). Effect of zinc deficiency in wheat on the release of zinc and iron mobilizing root exudates. *Zeitschrift Für Pflanzenernährung Und Bodenkunde*, 152(2), 205–210.
- Zhang, J., & Panthee, D. R. (2020). PyBSASeq: A simple and effective algorithm for bulked segregant analysis with whole-genome sequencing data. *BMC Bioinformatics*, 21(1), 1–10. <https://doi.org/10.1186/s12859-020-3435-8>
- Zhang, P., Wang, Y., Sun, T., Wu, X., Xia, W., Fang, P., Pandey, A. K., & Xu, P. (2022). Fine mapping *PsPS1*, a gene controlling pod softness that defines market type in pea (*Pisum sativum*). *Plant Breeding*, 141(3), 418–428. <https://doi.org/10.1111/pbr.13020>
- Zhang, Y., Sun, Y., Ye, Y., Karim, R., Xue, Y., Yan, P., Meng, Q., Cui, Z., Cakmak, I., Zhang, F., & Zou, C. (2012). Field Crops Research Zinc biofortification of wheat through fertilizer applications in different locations of China. *Field Crops Research*, 125, 1–7. <https://doi.org/10.1016/j.fcr.2011.08.003>
- Zhang, Y., Xu, Y. H., Yi, H. Y., & Gong, J. M. (2012). Vacuolar membrane transporters *OsVIT1* and *OsVIT2* modulate iron translocation between flag leaves and seeds in rice. *Plant Journal*, 72(3), 400–410. <https://doi.org/10.1111/j.1365-313X.2012.05088.x>
- Zhao, F. J., Su, Y. H., Dunham, S. J., Rakszegi, M., Bedo, Z., McGrath, S. P., & Shewry, P. R. (2009). Variation in mineral micronutrient concentrations in grain of wheat lines of diverse origin. *Journal of Cereal Science*, 49(2), 290–295. <https://doi.org/10.1016/j.jcs.2008.11.007>
- Zhao, L., Liu, X., Hu, Z., Li, L., & Li, B. (2017). Molecular Structure Evaluation of Wheat

Gluten during Frozen Storage. *Food Biophysics*, 12(1), 60–68.

<https://doi.org/10.1007/s11483-016-9463-2>

Zielińska-Dawidziak, M. (2015). Plant Ferritin—A Source of Iron to Prevent Its Deficiency. In *Nutrients* (Vol. 7, Issue 2). <https://doi.org/10.3390/nu7021184>